ROLE OF THE CXCR3 CHEMOKINE RECEPTOR AXIS IN THE COMBINATION OF ONCOLYTIC VESICULAR STOMATITIS VIRUS THERAPY AND NATURAL KILLER T CELL IMMUNOTHERAPY IN MELANOMA

by

Rhea Nickerson

Submitted in partial fulfilment of the requirements
for the degree of Master of Science

at

Dalhousie University
Halifax, Nova Scotia
January 2023

Dalhousie University is located in Mi'kma'ki, the
ancestral and unceded territory of the Mi'kmaq.
We are all Treaty people.

TABLE OF CONTENTS

LIST OF TABLES

LIST OF FIGURES

ABSTRACT

Advanced melanoma is highly metastatic and resistant to traditional chemotherapies, resulting in a 5-year survival rate of less than 30%. This study investigated Natural Killer T (NKT) cell-based immunotherapy in combination with oncolytic vesicular stomatitis virus (VSV-ΔM51). VSV-ΔM51 infection increases the production of CXCR3 chemokine receptor ligands CXCL9, -10, and -11, potentially recruiting CXCR3-expressing NKT cells into the tumor microenvironment; however, the specific role of the CXCR3 axis in treatment efficacy is unknown. Using a melanoma model, responses to NKT cell immunotherapy, alone and in combination with recombinant VSV-ΔM51 constructs, were tested in wild-type and $CXCR3^{-/-}$ mice. Mice received oncolytic VSV-GFP or VSV engineered to express reovirus fusion associated small transmembrane (FAST) protein p14 (VSV-p14). Combined treatments enhanced survival compared to monotherapies in both WT and $CXCR3^{-/-}$ mice. Loss of CXCR3 impaired accumulation of NKT cells within tumors, but did not impair recruitment of other key immune populations or significantly impact treatment efficacy. In fact, $CXCR3^{-/-}$ mice exhibited trends towards improved tumor regression and survival in response to VSV, as well as increased viral persistence post-treatment. These results demonstrate that oncolytic VSV in combination with NKT cell immunotherapy provides superior survival benefits compared to monotherapies. However, the CXCR3 axis appears dispensable in our combined therapy. Factors including chemokine axis redundancy, as well as reduced viral clearance and enhanced oncolytic activity may compensate for the loss of CXCR3 in this model.

LIST OF ABBREVIATIONS USED

αGalCer	α-galactosylceramide
ADCC	Antibody-dependent cellular cytotoxicity
ANOVA	Analyses of variances
APC	Antigen-presenting cell
ARV	Avian reovirus
ATP	Adenosine triphosphate
BATF	Basic leucine zipper transcription factor, ATF-like
BRAF	B-raf proto-oncogene serine/threonine kinase
DN	CD4− CD8− double-negative
C	Cysteine
CAR	Chimeric antigen receptor
cDC	Conventional DC
CSD	Cumulative sun damage
CTL	Cytotoxic CD8 T cells
CTLA-4	Cytotoxic T-lymphocyte-associated antigen
DAMP	Danger associated molecular pattern
DC	Dendritic cell
ddPCR	Digital droplet PCR
DMEM	Dulbecco's modified Eagle medium
DPP 4	Dipeptidylpeptidase 4
EDTA	Trypsin-ethylenediamine-tetra acetic acid
EGF	Epithelial growth factor
EGFR	Epidermal growth factor receptor
ELISA	Enzyme-linked immunosorbent assay
ER	Estrogen receptor
ERK	Extracellular signal-regulated kinase
FasL	Fas ligand
FAST	Fusion associated small transmembrane protein
FBS	Fetal bovine serum
FoxP3	Forkhead box protein 3
G	Glycoprotein
GATA-3	GATA binding protein 3
GC	Germinal centre
GEM	Genetically engineered mouse
GFP	Green fluorescent protein
GM-CSF	Granulocyte-monocyte colony stimulating factor
GPCR	G protein coupled receptor

HER-2	Human epidermal growth factor receptor 2
HGF/SF	Hepatocyte growth factor/scatter factor
HMGB-1	High-mobility group box 1
HSV-1	Herpes simplex 1 virus
ICD	Immunogenic cell death
ICOS	Inducible T-cell costimulator
IFN	Interferon
IL	Interleukin
i.p.	Intraperitoneal
IP-10	Interferon gamma-induced protein 10 (a.k.a. CXCL10)
IRF3	Interferon regulatory factor 3
IRF7	Interferon regulatory factor 7
i.t.	Intratumoral
I-TAC	Interferon-inducible T-cell alpha chemoattractant (a.k.a. CXCL11)
i.v.	Intravenous
JAK	Janus kinase
KIR	Killer cell immunoglobulin-like receptors
L	Large polymerase protein
LAG-3	Lymphocyte activation gene-3
LCMV	Lymphocytic choriomeningitis virus
LDL receptor	Low density lipoprotein receptor
LN	Lymph node
M	Matrix protein
M	Methionine
MAP kinase	Mitogen-activated protein kinase
MDSC	Myeloid derived suppressor cell
MEK	Mitogen-activated protein kinase kinase
MHC	Major histocompatibility complex
MIG	Monokine induced by gamma interferon (a.k.a. CXCL9)
MMP	Matrix metalloproteinases
moDC	Monocyte-derived DC
MOI	Multiplicity of infection
mRNA	Messenger RNA
N	Nucleocapsid protein
NBV	Nelson bay reovirus
NFκB	Nuclear factor kappa B
NK cell	Natural killer cell
NKT cell	Natural killer T cell

NO	Nitric oxide
NOD/SCID	Non-obese diabetic/severe combined immunodeficiency
NSCLC	Non-small-cell lung carcinoma
OV	Oncolytic virus
OVA	Ovalbumin
P	Phosphoprotein
p14Δ	p14 triple mutant
PAMP	Pathogen-associated molecular pattern
PBS	Phosphate-buffered saline
PD-1	Programmed Death 1 receptor
PD-L1	Programmed Death 1 receptor ligand
PFU	Plaque forming units
PKR	Protein kinase R
PSA	Prostate-specific antigen
PTEN	Phosphatase and tensin homologue deleted on chromosome 10
RdRp	RNA dependent RNA polymerase
RIG-I	Retinoic acid-inducible gene I
RNP complex	Ribonucleoprotein complex
ROS	Reactive oxygen species
RORγT	Retineic-acid-receptor-related orphan nuclear receptor γ
RPMI	Roswell Park Memorial Institute
RT-qPCR	Real time quantitative polymerase chain reaction
sc.	Subcutaneous
scFv	Single chain variable fragment
SEM	Standard error of the mean
STAT	Signal transducer and activator of transcription proteins
STING	Stimulator of interferon genes
TAM	Tumor-associated macrophages
T-bet	T-box expressed in T cells
TCR	T cell receptor
TEM	Transendothelial migration
Tfh cell	T follicular helper cell
TGF-β	Transforming growth factor β
Th cell	T helper cell
TNF	Tumor necrosis factor
TNM	Tumor-node-metastasis
TLR	Toll-like receptor
TLS	Tertiary lymphoid structure
TRAIL	TNF-related apoptosis-inducing ligand

Treg	Regulatory T cell
TRP2	Tyrosinase related protein 2
T-VEC	Talimogene laherparepvec
UV	Ultraviolet
UV-VSV	UV-inactivated VSV
V_H	Variable heavy chain
V_L	Variable light chain
VSIV	Vesicular stomatitis Indiana virus serotype
VSV	Vesicular stomatitis virus
VSV-ΔM51	Vesicular stomatitis virus with matrix protein mutation
VSV-NJ	Vesicular stomatitis virus New Jersey serotype
WT	Wild-type

ACKNOWLEDGEMENTS

This work would not have been possible without the guidance and supervision of Dr. Brent Johnston, as well as the expertise and support of my committee members, Dr. Jean Marshall and Dr. Andrew Stadnyk. I would also like to thank the technicians who have kept the Carleton Animal Care facility running, as well as Flow Cytometry Core staff Derek Rowter and Tatjana Brauer-Chapin for their training and technical support.

I would like to thank the past and present members of the Johnston lab, who taught me everything I know about the realities of working in a lab. I would particularly like to thank Dr. Adam Nelson for his mentorship and unerring ability to have either coffee or beer on hand when it was most needed. I would also like to thank Jordan Lukacs, who kept the lab running during uncertain times, as well as Natasha Osborne, who taught me how to do qPCR the right way. Thank you to all the members of the 15th floor lab space, for making it a collaborative and fun place to work, and particularly Alexander Edgar, for his extensive help troubleshooting my VSV-N primers. Thank you as well to Roy Duncan's lab and Nichole McMullen for developing the VSV-FAST constructs we used.

Finally, I would like to thank my family and friends. First, my parents, for their support and guidance. Second, Marlene and Natasha, without whom I wouldn't have completed the first degree, let alone this one. Third, Owen and Emily, for helping me feel less far from home. Fourth, I owe an incredible thank you to Taylor, Eileigh, and Stacia, who made me feel welcome from my very first day at Dal –without you this would have been a very different, and much lonelier experience. I couldn't have asked for a better cohort to commiserate and celebrate with. Last but very much not least, thank you Mel, for your endless encouragement and support; for reminding me how to carve out space for joy and keep perspective; and, of course, for always getting my toothbrush ready.

CHAPTER 1: INTRODUCTION

1.1 Cancer

1.1.1 Definition, epidemiology, classification

Cancer is the leading cause of death in Canada, responsible for almost 30% of all deaths in 2019 [1]. Almost half of all Canadians are projected to receive a cancer diagnosis in their lifetime, and almost half of those diagnosed are expected to die from cancer [1]. Although the last several decades have ushered in significant advances in both our fundamental understanding of and ability to treat cancer, it still bears an immeasurably heavy burden on both individuals and society at large. Although rates of most cancers are declining due to these advances, actual cases continue to increase in Canada as a factor of our aging population, and globally due to population growth [2,3]. Beyond mortality, the burden of cancer can be measured by metrics including years of life lost, the lasting effects of cancer on those who survive it, and economic impact on both healthcare systems and individuals [3]. From 2010 to 2019, there was a 26.3% increase in global cancer cases, a 20.9% increase in global cancer deaths, and a 16% increase in disability-adjusted life years (which combines years of life lost and cancer-associated disability) [3]. In 2021 alone, the economic burden of cancer in Canada was $26 billion CAD, and approximately one-third of that cost was paid by patients and their families [4]. In countries without robust public health care systems, these costs are much higher. So, what are major challenges we still face in the treatment of cancer?

The last two decades have ushered in breakthroughs in our understanding of the molecular underpinnings and immunological landscapes of cancer, and with this

understanding have come increasingly nuanced and targeted therapies. Beyond treating cancers primarily based on morphological or histological features, cancers can now be targeted based on their specific mutational profiles [5]. Despite the many successes of targeted therapies, such as proto-oncogene serine/threonine kinase B-Raf (BRAF) inhibitors, and human epidermal growth factor receptor 2 (HER-2) inhibitors, many patients fail to respond or develop resistance [6]. These targeted therapies also are inherently limited to patients with specific mutational profiles, and require additional screening, which has butted up against the limits of our diagnostic capacity [5]. The immune system has also been harnessed against cancer, particularly with the advent of immune checkpoint inhibitor therapies in the early 2010s, including anti-Programmed Death 1 receptor (PD-1) and anti-cytotoxic T-lymphocyte-associated antigen 4 (CTLA-4) monoclonal antibodies, whose profound impact on cancer treatment resulted in the winning of a Nobel Prize in 2018. However, even anti-PD-1 can only induce long-lasting cures in about 10-20% of patients, and much work is still being done to determine which patient populations will benefit most from this therapy [5]. Some major remaining challenges include developing reliable mechanisms to determine which patient populations will benefit from specific therapies, and finding ways to overcome the ability of cancers to adapt and become refractory to treatment.

As we continue to develop increasingly specialized and personalized therapies, it becomes increasingly clear that there will likely be no “magic bullet” cure. The heterogeneity between and within cancer types, and between and within individuals, will require the development of novel single and combination therapies. As combination therapies prove their worth in the treatment of heterogenous and evolving cancers, it is

becoming increasingly important that we understand how to rationally combine therapies, which requires elucidating the mechanisms by which therapies synergize in combination.

1.1.2 Hallmarks of cancer

Cancer, at its most basic, is a term used to describe diseases driven by cells which have been transformed by genetic mutation to grow uncontrollably and spread throughout the body, eventually impacting the body's ability to function. Though cancers are incredibly diverse, arising in different tissues as a result of different mutations in different individuals, they are united by this ability to grow and spread in ways normal, healthy cells do not. Cancers share many similar functional characteristics, developed in the transition from normalcy to malignancy, which allow cancer cells to survive, proliferate, and disseminate to form metastases [7]. These characteristics, which have been referred to as the "hallmarks" of cancer, define cancer cells' abilities to replicate indefinitely, avoid apoptosis, sustain proliferative signaling while avoiding growth suppression, deregulate cellular energetics, induce angiogenesis, and avoid immune destruction [7]. The development of these characteristics is driven at its core by genome instability, which has different triggers in different cancers that can be either hereditary or environmental. Some cancers, like melanoma, are highly driven by DNA-damaging insults like ultraviolet (UV) radiation, as will be discussed further below [8]. Normal cells can become malignant by acquiring hallmark mutations through generations of replicating cells. And as cancer cells acquire more mutations which suppress apoptosis, prevent DNA repair, and enable replicative immortality, their mutational rate accelerates, allowing the accumulation of additional hallmarks necessary for their survival and expansion into multicellular tumors. As these malignant cells divide, the mutational diversity in

successive generations of cells increases, giving rise to clonally heterogeneous tumors, composed of subpopulations of cells which are able to evade immune destruction or resist various treatment strategies, allowing for tumors to “evolve” under these stressors and become refractory to treatment [9,10].

Though cancers share common hallmark capabilities that allow them to survive and proliferate, it is also crucial to identify their differences, generated by their mutational profiles, tissues of origin, metastatic burden, immune status, and other factors. Being able to classify tumors by type and disease stage is essential for treatment and prognosis.

Cancers have historically been classified according to their primary site of origin or by their tissue type. According to the International Classification of Diseases for Oncology, Third Edition, cancers can be classified by tissue type into five major categories: carcinoma, sarcoma, lymphoma, myeloma, and leukemia [11]. Carcinomas, the most common category of cancer, are cancers arising from epithelial tissue. Sarcomas are a broad category of cancers originating from connective and supportive tissues, including muscle, bone, cartilage, and adipose tissue. These two categories make up the solid tumors, which have complex and distinct tumor structures and microenvironments. Lymphomas, which are cancers originating from lymphocytes in the lymph nodes or other areas of the lymphatic system; myelomas, which arise from plasma cells; and leukemias, which arise from leukocytes originating in the bone marrow; comprise the hematologic or blood cancers, which operate very differently from solid tumors.

Disease stage has traditionally been stratified by the tumor-node-metastasis (TNM) system, which divides cancers into severity categories based on primary and metastatic

tumor burden [12]. The T "tumor" category defines the primary tumor based on several criteria, including thickness and ulceration status [13]. The N "node" category defines the extent of local metastatic disease both in regional lymph nodes and lymphatics (i.e. in-transit metastases) [13]. The M "metastatic" category defines distant metastatic disease by the extent of metastasis and tissue site(s) affected [13]. The combination of scores in each of these categories defines the overall clinical stage groups of stage I, II, III, and IV [13]. This staging system largely informs how patients are treated, with standardized treatment strategies being stratified by stage [14].

The last two decades have seen this histological or morphological stratification of cancers become less useful in determining the susceptibility of certain tumors to treatment, which has been recently reflected in updates to the American Joint Committee on Cancer Staging Manual, the eighth edition of which includes new considerations in classification, including gene expression profiles [12,13,15]. New means of classifying cancers have been developed, including grading cancers based on biomarker expression, molecular profiles, and immune infiltration. In fact, the "Immunoscore" classification system which will be discussed in greater detail below, has been shown to be a better predictor of prognosis and treatment responsiveness than the TNM staging system, highlighting the importance of the relationship between the immune system and cancer [16].

1.2 Melanoma

1.2.1 Epidemiology and classification of melanoma

Moving now to the specific cancer which is the focus of this thesis, melanoma is a type of skin carcinoma, and one of very few cancers whose incidence is steadily increasing in

Canada and other countries, against the trend of overall decline [1]. Melanoma incidence has been increasing at a rate of ~2% per year over the past twenty years [1]. As of 2021, 1 in 48 Canadians will be diagnosed with melanoma in their lifetime, a rate that is only set to increase. Unlike many other solid tumors, melanoma also affects a greater proportion of the young to middle-aged population [17]. In Canada, melanoma is the 4th most common cancer in adults aged 30 to 49, and the 5th most common cancer in young adults aged 15 to 29 years [1].

Melanoma is by far the most aggressive form of skin cancer, accounting for less than 5% of all skin cancer cases but over 75% of skin cancer deaths [1]. It originates from melanocytes, cells which produce pigment in the form of melanin, and are found primarily in the skin but also in mucosal sites and the uvea [18]. Melanocytes are derived from neural crest stem cells, which is one reason why melanoma cells so successfully metastasize to the brain and other organs [18].

There are three major categories of melanoma based on site of origin: cutaneous, mucosal, and uveal [8]. Cutaneous melanoma arises in the skin and is most frequently driven by sun damage, possessing specific mutational signatures attributable to UV radiation [17,19]. A specific subcategory of cutaneous melanoma that is less-associated with sun exposure is acral melanoma, which arises in the glabrous skin of the hands and feet [8]. This skin has a different structure which protects the underlying epithelium from UV penetration and subsequent damage [8]. Mucosal and uveal melanomas are also less-associated with sun damage, and possess very different mutational signatures from cutaneous, UV-driven melanomas [19]. Given their relative infrequency, location, and often later diagnoses, mucosal and uveal melanomas face their own unique treatment

challenges [8,19]. However, cutaneous melanoma is by far the most common form of melanoma, and will be the focus of this thesis.

As previously mentioned, melanoma incidence is highly correlated with exposure to UV radiation and skin type. There are two primary chemically distinct forms of melanin: eumelanin (brown-black pigment) and phaeomelanin (yellow-red pigment) [20]. These two forms of melanin have different abilities to absorb UV light: eumelanin is able to scatter and absorb UV radiation as well as the free radicals it generates, whereas phaeomelanin is photo-unstable and may even promote carcinogenesis [20]. Fair-skinned individuals have increased production of photo-unstable phaeomelanin relative to UV-absorbing eumelanin in their skin, which results in reduced UV protection leading to a 70-fold increase in skin cancer risk [18,20]. Because of this UV-driven DNA damage, melanoma tumors on average have the highest mutational load across human cancers [18,19]. The importance of sun damage in driving the development of melanoma has led the World Health Organization to develop a classification system for melanoma incorporating cumulative sun damage (CSD), which correlates with specific mutations driving melanoma development [17]. The three categories include high-CSD and low-CSD melanoma, which are primarily cutaneous melanomas, as well as low-to-no-CSD melanoma, which includes acral, mucosal, and uveal melanoma [21]. In the low-CSD category, the most frequent molecular alteration is the $BRAF^{V600E}$ mutation, against which targeted therapies have been developed [17]. BRAF is an important regulator of the mitogen-activated protein (MAP) kinase/extracellular signal-regulated kinase (ERK) signaling pathway, which affects cell division, differentiation, and secretion [21]. Mutation of BRAF results in overactivation of the MAP kinase pathway triggering aberrant cell

proliferation, inhibiting apoptosis, and eventually promoting tumor progression [21]. V600E is the most common BRAF mutation, but other minor BRAF mutations do exist [21]. The overall high mutational burden of melanoma means that melanoma tumors are often highly clonally diverse and antigenic [9]. However, despite the therapeutic potential of targeting mutated antigens, the majority of tumor antigens are highly patient-specific and heterogenous within both the tumor and metastatic sites [9]. This diversity drives the ability of melanoma tumors to mutate in response to various therapies and become treatment-refractory, which is often seen in advanced melanoma tumors that are unable to be fully surgically-excised [9].

1.2.2 Melanoma treatment

Cutaneous melanoma is staged as follows: primary tumor with no evidence of distant or regional metastasis (stage I-II), regional/in-transit metastasis (stage III), and distant metastasis (stage IV) [22,23]. Around 85% of cutaneous melanoma cases present as stage I or stage II, which have very high cure rates when treated appropriately and promptly [14,15]. The first line treatment for cutaneous melanoma is surgical resection, with a five-year survival rate of over 90% after surgery [23]. If the primary tumor is non-resectable, or if the cancer has metastasized, prognosis is far more dire. Less than two decades ago, metastatic melanoma was widely viewed as incurable, with median survival rates of 6 to 10 months [18,24,25]. The only clinically-approved therapies for metastatic melanoma until the 2010s included chemotherapeutic agents such as dacarbazine, which exhibited little to no clinical benefit [26,27]. Melanoma is notoriously resistant to chemotherapy for several reasons, including dysregulated apoptotic pathways, altered drug transport, and over-activation of autophagy pathways to overcome cellular stressors [26,28].

Today, the 5-year survival rate for metastatic stage IV melanoma remains below 30% [1]. As dire as this is, it still represents a series of significant breakthroughs over the last decade, which began in the early 2010s first with the clinical approval of immune checkpoint inhibitors anti-CTLA-4 and anti-PD-1 and then mutation-targeting BRAF and mitogen-activated protein kinase kinase (MEK) inhibitors [18]. These therapies are primarily used in metastatic stage III and IV patients following surgical resection of primary and accessible metastatic tumors (adjuvant use), but are now being evaluated for neoadjuvant use (pre-resection) to render previously unresectable tumors amenable to surgery [14].

For the 40-50% of patients with BRAF-mutant melanoma, combination BRAF/MEK inhibitor targeted therapy has resulted in response rates of almost 80% [13,29,30]. However, more than 80% of these treatment responders eventually relapse [18,30]. Since BRAF mutations typically act as a driver at the earliest stage of melanoma development, tumors generally display limited intratumoral BRAF-mutation heterogeneity, but ~16% of BRAF-mutated tumors do display intratumoral heterogeneity in expression. [21]. BRAF mutation status also differs between primary and metastatic tumors with ~12% of primary/metastatic tumors having mismatched BRAF-mutation expression status [21]. This heterogeneity has important implications for responses to BRAF-targeted therapies, and is an important mechanism by which treatment resistance may develop. The nature of this targeted therapy also means that more than half of melanoma patients with wild-type BRAF are unable to derive any benefit from it, rendering other approaches necessary.

The other breakthrough in advanced melanoma treatment were immune checkpoint inhibitors, specifically anti-PD-1 and anti-CTLA-4 antibodies, which have the benefit of

being able to theoretically treat all patients, not just those with a specific targetable mutation [18]. Immune checkpoint inhibitors were first approved for use in melanoma, with the FDA approval of ipilimaumab (anti-CTLA-4) in 2011 [28]. Immune checkpoint inhibitors are monoclonal antibodies which block the interaction between inhibitory immune checkpoint receptors and their ligands, preventing inhibitory signaling and ultimately enhancing the host's anti-tumor response [25]. However, while checkpoint inhibitors have been shown to induce long-lasting remission in a subset of patients, the majority (60-70%) of patients still experience limited therapeutic responses [18,25]. Part of this therapeutic failure is attributable to intrinsic or acquired resistance associated with T cell exclusion and immune evasion within tumors [31], which will be discussed in more depth in later sections. There are also significant immune-related adverse events associated with immune checkpoint blockade, most commonly affecting the gastrointestinal tract (colitis) and skin (dermatitis), but also including hepatitis and endocrinopathies [28]. Toxicities such as colitis, dermatitis and hepatitis are generally reversible with steroid treatment, but patients who develop endocrine toxicities usually require life-long hormone replacement therapy [28]. These side effects are generally more common and more severe for anti-CTLA-4 therapy than anti-PD-1 or anti-Programmed Death 1 receptor ligand (PD-L1) [28].

Another recent breakthrough in advanced melanoma treatment was the landmark approval of the first oncolytic virus for use in human cancer in the USA and Europe. Talimogene laherparepvec (T-VEC) is a herpes simplex 1 virus (HSV-1) engineered to express the cytokine granulocyte-monocyte colony stimulating factor (GM-CSF) [32,33]. The specifics of T-VEC will be discussed at greater length in a later section. In brief, T-

VEC is administered by direct injection into accessible melanoma lesions, and can generate not only local but systemic anti-tumor immune responses, reducing the size of un-injected, metastatic lesions by greater than 50% in 15% of cases [34]. However, physicians' logistical and biosafety concerns, arising from lack of familiarity with the concept or application of oncolytic virus therapy, have limited its delivery to patients [34].

Despite the success of targeted and immune checkpoint therapies in advanced melanoma, there is still significant room for improvement in overall and sustained response rates, as well as limiting adverse events. To address this, there are many therapies in pre-clinical and clinical development for melanoma. Novel therapies in clinical trials include melanoma cancer vaccines and adoptive transfer of tumor-infiltrating lymphocytes as well as engineered chimeric antigen receptor (CAR)-T cells [28]. Many other immunotherapeutic approaches are being developed including those targeting natural killer (NK) and natural killer T (NKT) cells, as well as novel oncolytic virus platforms and alternate checkpoint inhibitors, such as Lymphocyte activation gene-3 (LAG-3) antibodies [25]. Many existing therapies are also being tested in new combinations in clinical trials, including combinations of anti-PD-1 and BRAF/MEK inhibitors, to great success; as well as combination of anti-PD-1 and anti-CTLA-4, also to great success, particularly in brain metastasis, but also with significantly higher toxicities [25]. T-VEC is also being tested in a stage III clinical trial in combination with anti-PD-1 [25,34]. The success of combination therapies in these clinical trials once again highlights the potential of combination therapies to overcome treatment challenges.

There are numerous challenges in the treatment of advanced metastatic melanoma. One is the acquisition of therapy resistance, which occurs through multiple mechanisms. One

elegant mechanism described in melanoma was the characterization of small populations of rare cells which transiently express high levels of resistance marker transcription driven to stable phenotypic expression by therapy initiation, allowing a small subpopulation of tumor cells to survive until some acquire secondary mutations and the tumor becomes overall refractory to treatment [10]. This is also combined with pre-existing clonal heterogeneity, where treatment selects for existing resistant mutants which then come to dominate, as can be seen in the example of BRAF-heterogenous tumors that acquire BRAF/MEK inhibitor resistance [21]. Other challenges include the organs to which melanoma metastasizes. Melanoma has a very high frequency of brain metastasis, which is a challenging tissue to target therapeutically for various reasons including the relative impermeability of the blood-brain barrier, and its status as an immune-privileged site [18,22]. Finally, more broadly, the tumor immune environment can have a major impact on the success of immune checkpoint inhibitors and other immunotherapies, as will be discussed in more detail in the following section.

1.3 Cancer and the immune system

1.3.1 Immune hallmarks of cancer

The immune system plays a complicated and often contradictory role in cancer whose critical importance has only come into the spotlight in the last few decades. The concept of cancer immunosurveillance, first proposed by Ehrlich in 1909 and refined in 1957 by Burnet and Thomas, underpins our understanding of how cancer develops in immunocompetent hosts [35]. This concept has since been refined to account for the complex pro- and anti-tumorigenic roles played by the immune system. The term “cancer immunoediting” was proposed by Robert Schreiber to encompass the various ways in

which the immune system both promotes and antagonizes tumor development. Tumor development is divided into three main stages: elimination, equilibrium, and escape [35]. Malignant cells arise regularly in our bodies, and are routinely recognized and eliminated by surveying immune cells. Most malignant cells do not pass this first stage. The importance of this elimination stage can be seen in the real-world in immunocompromised patients who have significantly higher risks of *de novo* cancer development [35]. But, of course, cancer still develops in immunocompetent hosts, through the remaining two stages of equilibrium and eventual cancer escape. Equilibrium describes the process by which the immune system, by destroying susceptible cells, selects for and drives the generation of malignant cells increasingly able to resist and evade immune attack [35]. The end result of this process is escape, in which these evasive and/or resistant cancer cells are able to proliferate and form clinically detectable tumors [35].

This acquired ability of cancer to evade and manipulate the immune system was only recognized as a hallmark of cancer in the past ten years [7,36]. The mechanisms by which cancers accomplish this are highly varied, but can be grouped into three main categories: to evade the immune system, cancers must be able to thrive in a chronically inflamed microenvironment, evade immune recognition, and suppress immune reactivity [36]. Cancers are able to not only persist in inflammatory conditions, but can actually wield chronic inflammation to their advantage and use it to drive tumorigenesis [7]. Inflammation has been shown to be present during even the earliest stages of tumor formation, and it can contribute to the development of several of cancer's hallmark capabilities in a variety of ways; for example, by providing growth factors and cytokines which can sustain

proliferative and anti-apoptotic signaling; pro-angiogenic factors that induce tumor neovascularization; extracellular-matrix remodeling enzymes which facilitate angiogenesis as well as metastasis; and reactive oxygen species (ROS) which can induce further DNA damage and mutation in malignant cells, driving their acquisition of other hallmark characteristics [7]. Chronic inflammation is also important for maintaining tumors, as chronic inflammatory signaling can exhaust effector immune cell populations, like CD8+ T cells, and promote the formation of dysfunctional suppressive cell populations like myeloid-derived suppressor cells (MDSCs) [7,37]. However, despite this ability of cancer cells to twist inflammation to their benefit, they must still find ways to evade immune cells and their anti-tumor cytotoxic effector mechanisms. To evade recognition by cytotoxic CD8+ T cells, whose critical role in anti-tumor immunity will be discussed in greater detail below, cancer cells frequently downregulate their expression of major histocompatibility complex (MHC) Class I [36]. Cancer cells can also hide their expression of tumor antigens and manipulate their expression of certain cytokines and chemokines to avoid recruiting and activating immune cells [38,39,40]. Many tumor cells fail to express costimulatory molecules and can thereby induce anergy or tolerance in T cells by engaging antigen-specific T cells in the absence of co-stimulation [41]. Finally, tumor cells have also developed several mechanisms to suppress any anti-tumor immune responses that still occur. Tumor cells can indirectly induce immunosuppression by producing chemokines (ex. CCL2) that recruit immunosuppressive immune populations, like CD4+ regulatory T cells (Tregs) [42]. The chronically inflamed tumor microenvironment can also, as mentioned previously, promote the differentiation of immune populations into dysregulated suppressive subsets like MDSCs and tumor-

associated macrophages (TAMs) [43]. These suppressive immune populations produce cytokines like interleukin (IL)-10 and transforming growth factor β (TGF-β) which antagonize and counter-regulate pro-inflammatory signals to induce a broadly immunosuppressive tumor microenvironment [43,44]. Cancer cells can also directly suppress immune responses in a variety of ways. For example, cancer cells frequently upregulate their expression of PD-L1 and other co-inhibitory immune checkpoint ligands to inhibit activation of anti-tumor immune cells like CD8+ T cells [45,46].

1.3.2 Hot and cold tumors

Over a decade ago, the first study was published which used tumor immune infiltration (type, density and location of immune cells within colorectal tumors) to more accurately predict survival than the classic TNM staging system [47]. This kickstarted the development of the "Immunoscore", a means of classifying tumors by the presence of specific immune populations at distinct sites within or at the margins of tumors [16]. This led to the classification of tumor immune landscapes by immune infiltration, placing tumors along a scale from "hot" (highly immune infiltrated, specifically by cytotoxic CD8+ T cells), to "cold" (low to absent immune infiltration) [16,31]. This "hot" and "cold" paradigm has been further subdivided into "hot", "cold", and "altered". "Hot" tumors are defined as highly immune-infiltrated and inflamed, "cold tumors" have minimal immune infiltration and inflammation, and "altered" tumors are an intermediate category which can fall into one of two subgroups, either "immunosuppressed" (meaning that immune cells are present but have limited functionality), or "immune excluded" (closer to the cold end, key immune effector subsets are present in very limited numbers) [16]. This categorization of tumor immune landscapes has been shown to predict and correlate with responsiveness to

immunotherapies like immune checkpoint inhibitors in a variety of cancers, including melanoma [16]. A large part of current immunotherapy research is figuring out how to turn cold or altered tumors into hot tumors. Key considerations include how to recruit anti-tumor immune populations into tumors, and how to reverse or interrupt the suppressive mechanisms of tumor-promoting immune cells. So, what are the key immune cell subsets which populate the multifaceted tumor immune landscape?

1.3.3 Tumor-promoting immune cells

Several specific kinds of immune cells, spanning innate and adaptive immunity, have been categorized as "tumor-promoting" immune cells. Key players include forkhead box protein 3 (FoxP3)+ Tregs, as well as anti-inflammatory or dysregulated innate immune cells, particularly from the myeloid lineage.

Looking first to the innate compartment, M2-polarized TAMs and MDSCs are two major cell types which have been implicated in many pro-tumorigenic functions, from the induction of invasion and metastasis to suppression of anti-tumor immune function [7,48]. MDSCs can be divided into two main morphological groups: granulocytic/polymorphonuclear MDSCs, which resemble neutrophils, and monocytic MDSCs, which resemble monocytes [37]. Chronic disease states like cancer, which provide weak and sustained "pathologic" activating signals (in the form of growth factors and inflammatory cytokines), give rise to these morphologically and phenotypically immature neutrophils and granulocytes which can be termed MDSCs [37]. Functionally, MDSCs are weakly phagocytic, consistently produce ROS and nitric oxide (NO), and anti-inflammatory cytokines such as IL-10 and TGF-β which inhibit the function of T cells,

NK cells, NKT cells, and dendritic cells (DCs) [37,49]. Release of these cytokines and other mediators also supports the function of other immunosuppressive subsets including Tregs and TAMs in a positive feedback loop [50]. MDSCs also express high levels of PD-L1, which they use to bind PD-1 expressed on activated T, NK, and NKT cells to inhibit their function by inducing immune exhaustion, anergy, and apoptosis [51]. MDSCs can also promote metastasis by inducing tumor angiogenesis and producing matrix metalloproteases (MMPs) which degrade extracellular matrix proteins and disrupt cell-cell attachment to allow tumor cells to migrate across tumor vasculature [52]. TAMs can be recruited to tumors as circulating or bone-marrow monocytes by chemokines including CCL2 and CCL5 [53]. Once in tumors, TAMs can be polarized along a gradient that has two extremes: M1 "inflammatory" macrophages and M2 "regulatory" or "anti-inflammatory" macrophages. In tumors, the TAM population is able to shift transiently between M1 and M2 populations depending on the type and concentration of signals in the tumor microenvironment [53]. M2 macrophages are pro-tumorigenic, and like MDSCs, can inhibit anti-tumor immune cell function through production of ROS, NO, IL-10, and TGF-β. They can also recruit Tregs by producing CCL22. M2 macrophages are also able to stimulate tumor cell proliferation and survival directly by producing epithelial growth factor (EGF) and other EGF receptor ligands [53,54]. Finally, like MDSCs, M2 macrophages can promote metastasis by inducing tumor angiogenesis and producing MMPs [53].

CD4+ Tregs, defined by their expression of the transcription factor FoxP3, function in health to maintain immune homeostasis and peripheral tolerance, by bringing the body back to baseline after infection and suppressing autoimmunity [55]. Patients with cancer tend to have higher levels of Tregs compared to healthy individuals, and tumor-derived

Tregs also appear to have higher suppressive activity than naturally-occurring Tregs [40,55]. The primary Treg population involved in cancer immunity are inducible Tregs, which are generated in the periphery and do not require costimulatory molecules for activation, although they do require antigen-specific T cell receptor (TCR) signaling and cytokine signals such as TGF-β and IL-2 [55]. Tregs express high levels of CD25, also known as the high affinity IL-2 receptor, which allows Tregs to outcompete other T cell populations in binding of free IL-2, depleting it from the environment and inhibiting the proliferation of other IL-2 dependent T cell populations [56]. Tregs also constitutively express immune checkpoint receptors including PD-L1 and CTLA-4 [57]. Tregs, like the populations described above, also produce high levels of IL-10 and TGF-β, as well as other anti-inflammatory cytokines like IL-35, which in addition to inhibiting the function of pro-inflammatory anti-tumor immune populations, also promote the polarization of anti-inflammatory subsets like MDSCs [40,55]. Tregs have also been shown to be able to release granzyme B to cytolytically kill effector NK cells, T cells, and DCs [55,58]. Tregs are recruited to tumor sites by chemokines such as CCL2, CCL4, CCL5, CCL20, and in some contexts, CXCL9, CXCL10, and CXCL11 [55,59,60,61,62]. Higher intratumoral presence and activity of Tregs have been directly linked to decreased survival and poor prognosis in a wide range of cancers [55].

B cells, which comprise the humoral component of the adaptive immune response, have a more controversial role in tumor immunity. Tumor-infiltrating B cells can activate and secrete tumor-antigen specific antibodies, sometimes even forming germinal centres (GCs) in tumor-associated tertiary lymphoid structures (TLS) [63]. This B cell presence has emerging associations with improved prognosis and survival [63,64]. The presence of tumor-

infiltrating B cells can promote anti-tumor immunity by enhancing CD8+ T cell function, and driving "hot" tumor microenvironments [64,65]. However, B cells, particularly in tumors with immature TLS and limited/no GC formation, can also adopt a regulatory phenotype (Bregs) and mediate pro-tumorigenic effects through secretion of cytokines like IL-10 and expression of PD-L1 [63,66].

1.3.4 Anti-tumor immune cells

As with the tumor-promoting population, there are diverse immune populations spanning innate and adaptive immunity which have been categorized as "anti-tumor" immune cells. Key players include cells from both the adaptive compartment, specifically CD4+ T helper (Th) 1 cells, cytotoxic CD8+ T cells, and NKT cells, as well as innate NK cells, antigen-presenting DCs, and inflammatory M1 macrophages.

First, M1 macrophages compose the "pro-inflammatory" TAM population. In a tumor context, M1 macrophages can be polarized by inflammatory signals such as interferon γ (IFNγ) [53]. M1 macrophages can mediate anti-tumor effects by two main mechanisms. First, macrophage-mediated cytotoxicity, which involves the release of molecules such as ROS and NO, has cytotoxic effects on tumor cells (although these molecules are also implicated in driving pro-tumor inflammation and can harm other bystander cells, including anti-tumor immune cells). The other is antibody-dependent phagocytosis, which requires macrophage-expressed CD16 to bind anti-tumor antibodies on tumor cells [53]. M1 macrophages can also produce a variety of inflammatory cytokines such as IFNγ which help polarize a protective anti-tumor immune response [53].

Next, DCs function as professional antigen-presenting cells (APCs), and thus play a crucial role in orchestrating immune responses and activating adaptive lymphocyte populations, particularly CD8+ T cells. Tumor-infiltrating DCs internalize tumor antigens and present them to CD4+ and CD8+ T cells in tumor-draining lymph nodes to initiate anti-tumor immune responses [67]. Tumor-infiltrating DCs also crucially secrete pro-inflammatory cytokines which help shape T cell responses by polarizing CD4+ T cells towards the Th1 subset and providing important pro-inflammatory activating signals for CD8+ T cells and NK cells. Tumor-infiltrating DCs are also key producers of lymphocyte-recruiting chemokines such as CXCL9, -10, and -11 [68,69,70] , which will be discussed in greater depth later. Tumors with limited DC infiltration also have limited T cell infiltration and generally poorer prognoses [68,70].

NK cells are innate lymphoid cells that mediate anti-tumor effects through both direct cytotoxic tumor cell killing and cytokine production. NK cells express a wide range of activating and inhibitory receptors, and identify target cells by the precise balance between the activating co-stimulatory and inhibitory signals they receive [71]. In tumor settings, NK cells play an especially key role by recognizing tumor cells which have downregulated MHC I expression to evade CD8+ T cell-mediated killing. NK cells express inhibitory receptors Ly49 (mouse) or killer cell immunoglobulin-like receptors (KIR) (human) which bind MHC I [71]. The absence of MHC I on tumor cells activates NK cells by a process called missing-self recognition, allowing them to mediate their anti-tumor effector functions. NK cells also express a variety of other inhibitory receptors, as well as activating receptors including cytokine-binding receptors, integrins, and killing-receptors (such as CD16, which mediates antibody-dependent cellular cytotoxicity

(ADCC)) [71]. NK cells, as well as a variety of other cell types, including NKT cells and CD8+ T cells, also express the activating receptor NKG2D, which binds stress-induced NKG2D ligands on tumor cells [72]. Tumor cells are able to shed NKG2D ligands from their cell surface as an additional mechanism of immune escape [72].

In humans, NK cells are identified as CD3−CD56+ cells which can be subdivided into $CD56^{bright}$ and $CD56^{dim}$ functional subsets [71]. $CD56^{bright}$ NK cells mediate primarily cytokine release, whereas the more terminally differentiated $CD56^{dim}$ NK cells are highly cytotoxic. In mice, NK cells are CD3−NK1.1+ and CD3−CD49b+ [71]. NK cells can be attracted to tumors by chemokines such as CXCL9, -10, and -11 [73].

Following activation, NK cells mediate anti-tumor responses by secreting pro-inflammatory cytokines, particularly IFNγ but also tumor necrosis factor (TNF), IL-6, and GM-CSF [48]. They also directly kill tumor cells by releasing cytotoxic granules containing perforin and granzyme B which induce tumor cell apoptosis. They can also kill tumor cells by engaging TNF-related apoptosis-inducing ligand (TRAIL) and Fas ligand (FasL) with their corresponding receptors on tumor cells, sending pro-apoptotic signals [48,59]. Mice with depleted NK cell numbers or deficient NK cell function often have more aggressive tumor growth and increased metastasis, demonstrating a crucial role for NK cells in tumor immunosurveillance and control [74].

Adaptive lymphocyte populations, both CD4+ and especially CD8+ T cells, also play critical roles in the anti-tumor response. CD4+ T cells are known as helper cells because of their roles in regulating and orchestrating immune responses through their release of specific cytokines. CD4+ T cells recognize peptide antigens presented by MHC II on

APCs such as DCs. Following this antigen-specific activation, CD4+ T cells proliferate and differentiate into a variety of effector subsets based on the cytokine milieu in which they were activated. These effector subsets can be defined based on the primary transcription factor which controls their development, and the specific cytokines they produce. The subsets whose roles in cancer are best defined are Th1 cells, which express T-box expressed in T cells (T-bet) and produce IFNγ; Th2 cells, which express GATA binding protein 3 (GATA-3) and produce IL-4, IL-5, and IL-13; Th-17 cells, which express retineic-acid-receptor-related orphan nuclear receptor γ (RORγT) and produce IL-17; and Treg cells, which express FoxP3 and produce IL-10 and TGF-β [48,75]. Each Th subset plays a unique role in tumor immunity based on their lineage and cytokine profile.

The most clearly anti-tumor CD4+ subset are Th1 cells. They play important roles in priming the anti-tumor immune response by activating tumor-specific CD8+ T cells in lymph nodes [48,76], as well as licensing DCs to cross-present exogenous antigens to CD8+ T cells [67]. By promoting tumor-specific CD8+ T cell activation, tumor-specific CD4+ Th1 cells can drive the expansion and trafficking of CD8+ T cells into tumors to exert cytotoxic functions. Accordingly, reduced CD4+ Th1 cells in tumors correlate with reduced CD8+ T cell recruitment and function [77]. Th1 cells also produce high levels of IFNγ in the tumor microenvironment, which is an important pro-inflammatory cytokine.

Th2 and Th17 CD4+ T cells play more controversial roles in tumor immunity, which appear to be at least partially cancer-dependent [78,79,80]. Th2 cells polarize the immune system towards a type 2 immune response, which is able to antagonize the development and function of Th1 cells [75]. Different cytokines produced by Th17 cells appear to both promote and inhibit tumor angiogenesis, meaning that they may be able to mediate

simultaneous pro and anti-tumorigenic effects which may ultimately influence different outcomes in different tumors [80].

Cytotoxic CD8+ T cells are crucial mediators of anti-tumor immune responses. CD8+ T cells are activated by peptide antigens displayed by MHC I presented on APCs in the correct context of costimulatory ligand and cytokine expression [67]. Primed CD8+ T cells directly recognize neoantigens and tumor antigens presented on MHC I by tumor cells, resulting in direct killing of those cells, which provides selective pressure for tumor cells to downregulate MHC I expression as a key mechanism of immune escape. Like their innate counterpart NK cells, activated CD8+ T cells mediate direct cytotoxicity and indirectly enhance anti-tumor immunity by release of pro-inflammatory cytokines like IFNγ and TNF. Cytotoxic activity is mediated by release of cytotoxic granules containing perforin and granzyme B, as well as inducing apoptosis via TRAIL and FasL [48,81]. After their initial activation, CD8+ T cells can crucially also become memory T cells that are able to contribute to long-term cancer immunosurveillance and prevent cancer recurrence [82].

NKT cells are another key anti-tumor immune population. They bridge the innate and adaptive immune systems and are a crucial focus of this thesis. They will be discussed in greater detail in the following section.

1.4 Natural killer T cells

1.4.1 Overview

NKT cells are a subset of CD3+ innate-like T cells that express conserved TCR rearrangements that recognize endogenous and exogenous glycolipid antigens presented

by the MHC I-like molecule CD1d [83]. CD1d, unlike conventional MHC molecules, is non-polymorphic and highly conserved between individuals and even between species, allowing NKT cells to recognize glycolipid antigens presented on CD1d across species [84]. The discovery of the marine sponge-derived glycolipid α-galactosylceramide (αGalCer) as a potent activator of NKT cells represented a significant advance in our ability to detect and study NKT cell populations [84]. NKT cells can be divided into two subtypes: Type I and Type II. Type I NKT cells, also known as invariant NKT cells, express a semi-invariant TCRα chain composed of Vα14-Jα18 paired with Vβ8.2/7/2 in mice and Vα24-Jα18 paired with Vβ11 in humans [85]. Type II NKT cells exhibit a more diverse array of TCR rearrangements, and preferentially recognize sulfatides and other lipids rather than αGalCer [85,86]. Type I NKT cells, which comprise the prototypic NKT cell population, are involved in tumor surveillance, and can exert potent anti-tumor effects through both direct and indirect mechanisms [83,85,86]. Type II NKT cells, by contrast, have been implicated in tumorigenesis and the formation of metastases, and thus are associated with pro-tumor rather than anti-tumor functions, including cross-regulation of Type I NKT cells [86]. For the purpose of this thesis, the term "NKT cells" moving forward will refer specifically to Type I NKT cells.

NKT cells were first defined by their expression of a variety of NK cell receptors in mice, such as NK1.1, NKG2D, and Ly49. However, this receptor expression varies with developmental stage and genetic background [84]. NKT cells in mice can be either CD4+ or double negative (DN), whereas humans also have CD8+ NKT cells [85,87]. NKT cells develop in the thymus in a CD1d-dependent manner, and selectively home to peripheral organs after maturation [85]. NKT cells can be divided into 3 major subsets: NKT1, NKT2,

and NKT17, which are roughly analogous to Th1, Th2, and Th17 subsets in conventional CD4+ T cells. NKT10 and NKTfh subsets have also been proposed which mirror Treg and T follicular helper (Tfh) subsets [85]. NKT1 cells produce high levels of Type I cytokines such as IFNγ, and are abundant in the spleen and liver [85]. The NKT1 subset appears to be the primary mediator of anti-tumor immune responses, analogous again to Th1 cells [83,85,88]. NKT2 cells produce primarily Th2-skewed cytokines such as IL-4 and IL-13, and are located primarily in the thymus, spleen, lung, and mesenteric lymph nodes [85]. NKT17 cells produce cytokines such as IL-17 and are enriched in lungs and lymph nodes [85,89]. NKT10 cells produce IL-10 and are enriched in white adipose tissue [90]. NKTfh cells can be found in germinal centres of B cell follicles [91]. NKT cell levels differ between mice and humans, with mice possessing high NKT cell levels, particularly in the spleen and liver, where they can constitute up to 30% of total lymphocytes [92]. Human CD1d exhibits altered intracellular trafficking and localization that results in lower levels of NKT cell selection [93]. Humans not only have significantly lower levels of NKT cells than mice in most tissues, with the exception of adipose tissue, but also have more variable NKT cell frequencies, with blood NKT cell levels ranging from 0.001% to 1% between healthy individuals [94]. Expression of human CD1d in mice reduces the number of NKT cells to similar levels to humans, but robust anti-tumor functions are maintained [93].

Referred to as the “Swiss-army knife of the immune system”, NKT cells have wide-reaching roles and implications in a variety of disease states from autoimmunity to cancer [84]. As “innate-like” cells, NKT cells respond quickly upon recognizing their glycolipid antigens with both cytokine production and cytolytic functions. NKT cells can also be

activated in a CD1d-independent manner by cytokines alone, specifically the combination of IL-12 and IL-18 which have been shown to be sufficient for NKT cell activation[92]. Once activated, NKT cells rapidly produce a wide array of cytokines, primarily IFNγ and IL-4, but also IL-2, IL-6, IL-10, IL-17, TNF, TGF-β, GM-CSF, and various chemokines [84]. Which cytokines are produced depends on the structure of the glycolipid ligand and the NKT cell subset that is stimulated. This cytokine production allows NKT cells to regulate the broader immune response. NKT cells can activate and recruit conventional CD4+ and CD8+ T cells; recruit B cells and macrophages; recruit and transactivate NK cells; and recruit and induce maturation in DCs [84,95]. NKT cells also have cytolytic granules containing granzyme B and perforin, and express death ligand receptors like FasL and TRAIL, allowing them to directly kill cells presenting glycolipid antigens in a CD1d-dependent manner [84].

1.4.2 NKT cells in cancer

In the context of cancer, NKT cells play an important role in both cancer immunosurveillance and tumor rejection. Several studies have demonstrated accelerated rates of tumor growth and metastasis in mice lacking Jα18$^{-/-}$ and thus Type I NKT cells [96,97]. In humans, increased NKT cell infiltration is associated with improved prognosis in a variety of cancers, including melanoma [85,98,99]. In a tumor setting, NKT cells can be directly activated by CD1d-expressing tumor cells presenting endogenous glycolipid antigens. These antigens can be either stress-associated or tumor-associated, although much work remains to be done to identify what these endogenous tumor-associated glycolipids are [100]. The importance of this direct recognition is underscored by the fact that CD1d-expressing tumors will often downregulate CD1d to avoid detection by NKT

cells [101]. For tumor cells that downregulate or do not express CD1d, NKT cells can also exhibit cytotoxicity through other receptors (NKG2D, FasL, TRAIL) or be indirectly activated by CD1d-expressing APCs in the tumor microenvironment or by CD1d-independent cytokine activation. Some tumor cells have also been shown to drive downregulation of CD1d expression by APCs in the tumor environment to further avoid NKT cell-mediated killing [102]. It is important to note that the B16 melanoma model used in this thesis expresses limited to no CD1d, meaning that NKT cells are likely mediating their anti-tumor effects primarily indirectly in this model [101,103]. Information regarding expression of CD1d by human melanomas is limited, but variable CD1d expression has been noted in other human cancers, and it is likely that melanomas follow this trend [104].

In addition to mediating direct tumor lysis and indirect immune cell activation and recruitment, NKT cells can also reduce the numbers and efficacy of pro-tumorigenic populations such as M2 macrophages and MDSCs [92]. In primary human neuroblastoma, NKT cells were able to directly kill tumor antigen-expressing TAMs, leading to decreased metastasis [105]. NKT cells have also been shown to reduce the numbers and immunosuppressive activity of MDSCs [106,107]. NKT cells have also shown greater resistance to immunosuppressive tumor environments than conventional T cells, and so may be able to help reshape immunosuppressed tumors towards states of greater immune activation [92,108].

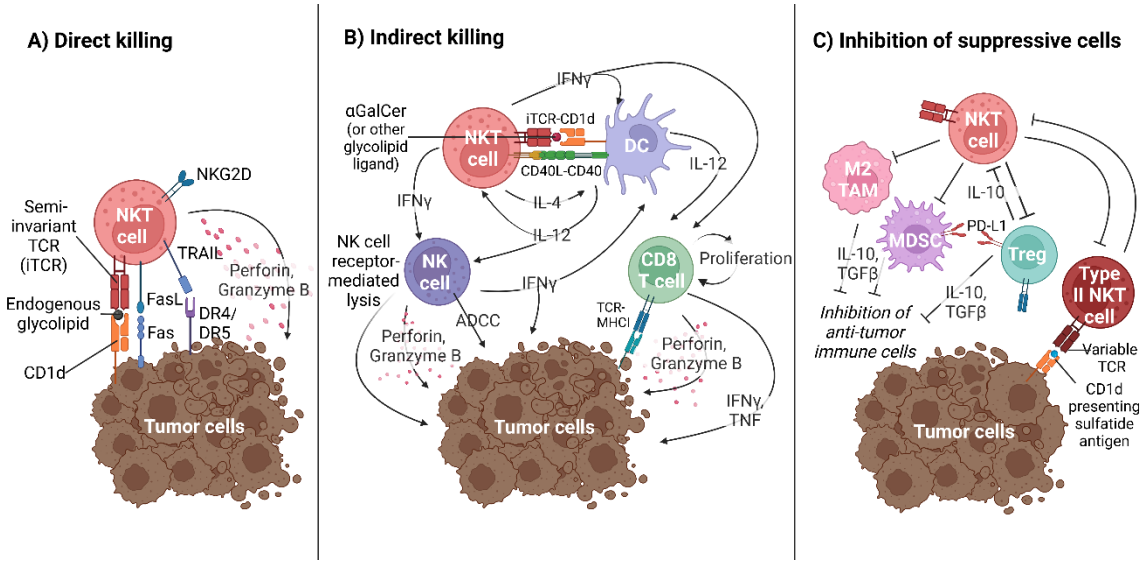

Figure 1. Roles of NKT cells in anti-tumor immunity. A) Type I NKT cells (NKT cells) can be activated via their conserved semi-invariant TCR (iTCR) recognizing CD1d-expressing tumor cells presenting endogenous glycolipid antigens. NKT cells can also be activated by NKG2D-ligand binding or IL-12. Activated NKT cells can directly induce tumor lysis by releasing cytotoxic granules such as perforin and granzyme B, or activating apoptotic signaling through death receptors (FasL, TRAIL on NKT cells bind Fas, DR4/DR5 on tumor cells). B) NKT cells can also be indirectly activated by APCs like DCs presenting glycolipid antigens, such as the synthetic glycolipid αGalCer, on CD1d, alongside costimulatory (CD40L-CD40) and cytokine (IL-12) signals. NKT cells can indirectly promote anti-tumor immunity through release of cytokines (IFNγ, IL-4) which promote APC maturation as well as proliferation and lytic function of effector immune cells including NK cells and cytotoxic CD8+ T cells. C) NKT cells can inhibit immunosuppressive cells in the tumor microenvironment including Tregs, MDSCs, and M2-polarized TAMs which inhibit anti-tumor immunity through production of anti-inflammatory cytokines (IL-10, TGFβ), expression of inhibitory coreceptors (PD-L1), and other factors. NKT cells can produce pro-inflammatory cytokines to polarize TAMs towards an anti-tumorigenic M1 phenotype, inhibit suppressive functions of MDSCs, and directly lyse MDSCs and TAMs. Anti-tumorigenic Type I NKT cells and pro-tumorigenic Type II NKT cells cross-regulate each other by mechanisms that remain to be fully elucidated. Adapted from Nelson et al. [109] and McEwen-Smith et al. [110]. Figure created with BioRender.com.

1.4.3 Harnessing NKT cells as an immunotherapy

As mentioned previously, αGalCer is a potent activator of NKT cells. Structurally, αGalCer is composed of a galactose carbohydrate α-linked to a ceramide backbone comprised of a C26:0 acyl chain and 18-carbon phytosphingosine chain. The acyl chain and phytosphingosine fit into the A' and F' pockets of the CD1d binding groove, leaving the galactose carbohydrate exposed directly to the NKT cell which then recognizes it via its semi-invariant TCR [111]. Other synthetic αGalCer analogues have been developed with different bioactive properties and resistances to degradation that allow them to skew NKT cell responses to either more Th1 or Th2-dominant types [112]. These αGalCer analogues are still being tested in clinical and pre-clinical trials, and may represent a future direction for more precise activation of NKT cells in cancer [112,113].

Numerous clinical trials have been conducted attempting to harness the anti-tumor potential of NKT cells. Early trials activated endogenous NKT cells in patients by direct administration of free αGalCer [114]. In one of the first phase I trials conducted, direct administration of αGalCer was well-tolerated, with no dose-limiting toxicities observed in any of the 24 patients [114]. However, there were no clinical responses and biological effects were limited, with increased serum levels of TNF and GM-CSF in only 5/24 patients, and a transient decrease in peripheral blood NK cells in 7/24 patients [114]. These effects depended on pre-treatment NKT cell levels rather than αGalCer dosage, and authors noted that cancer patients had significantly lower NKT cell levels than healthy controls, which represents a potential obstacle in NKT cell immunotherapy [114]. Delivery of free αGalCer is now known to induce NKT cell anergy, as defined by reduced NKT cell function upon re-activation [115]. This is likely mediated by the ability of αGalCer to be

taken up and presented on a wide range of APCs, some of which, namely B cells, have been reported to induce greater anergy than professional APCs like DCs [63,92,115]. One study demonstrated that induction of NKT cell anergy in mice could be overcome through delivery of αGalCer through nanoparticles which targeted αGalCer to be preferentially taken up and presented by macrophages and DCs [116]. Subsequent clinical trials have delivered αGalCer pre-loaded on autologous patient-derived DCs. Clinical trials in several cancers, including multiple myeloma, lung cancer, and head and neck cancer, demonstrated that αGalCer-loaded-DCs were well tolerated with no serious adverse events [117,118,119,120]. Furthermore, αGalCer-loaded DC treatment successfully induced clinical responses, with increased IFNγ production and expansion of NKT cells noted as biological effects, which led to stable disease and increased median survival times [117,118,119,120]. Drawbacks to this approach include difficulties in obtaining sufficient autologous DCs from patients, as well as the continued dependence on baseline levels of NKT cells in often NKT-cell depleted cancer patients [121,122]. To counter these drawbacks, other clinical trials in lung cancer and advanced melanoma have adoptively transferred *ex vivo* expanded and activated NKT cells back into patients [99,123,124]. In these trials, adoptively-transferred NKT cells were again well-tolerated with minor adverse events, and successfully increased IFNγ production and overall numbers of circulating NKT cells, but overall clinical responses were limited [99,123,124]. One benefit of such an approach is that NKT cells could be relatively easily-adapted for allogenic cell transfer since they recognize non-polymorphic CD1d. In fact, a recent clinical trial has combined allogeneic NKT cells with gefitinib, an epidermal growth factor receptor (EGFR) inhibitor, in patients with advanced EGFR-mutated non-small-cell lung carcinoma (NSCLC) [125]. The

trial appears to be ongoing; however, a recent single case report described one patient who achieved a surgical opportunity and long-term survival in response to treatment [126]. NKT cell therapy has also been combined with chemotherapeutic agents in several clinical trials [127]. Other combination therapies, such as combination with oncolytic viruses and anti-PD-1 checkpoint blockade, appear promising in pre-clinical models of murine ovarian, breast, and pancreatic cancer, but have not been translated to clinical trial [128,129].

1.5 Oncolytic viruses

1.5.1 Overview of oncolytic virus therapy

Oncolytic viruses (OVs) are viruses that selectively infect and kill tumor cells [130]. This tumor-specific tropism is often a combination of natural and engineered selectivity. For example, viruses can be selected based on their preferential binding to entry receptors disproportionately displayed on tumor cells, or engineered to selectively bind to tumor-specific entry receptors [130]. Viruses are also able to exploit a variety of tumor cell survival mechanisms, such as inhibited apoptosis, hyperactive replication machinery, and defective antiviral machinery [130,131]. Cancer cells often downregulate key innate immune signaling pathways in order to become resistant to apoptosis and dysregulate cell cycle control [131]. For example, cancer cells can downregulate retinoic acid-inducible gene I (RIG-I) sensing of viral dsRNA [131]. They also downregulate transcription factors downstream of Toll-like receptor (TLR) signaling, including Interferon regulatory factor (IRF) 3 and IRF7, preventing induction of Type I IFNs IFNα and IFNβ [131]. In addition to this reduced induction of Type I IFNs, cancer cells also downregulate Protein kinase R (PKR) and Janus kinase (JAK)/signal transducer and activator of transcription proteins

(STAT) pathways, decreasing their responsiveness to Type I IFNs [131]. These and other mechanisms decrease the ability of cancer cells to detect and eliminate viruses, and improve viral replication within tumor cells.

OVs mediate anti-tumor effects through two related mechanisms: they are able to directly infect and lyse tumor cells, and stimulate local immunity via the release of factors that mediate the recruitment and activation of immune cells, which can precipitate systemic adaptive immune targeting of distant metastases [130,132]. Unlike many other cancer therapies, particularly immunotherapies, OV therapy can actually benefit from immunosuppressive tumor environments, which can slow otherwise rapid inactivation of the therapeutic virus by innate immune mechanisms [130]. Viral replication in tumor cells ultimately leads directly to tumor cell death via immunogenic cell death (ICD) pathways, including necrosis, pyroptosis, and autophagic cell death [130,133]. Immunogenic cancer cell death mobilizes danger associated molecular patterns (DAMPs), such as surface calreticulin exposure, and release of extracellular adenosine triphosphate (ATP), high-mobility group box 1 (HMGB-1), and uric acid. Viral pathogen-associated molecular patterns (PAMPs) are also released which can activate innate immune sensors in surrounding cells and lead to production of proinflammatory and immunostimulatory cytokines. ICD can also release novel tumor antigens that can be recognized by the immune system [130,133]. These pathways support recruitment and maturation of APCs such as DCs to stimulate the activation and proliferation of tumor antigen-specific CD4+ and CD8+ T cells, as well as the recruitment and activation of other immune subsets [130]. This increased activation and recruitment of tumor-specific immune populations can transform an immunosuppressed “cold” or immune-excluded tumor landscape into a hotter

immune-infiltrated tumor over time [16,134,135]. This ability of OVs to convert "cold" tumors into "hot" tumors could have even greater potential when combined with immunotherapies that rely on "hot" tumors for efficacy. Beyond this, OV-mediated immune activation has the potential to cause systemic anti-tumor immune responses and regression of distant non-injected tumor sites, as has been observed with T-VEC [32,33,34]. In addition to their ability to directly and indirectly target tumor cells themselves, oncolytic viruses are also able to target and destroy tumor vasculature while leaving normal vasculature intact, reducing tumor perfusion and leading to massive death of tumor cells well beyond limited sites of infection [136].

Interest in OV-based therapies was greatly bolstered by the 2015 approval in Europe and the USA, of T-VEC, a HSV-1 virus engineered to express the cytokine GM-CSF [32,137]. T-VEC preferentially replicates in tumor cells, and deletion of its ICP34.5 genes, which are involved in shutting off the host antiviral response, have improved its tumor-specific tropism and reduced its pathogenicity [34]. T-VEC can infect and lyse tumor cells directly, resulting in the release of tumor-derived antigens in an immunogenic fashion, which, along with its release of GM-CSF, can enhance antigen presentation and prime CD8+ T cell responses to enhance anti-tumor immunity [34]. In a phase III clinical trial, T-VEC led to complete resolution in almost 50% of injected melanoma tumors, and displayed systemic effects by initiating the resolution of 9% of distant non-injected metastatic tumors [33]. These results have been confirmed and bolstered by clinical use [34]. However, T-VEC has faced roadblocks in clinical use due to lack of education regarding the safety and logistics of T-VEC delivery amongst physicians as well as patients [34]. Melanoma tumors treated with T-VEC also frequently experience pseudoprogression, which can be

difficult to distinguish from true progression when deciding whether or not to continue treatment [130].

There are several other challenges faced by OV therapies more broadly. One is delivery – depending on delivery mechanism (for example, intravenous versus intratumoral), the inoculated virus may face significant barriers to disseminating within the tumor [130]. Intratumoral delivery strategies, however, limit OV targeting to tumors that are surface-accessible. Intravenous and intratumoral OV delivery may also have different safety profiles, as intravenous delivery may lead to broader dissemination of the virus. The cellular structure of the tumor itself may also pose a barrier. Dose is also difficult to control with delivery of live, replication-competent virus, and peak viral replication levels will depend on many factors [130]. Therapeutic efficacy may also be compromised by a host's pre-existing immunity against a viral vector, particularly if it is a common human virus, as is the case for adenovirus-based OVs and HSV-based OVs. Pre-existing antibodies may be able to neutralize an OV before it is able to invade tumors [131]. Development of antibodies against OVs even without a pre-existing immune response may limit the ability of OVs to function repeatedly. And, while the strong immune response elicited by OVs is beneficial for carrying out their broader anti-tumor effects, it may also enhance clearance of the virus and limit any further anti-tumor function [130]. Rates of clearance also vary between individual patients, making it difficult to generate standardized re-treatment strategies for patients.

Although T-VEC is the only oncolytic virus which has been clinically approved for use in North America, other oncolytic viruses have been approved in other regions. The oncolytic adenovirus H101 was approved in China in 2006, years before T-VEC, for

treatment of head and neck cancer, and Japan very recently approved the recombinant HSV-1-based Teserpaturev/G47Δ for glioma [138,139]. Numerous other oncolytic virus platforms are also being tested in clinical trials, including adenoviruses, vaccinia viruses, coxsackie virus, and vesicular stomatitis virus [130,140].

1.6 VSV

1.6.1 VSV overview

Vesicular stomatitis virus (VSV) is a bullet-shaped, enveloped, negative-sense RNA virus in the family *Rhabdoviridae* [141].There are two major serotypes of VSV: New Jersey (VSV-NJ) and Indiana (VSIV) [142,143]. Both serotypes are endemic to the United States as well as Central and South America [141]. The natural hosts for VSV include livestock animals, such as cattle and pigs, as well as their insect vectors [141]. Rare cases of human VSV infection have been documented, primarily in agricultural workers, where it has caused mild flu-like symptoms in adults, which have served to demonstrate that VSV is naturally not highly pathogenic [141]. Oncolytic VSV constructs have been derived from the Indiana serotype [142,143,144,145]. VSV has many properties which make it an appealing oncolytic platform, including a broad cell tropism, cell-cycle independent replication, inability to transform host cells, natural IFN sensitivity, and minimal pre-existing human immunity [141,146]. The 11-kilobase VSV genome encodes 5 genes: the nucleocapsid (N) protein, phosphoprotein (P), large polymerase (L), glycoprotein (G), and matrix (M) protein [141]. The VSV G protein mediates viral entry into cells by binding the low-density lipoprotein (LDL) receptor, which is widely-expressed on many cell types, including cancer cells, allowing VSV to be targeted to a wide range of cancers [141,147]. After viral entry into the cell, the VSV N protein associates with the P protein, a multifunctional

polymerase co-factor, and the L protein, an RNA dependent RNA polymerase (RdRp), to form the VSV ribonucleoprotein (RNP) complex which mediates transcription of viral mRNAs [141]. VSV N is also required for VSV genome replication and encapsidates newly-produced genomic RNA [141]. The VSV M protein is involved in several key viral functions including virion assembly, budding, and inhibition of host gene expression [143]. Importantly, the VSV M protein is involved in inhibiting the host cell's antiviral response, specifically by blocking the nuclear export of IFNβ mRNA [143]. To improve VSV's tropism for cancer cells, a VSV M mutant virus (of the Indiana serotype) was generated with a complete deletion of methionine 51 (M51) from its genome (VSV-ΔM51) [143]. The complete deletion, rather than mutation, of methionine 51, makes it considerably more difficult for VSV-ΔM51 to revert to wild-type, a factor which is important for its safety profile [143]. Crucially, this VSV-ΔM51 mutant is unable to replicate in Type I IFN-producing cells, but retains its ability to infect and kill tumor cells, which, as mentioned earlier, often possess defective Type IFN signaling mechanisms [143].

The VSV-ΔM51 mutant has since been broadly used as an oncolytic platform, and has seen success in a wide variety of cancer types, including pancreatic cancer, metastatic breast cancer, and ovarian cancer, as well as non-solid tumors [128,129,148]. VSV-ΔM51, like other oncolytic viruses, can mediate its anti-tumor effects by both direct tumor lysis of a wide range of cancer types, as well as enhancing the anti-tumor immune response [141,146,149]. Tumor cell oncolysis by VSV-ΔM51 has been documented to release DAMPs such as calreticulin, ATP, and HMGB-1, and induce CXCL10, indicating that VSV-ΔM51 is capable of inducing ICD [128]. VSV-ΔM51 has also been shown in CT26 colon

carcinoma to selectively destroy tumor vasculature, greatly increasing its capacity to kill even uninfected tumor cells [136].

VSV-ΔM51 has also been used as an oncolytic platform in clinical trials. A phase I trial (NCT03017820) used VSV-ΔM51 engineered to express IFNβ (VSV-IFNβ) to treat patients with relapsed refractory T cell lymphoma [150]. No dose-limiting toxicities were observed, and of the 7 patients enrolled 2 had partial responses lasting 3 and 6 months respectively, and one patient experienced an ongoing complete response [150]. The patient who responded completely experienced robust viral replication, high plasma IFN-β, a strong anti-VSV neutralizing antibody response, and increased numbers of tumor-specific T cells [150]. This study demonstrated potential for VSV monotherapy to induce clinical responses in patients, although patients were heavily-pretreated. VSV-IFNβ is now being tested in ongoing phase I/II clinical trials in combination with either chemotherapy or immune checkpoint inhibitors. Combined VSV-IFNβ with pembrolizumab (anti-PD-1) is being used to treat treatment-refractory head and neck squamous cell carcinoma and NSCLC (NCT03647163), and combined VSV-IFNβ with ruxolitinib phosphate (a JAK inhibitor) is being tested in endometrial cancer (NCT03120624).

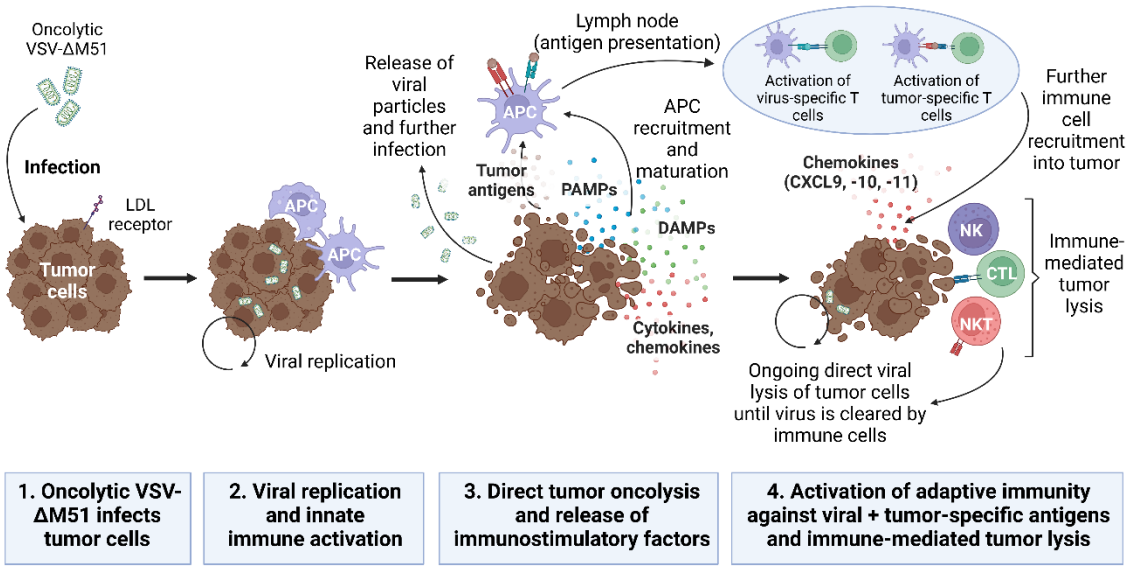

Figure 2. Mechanisms of oncolytic VSV-ΔM51-mediated tumor lysis. Oncolytic VSV-ΔM51 infects tumor cells using the LDL receptor for entry. VSV-ΔM51 infection leads to direct tumor oncolysis, resulting in the release of immunostimulatory molecules including PAMPs, DAMPs, cytokines, chemokines, and tumor antigens, alongside release of viral particles. Local APCs are recruited and activated by the products of tumor oncolysis, and present tumor and viral antigens to T and B cells in local lymphoid tissues, leading to activation of adaptive immunity against both tumor and viral products. This results in increased recruitment of both innate and adaptive immune cells to tumor sites and enhanced immune-mediated tumor lysis. Adapted from Peruzzi and Chiocca [151]. Created with BioRender.com.

1.6.2 FAST proteins

VSV-ΔM51 is amenable to genetic engineering, and has been engineered to express a variety of molecules to increase its virulence and immunogenicity [152,153]. This insertion occurs between the VSV-G and VSV-L genes. Among the molecules which VSV-ΔM51 has been engineered to express are reovirus fusion-associated small transmembrane (FAST) proteins, which allow VSV to spread by cell-cell fusion and enhance immunogenic tumor cell killing [154]. FAST proteins are non-structural accessory proteins derived from the *Reoviridae* genera *Orthoreoviruses* and *Aquareoviruses* [155]. FAST proteins are notable for several reasons: they are the smallest viral membrane fusion proteins (~100 to 200 amino acids), the only fusion proteins produced by non-enveloped viruses, and they induce cell-to-cell rather than virus-to-cell membrane fusion [155]. FAST proteins are promiscuous, and can fuse almost all cell types at neutral pH in a receptor-independent manner [155]. FAST proteins mediate the formation of syncytia: large multinucleated cells which arise as a result of cell-cell fusion. FAST proteins have been shown to contribute to the virulence of naturally fusogenic reoviruses by enhancing viral egress and viral spread [155].

The ability of FAST proteins to promiscuously fuse cells, including cancer cells, to form large syncytia which enhance virus dissemination and apoptosis, has made them appealing candidates to augment oncolytic virotherapy [156]. VSV-ΔM51 has been engineered to express several different FAST proteins, including reptilian reovirus p14; baboon reovirus p15; and p10 homologues encoded by avian reovirus (ARV) and Nelson Bay reovirus (NBV) [156]. VSV has also been engineered to express genetically modified FAST proteins. Recombinant p14endop15, which contains the ectodomain and

transmembrane domain of p14 and the endodomain of p15, was shown to induce greater cell fusion than either wild-type virus in QM5 quail fibrosarcoma cells (R. Duncan, unpublished data). A triple mutant of p14 (p14Δ) also induced greater cell-fusion than wild-type p14 in QM5 cells (R. Duncan, unpublished data). Of these VSV-FAST constructs, VSV-p14 has been shown to induce improved tumor regression and survival compared to VSV-ΔM51 in murine models of breast and colon cancer [154].

In a model of primary 4T1 breast cancer, treatment with VSV-p14 slowed tumor progression and increased survival significantly relative to VSV-GFP (VSV-ΔM51 expressing a green fluorescent protein (GFP) construct in the same location as p14), which had very limited impact on survival [154]. In a model of resected metastatic 4T1 breast cancer, VSV-p14 was able to target distant metastases and significantly reduce metastatic burden relative to VSV-GFP, and improved survival time in that model >30% over VSV-GFP [154]. VSV-p14 treatment also increased activation and infiltration of splenic and intratumoral CD4+ and CD8+ T cells compared to VSV-GFP, suggesting that p14 augmented the immunogenicity of VSV-ΔM51 to potentiate anti-tumor immunity [154]. Additionally, the biodistribution of VSV-p14 remained unchanged relative to VSV-GFP, suggesting that the enhanced ability of VSV-p14 to spread by cell-cell fusion did not negatively affect its safety profile [154]. In a model of 4T1 breast cancer, VSV-p15 was tested against VSV-p14 and shown to mediate significantly more potent anti-tumor effects, with a log lower dose of VSV-p15 mediating the same tumor regression and survival as a log higher dose of VSV-p14 [157].

1.7 Chemokines and their receptors

1.7.1 Chemokine overview

Chemokines are chemotactic cytokines that mediate immune cell trafficking and differentiation, amongst other functions. Chemokines are the largest family of cytokines, small (8-15 kDa) proteins which function primarily as soluble messengers of the immune system [158]. Chemokines are subdivided into 4 groups based on the location of the conserved cysteine (C) residues in their amino acid sequence: the CXC-chemokines, CC-chemokines, C-chemokines, and CX_3C-chemokines [158]. Chemokines bind chemokine receptors, which are seven transmembrane spanning G-protein coupled receptors (GPCRs) that are divided into 4 categories corresponding with the family of chemokines they bind. Chemokine receptors associate with intracellular G proteins, primarily Gαi, through which they signal [158]. Chemokine receptor signaling directs cell migration, adhesion, and various immune cell programs including immune polarization and release of immune mediators [158]. Many chemokines share redundant or overlapping functions, with several chemokines binding a single chemokine receptor, and receptors binding more than one chemokine ligand. Chemokines are produced by both immune and non-immune cells, either constitutively or in response to various immune signaling pathways.

In the context of the tumor microenvironment, chemokines can be produced by tumor cells, tumor stromal cells, and tumor-infiltrating immune cells [159]. Chemokines play key roles in recruiting immune cells to tumor microenvironments, as well as modulating the responses of these immune cells in the tumor microenvironment and coordinating interactions between immune cells [159]. Chemokines can also act on tumor cells themselves in both pro-and-anti-tumorigenic ways. There are numerous chemokine axes operating in cooperative and antagonistic ways in the tumor environment. For example, the CXCR4-CXCL12 axis is primarily pro-tumorigenic, mediating recruitment of several

immune populations including B cells, plasmacytoid DCs, Tregs, and Th17 cells, and can also promote angiogenesis, cancer cell proliferation, survival, and metastasis [159]. CCR9, which binds CCL25, can be expressed on cancer cells and can increase their chemotherapy resistance and metastatic potential [159]. CCR4-CCL20,CCR6-CCL20, and CCR5-CCL5 have been shown to recruit Tregs [159,160]. CCR2-CCL2 signaling can recruit macrophages, CD8+ T cells, and NKT cells, but can also have some negative effects, including CCL2-mediated promotion of metastasis [159,161]. CCR5 binds CCL3, -4, and -5 and is involved in recruitment of a variety of tumor-infiltrating subsets including myeloid cells, DCs, CD8+ T cells, NKT cells, and NK cells [159,162]. A final key player is CXCR3, which will be discussed below.

1.7.2 CXCR3 axis in cancer

The chemokine receptor CXCR3 binds the chemokines CXCL9, CXCL10, and CXCL11. This axis is crucial for orchestrating immune cell migration, activation, and polarization, and plays a key role in cellular anti-tumor immunity [163,164]. CXCR3 is an important marker of a Th1 immune response and can help drive differentiation of naïve CD4+ T cells into effector Th1 cells [164]. CXCR3 ligands CXCL9 (also known as monokine induced by gamma interferon, or MIG), CXCL10 (also known as Interferon gamma-induced protein 10, or IP-10), and CXCL11 (interferon-inducible T-cell alpha chemoattractant, or I-TAC) are, as their alternate names suggests, induced by IFN signaling, particularly IFNγ (for all three) and Type I IFNs IFNα and IFNβ (for CXCL10 and CXCL11) [164]. These chemokines are able to directly mediate anti-tumor effects by inhibiting tumor angiogenesis [164]. More important, though, are their roles in recruiting and localizing key anti-tumor immune populations in tumors. CXCR3 is expressed by a

variety of cell types, including monocytes, macrophages, and some cancer cells, but most importantly, activated cytotoxic CD8+ T cells, Th1 CD4+ T cells, NK cells, and NKT cells, populations which, as discussed previously, play key roles in anti-tumor immunity and whose infiltration into tumors is highly correlated with improved prognosis in numerous cancers.

CXCR3 expression on these tumor-infiltrating immune cells, particularly NK cells and CD8+ T cells, has been directly positively associated with improved prognosis in many cancers, including both pre-clinical and clinical melanoma [73,165,166]. While NKT cells also express CXCR3 and migrate in response to CXCR3 ligands [167], the role of CXCR3 in infiltration of NKT cells into tumors remains understudied. Increased CXCR3 expression has also been found to positively correlate with increased responsiveness to a variety of immunotherapies, including adoptive T-cell therapy and anti-PD-1 immune checkpoint blockade [69,165].

The mechanisms by which the CXCR3 axis mediates infiltration of key anti-tumor immune populations, as well as the efficacy of various immunotherapies, still remain to be fully elucidated, and may be complicated by tumor model and cell-type-specific differences in CXCR3-dependent immune cell recruitment. Recent findings are also beginning to highlight potential differences in chemokine requirements between early recruitment of lymphocytes in the early stages of tumor development, and subsequent recruitment of lymphocytes, including adoptively-transferred populations, into established tumors.

Work by Mikucki et al. [165] found a non-redundant requirement for the CXCR3 axis in trafficking of adoptively-transferred CD8+ T cells into tumors using both the B16-ovalbumin (OVA) model and human melanoma patient samples. Using competitive homing assays, they determined that loss of CXCR3 alone significantly abrogated intratumoral T cell infiltration, to the same extent as global blockade of chemokine receptor signaling (by pertussis toxin), despite the high expression of additional chemokine receptors CCR5 and CCR2 on tumor-infiltrating T cells [165]. The authors determined that CXCR3 was specifically mediating the transition to firm arrest during lymphocyte migration into tumor vessels, by binding CXCL9 and CXCL10 displayed on tumor vessel walls [165]. This finding suggested that the CXCR3 axis may play a critical role in mediating the efficacy of adoptive T-cell immunotherapy, for which the CCR5 and CCR2 axes were dispensable. An earlier paper by Wendel et al. [73] reported similar findings for NK cells. They found that $CXCR3^{-/-}$ mice had significantly reduced numbers of tumor-infiltrating NK cells in subcutaneous RMA-S lymphoma and B16-RAE-1ε melanoma tumors, and that adoptively-transferred $CXCR3^{-/-}$ NK cells also experienced significantly impaired trafficking into tumors [73]. Supplementation of tumors with exogenous CXCL10 or ectopic expression of CXCL10 on RMA-S cells increased intratumoral NK cell accumulation in a dose-dependent manner, slowing the rate of tumor growth and prolonging survival [73].

However, interpretations of this work have been complicated by others who have reported that CXCR3 may be playing a more complex role than described above. A paper by Chow et al. [69], looking not at trafficking of adoptively-transferred CD8+ T cells into tumors but responsiveness of endogenous CD8+ T cells to anti-PD-1 blockade, found

instead that CXCR3 was dispensable for the recruitment of these effector cells into tumors. Instead of competitive homing assays, they compared intratumoral infiltration of endogenous CD8+ T cells into MC38 colon adenocarcinomas on the C57BL/6 wild-type (WT) and CXCR3$^{-/-}$ backgrounds, and found comparable cell numbers and functionality, indicated by similar expression of cell surface molecules including PD-1, LAG-3, CD44, and inducible T-cell costimulator (ICOS) and similar cytokine expression profiles prior to anti-PD-1 treatment [69]. However, following treatment, intratumoral levels of CD8+ T cells were significantly higher in WT mice –but, this was not due to CXCR3-dependent differences in homing following treatment initiation [69]. Instead, CXCR3 on CD8+ T cells was playing a critical role in mediating their activation and proliferation during anti-PD-1 treatment, specifically through interactions with CXCL9-expressing CD103+-DCs, a population which has been noted by others to be crucial for intratumoral CXCL9 and -10 production [68,69]. The importance of the CXCR3 axis in mediating the positioning of CD8+ T cells in tissues, rather than their entry into tissues, has also been reported in models of viral infection [168]. Finally, they found that upregulating CXCR3 ligand expression within anti-PD-1-resistant AT-3 tumors using epigenetic modulators significantly enhanced expression of CXCL9 and CXCL10 and thus responsiveness to anti-PD-1 treatment [69]. This work still emphasizes a central role for CXCR3 in responsiveness to immunotherapies, but leaves questions about other chemokine axes which may cooperate with CXCR3 in tumor lymphocyte infiltration.

One other chemokine axis emerging as a potential key player in this recruitment of tumor-infiltrating lymphocytes is CCR5 (and its ligands CCL3, -4, and -5) [169]. CCR5 is expressed at high levels on tumor-infiltrating T cells, and has been variably associated

with intratumoral T cell infiltration and survival [165]. A paper by Dangaj et al. [169] found, in human and mouse models of ovarian cancer, that T cell infiltration required intrinsic tumor cell-derived CCL5 and was amplified by IFNγ-inducible, myeloid cell-secreted CXCL9. They found that constitutive CCL5 production by tumor cells early in tumor development recruited tumor-specific T cells which then recognized their cognate tumor antigens, triggering IFNγ release and activating tumor-associated macrophages and DCs to produce CXCL9 (and CXCL10), leading to an amplified second wave of CXCR3-mediated T cell recruitment [169]. This "multi-stage" infiltration was mirrored in another paper by Srivastava et al. [170], where they looked at CAR-T cell recruitment in a genetically engineered model of inducible lung adenocarcinoma. They found that initial recruitment of CAR-T cells to tumors was partially dependent on their expression of CCR5 and CXCR6, and that once the first wave of CAR-T cells infiltrated the tumor they produced IFNγ and stimulated inflammatory "M1" macrophages to express CXCL9 and CXCL10, initiating an amplified second wave of CXCR3-dependent CAR-T cell recruitment [170]. This mechanism is very similar to that reported by Dangaj et al., and highlights that recruitment of various immune populations into tumors may in fact involve the efforts of multiple chemokine axes working together [169]. These findings also have implications for NK and NKT cell trafficking into tumors, as NK cells (particularly the $CD56^{bright}$ population) as well as NKT cells can also co-express CCR5 and CXCR3 [162,167,171]. Earlier findings by Mikucki et al. [165] can potentially be understood in the context of multi-stage tumor lymphocyte recruitment posed by this later work, in that adoptively-transferred T cells are being delivered to established tumors, where CXCR3 appears to play a more critical role. In this context, these findings suggest that the

CXCR3 axis may play a particularly critical role in mediating the efficacy of adoptive T-cell immunotherapy, and potentially other therapies which aim to re-establish immune infiltration in non-inflamed tumors.

Ultimately, while these papers come to different conclusions regarding how the CXCR3 axis mediates immune cell migration and function, they all demonstrate its importance for responses to cancer immunotherapies, particularly in the expression of CXCR3 ligands in the tumor environment. This highlights again that strategies to boost expression of CXCR3 ligands could potentially benefit a variety of immunotherapies, especially as expression of these chemokines in tumor microenvironments appears to vary widely [165,172,173,174,175].

Within tumors, CXCR3 ligands can be produced by a variety of cell types. These chemokines are usually expressed at low levels under homeostatic conditions, but can be induced during inflammation, primarily in response to type I (IFNα, IFNβ) and type II IFN (IFNγ), through activation of STAT-1 and nuclear factor kappa B (NFκB) pathways [176]. IRF3 has also been shown to activate the CXCL10 promoter independent of IFN signaling, downstream of TLR and stimulator of interferon genes (STING) pathways [177]. Intratumoral DC subsets, particularly basic leucine zipper transcription factor ATF-like (BATF)-lineage CD103+ DCs, have been shown to be very important producers of CXCL9 and -10 in mice, as described above [68,69]. CD103+ DCs are a population of conventional DCs (cDCs) whose development is controlled by the transcription factor BATF3 [178]. CD103+ DCs are tissue-resident and are specialized to cross-present antigens to CD8+ T cells [70,178]. Their human counterpart are CD141+ DCs [70]. In a cancer context, tumor-infiltrating CD103+ DCs play an important role in presenting tumor antigens to

CD8+ T cells, and have been found to have a unique ability to transport intact antigens to tumor draining lymph nodes and prime tumor-specific CD8+ T cells there [70]. Various papers have noted that recruitment of BATF3-expressing DCs (mediated by CCR5-CCL4) is an important determinant of T cell inflammation and immunotherapy response in melanoma and other cancers [68,169]. Other myeloid populations in tumors are also able to contribute to expression of CXCR3 ligands, including TAMs, particularly activated inflammatory "M1" macrophages, whose production of CXCR3 ligands seems to be induced by IFNγ produced by infiltrating lymphocytes [169,170]. Profiling of pre-treatment human melanoma tumors revealed macrophages as the primary producer of CXCL10, with lesser contributions by DCs [174]. Tumor stromal cells, including endothelial cells and fibroblasts, can also secrete CXCL9, -10, and -11 under inflammatory conditions [176,179]. Finally, tumor cells themselves can also express CXCR3 ligands, and B16 melanoma cells have been reported to express CXCL9 and CXCL10 *in vitro* and *in vivo*, particularly when stimulated by therapeutic interventions [165,180]. Human primary and metastatic melanoma cells have also been found to produce CXCL9, -10, and -11 *in vivo* and *in vitro* [174,181]. Furthermore, one study found that B16 melanoma and MCA205 fibrosarcoma cells were able to shut off their CXCL9 production when grown *in vivo*, and that these CXCL9-deficient "escape" variants were more aggressive when re-transplanted into new hosts [39]. The authors found that these CXCL9-deficient tumor cell variants did not arise when grown in IFNγ-deficient or immune cell-deficient (RAG1/2$^{-/-}$) hosts, suggesting that loss of CXCR3 ligand production by cancer cells may be a means of immune escape [39]. Another study corroborated this in both murine and human ovarian cancer established in humanized mice, where they reported that epigenetic silencing

mechanisms repressed expression of CXCL9 and CXCL10 by tumor cells to evade primarily T cell-mediated anti-tumor immunity [38]. The silencing of CXCR3 ligand expression by cancer cells as a means of immune escape highlights the importance of this axis, particularly for immune-mediated cancer therapies.

Various strategies have been employed to increase the production of CXCR3 ligands within tumors. First, CXCR3 ligands have been directly administered in a variety of settings. In a model of renal cell carcinoma, intratumoral delivery of CXCL9 alongside systemic IL-2 reduced tumor growth and increased infiltration of CXCR3+ cells [182]. Intratumoral injection of CXCL10 additionally improved survival in a mouse model of lung carcinoma [183]. A variety of strategies have also directly exploited the IFN-inducible nature of CXCR3 ligands to upregulate them. Some of the earliest immunotherapies directly delivered IFNs, for example, adjuvant low-dose IFNα therapy, which in a clinical trial of stage II and III melanoma patients was able to upregulate CXCL10 levels over a sustained period of time [184]. Others have taken more sophisticated approaches, for example, using epigenetic modulators DZNeP and 5-AZA-dC to upregulate CXCL9 and -10 expression [69]**.** One interesting strategy focused not on upregulating CXCR3 ligands in tumors but preserving them from degradation [185]. The enzyme Dipeptidylpeptidase 4 (DPP 4) post-translationally processes several chemokines, including CXCL10, which it cleaves into an inactive form that serves as an antagonist for CXCR3 [185]. The authors repurposed a DPP 4 inhibitor in B16 melanoma tumors, to increase the levels of active intratumoral CXCL10, enhancing T cell infiltration as well as the efficacy of adoptive transfer and anti-PD-1 checkpoint blockade [185]. Other strategies, such as chemotherapy and radiation therapy, have been found to mediate some of their benefits through

upregulation of CXCR3 ligands [163,186,187]. Anthracyclines, a class of chemotherapeutic agents which mimic viral infection to stimulate RNA sensors in cancer cells, induce autocrine and paracrine production of Type I IFN, leading to enhanced CXCL10 production and infiltration of T cells to enhance anti-tumor responses [188]. But, rather than mimicking viral infection, why not go a step further and infect cancer cells with viruses that are able to mediate both direct viral oncolytic effects and indirectly stimulate CXCR3 ligand production to enhance immune cell infiltration into tumors? For these reasons, oncolytic viruses may represent a promising strategy, particularly in combination with other immunotherapies. Oncolytic viruses such as VSV-ΔM51 activate antiviral response pathways within the tumor microenvironment, including the tumor cells they are able to infect and lyse. Infection of 4T1 breast cancer cells with VSV-ΔM51 upregulated their expression of CXCL9, -10, and -11 highly significantly, suggesting that this may be one axis by which oncolytic VSV mediates its anti-tumor effects and possibly synergizes with other therapies, including NKT cell activation immunotherapy and anti-PD-1 checkpoint blockade [128,129].

But CXCR3 may also be a double-edged sword. Despite all of the positive associations between CXCR3 ligands and T cell infiltration, immunotherapy response, and overall prognosis, the CXCR3 axis has also been associated with poor prognosis in several cancer types [61,189,190,191]. Elevated CXCL9, -10, and -11 were negative indicators for overall survival and recurrence-free survival in non-metastatic renal cell carcinoma, and circulating CXCL9 has been associated with risk of lung cancer development [189,190]. Elevated CXCL10 has been associated with poor prognosis in pancreatic cancer, with multiple studies reporting a negative correlation between CXCL10 and survival time, and

one study reporting that CXCL10 expressed by pancreatic stromal cells recruited CXCR3+ Tregs [61,191]. Similarly, in ovarian carcinoma, it was found that CXCL10 expression recruited a unique population of CXCR3+ Tregs, which actually constituted the most prevalent Treg population in that cancer [62]. Another paper found that CXCL9, -10, and -11 upregulated expression of the immune checkpoint ligand PD-L1 on gastric cancer cells by activating the STAT and PI3K-Akt pathways, across numerous gastric cancer cell lines and patient tissues [192]. The angiostatic properties of CXCR3 ligands, while they may inhibit tumor proliferation by restricting blood flow and the delivery of key nutrients, may also restrict recruitment of immune cells by removing access points for immune cells to leave the circulation and migrate into tumors.

CXCR3 can also be expressed on tumor cells themselves, and several studies have implicated the CXCR3 axis in metastasis of CXCR3-expressing tumors, including colon cancer, gastric cancer, and melanoma [164,180,193,194,195]. In mouse models of these cancers, small molecule inhibitors of CXCR3, CXCR3 knockdown, and reduction of CXCR3 expression on tumor cells by antisense RNA, reduced metastasis to various organs [193,194,196,197]. Multiple studies have reported that murine B16 melanoma cells constitutively express CXCR3, and human metastatic melanoma cells have also been found to express CXCR3 regardless of the tissue from which they were removed [195,196,197]. Studies appear split between which CXCR3 ligands mediate these metastatic effects. One study found that co-expression of CXCL10 and CXCR3 was doubled in metastatic compared to primary human melanoma tumors [197]. They reported that autocrine CXCL10-CXCR3 signaling in B16 melanoma cells drove metastasis through regulation of cellular adhesion, invasion, and migration [197]. Another study found that

autocrine CXCL11-CXCR3 signaling via ERK1/2 promoted self-renewal and survival in hepatocellular carcinoma tumor-initiating cells [198]. A separate study found that production of CXCL9 by tumor endothelial cells was a major driver of human melanoma metastasis by accelerating melanoma-mediated transendothelial migration (TEM), a key step in the dissemination of tumor cells to form metastases [196]. These contradictory findings, which posit pro-tumorigenic as well as anti-tumorigenic roles for the CXCR3 axis are important to keep in mind when considering harnessing the CXCR3 axis in cancer therapy, particularly in cancers, like melanoma, which have been shown to express and perhaps exploit CXCR3.

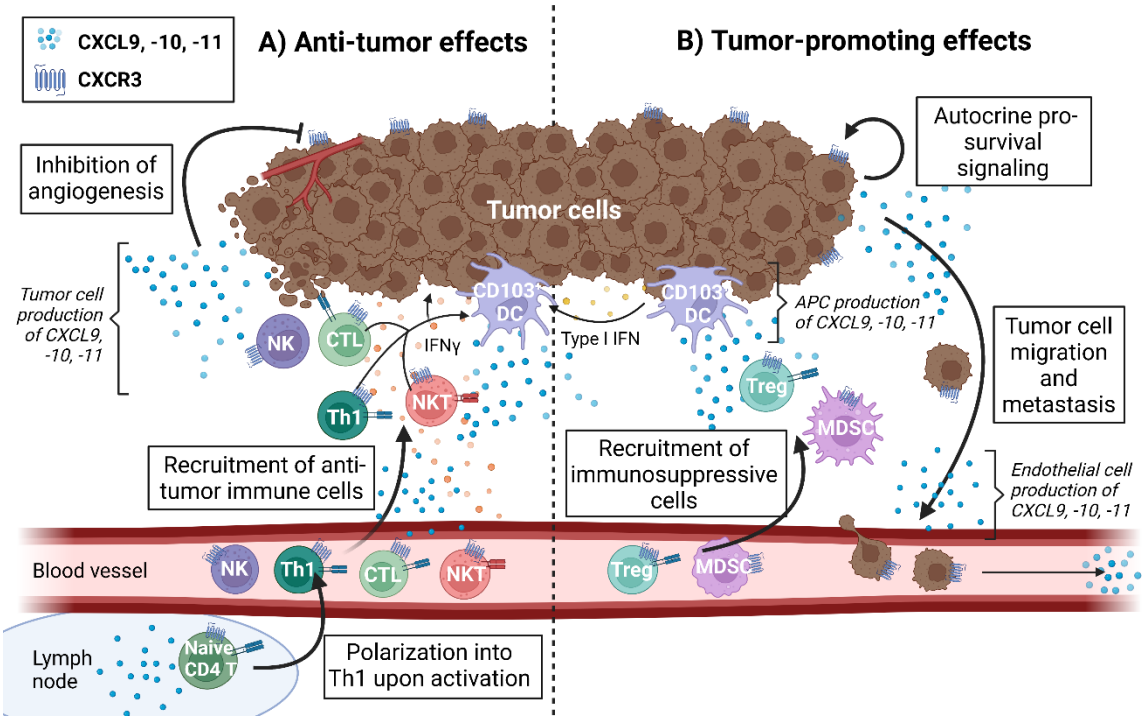

Figure 3. CXCR3 axis in cancer. CXCR3 ligands CXCL9, -10, and -11 can be produced in the tumor microenvironment by tumor cells, endothelial cells, and antigen-presenting cells such as CD103+ DCs. CXCL9, -10, and -11 production can be stimulated by Type I IFN produced by DCs and other cells in response to inflammatory signals, as well as IFNγ produced by immune cells including NKT cells, CD4 Th1 cells, and cytotoxic CD8+ T cells (CTLs). The CXCR3 axis has distinct anti-tumor and pro-tumorigenic effects. A) Anti-tumor effects mediated by the CXCR3 axis include recruitment of CXCR3-expressing anti-tumor immune cells such as NK cells, NKT cells, Th1 cells, and CTLs, as well as polarization of CD4+ T cells into Th1 effector cells. CXCL9, -10, and -11 can also directly inhibit angiogenesis and tumor neovascularization. B) The CXCR3 axis can promote tumorigenesis by recruiting CXCR3-expressing immunosuppressive subsets including Tregs and MDSCs. CXCR3-expressing tumor cells can also receive proliferative and pro-survival signals via autocrine CXCR3 signaling. CXCL9, -10, and -11 produced by endothelial cells can also drive migration and metastasis of CXCR3-expressing tumor cells. Figure created with BioRender.com.

Another nuance to be considered is the potential difference between CXCL9, -10, and -11. CXCL9, -10, and -11 expression is induced by different IFNs; all three are induced by IFNγ signaling, but only CXCL10 and CXCL11 are induced by Type I IFN signaling as well, which could affect the extent and context of their expression. CXCL9, -10, and -11 have also been shown to have different binding affinity for the CXCR3 receptor [164]. Certain models have demonstrated their redundancy; for example, a model of murine bronchiolitis found that deletion of CXCL9 or CXCL10 individually had no effect, whereas blockade of CXCR3 reduced airway damage [199]. In other contexts, CXCL9 and CXCL10 have been found to antagonize each other. In a murine cardiac transplant model, CXCL9 deficiency decreased the frequency of alloreactive CD8+ T cells, whereas CXCL10 deficiency increased their frequency in a manner that was CXCL9-dependent [200]. CXCL11 specifically has been shown to induce FoxP3+ Treg cells in a model of experimental autoimmune encephalomyelitis [60]. Many of the other studies described previously also highlight specifically one of CXCL9, -10, or -11 as the key mediator of either the anti- or pro-tumorigenic effects they describe. The non-redundant roles of CXCR3 ligands are likely dependent on context, including tissue and disease type, as well as spatial and temporal regulation of chemokine and receptor expression. These considerations should be taken into account in future investigations into the roles of CXCR3 and its ligands in various cancers.

Finally, there are also some structural differences between human and mouse CXCR3 which warrant consideration. In humans, there are three isoforms of CXCR3 (CXCR3A, CXCR3B, and CXCR3alt), whereas mice possess only one [164]. These different isoforms have been shown to activate different intracellular signaling pathways, which suggests

they possess different functions [164,201] . CXCR3A represents the classical CXCR3, and mediates immune cell chemotaxis and cell proliferation [163]. CXCR3B, which has a slightly extended N-terminus generated by alternative splicing, appears to have antagonistic functions including induction of cell apoptosis and inhibition of cell migration [163]. CXC3B can also bind CXCL4 in addition to CXCL9, -10, and -11 to mediate angiostasis [163]. CXCR3alt has a truncated C-terminus generated from exon skipping, and mainly mediates CXCL11 function [163]. The nuances of this variation are not able to be captured in murine models studying the CXCR3 axis. Additionally, the C57BL/6 mouse strain only produces functional CXCL9 and CXCL10, as it harbours a mutated CXCL11 gene that encodes an mRNA product with a single-nucleotide deletion in the 5' exon which targets it for nonsense-mediated mRNA decay [202]. Given this, models using B16 melanoma, which is derived from the C57BL/6 strain, are unable to interrogate the potential roles of CXCL11. However, a CRISPR/Cas9 system was recently used to correct this mutation on the C57BL/6 background, resulting in the production of functional CXCL11 [202]. Overall, the differences between the human and murine CXCR3 axis further complicate our ability to untangle the role of the CXCR3 axis in human cancer.

1.8 Thesis overview

Advanced melanoma is highly metastatic and resistant to traditional chemotherapies, resulting in a 5-year survival rate of <30% [1,24,203]. Recently, cancer immunotherapies have significantly improved patient outcomes, but their failure to fully resolve tumors highlights a need for new therapeutics [132]. Combined Natural Killer T (NKT) cell and oncolytic Vesicular stomatitis virus (VSV) therapy represent one promising approach.

Oncolytic VSV has been shown to enhance NKT cell infiltration into tumors, increasing the efficacy of subsequent NKT cell immunotherapy [128,129]. VSV infection increases the production of CXCR3 ligands in the tumor microenvironment, potentially recruiting NKT cells that highly express CXCR3; however, the specific role of the CXCR3 axis in overall treatment efficacy is unknown [128].

I hypothesized that VSV, by increasing expression of CXCL9, -10, and -11 in the tumor microenvironment, would enhance recruitment of CXCR3+ effector cells, including NKT cells, providing a basis for the synergistic combination of oncolytic VSV and NKT cell immunotherapies. I aimed to characterize VSV-mediated upregulation of CXCL9, -10, and -11 by B16 melanoma cells *in vitro*, determine the impact of the CXCR3 axis on the efficacy of VSV and NKT cell immunotherapies *in vivo,* and investigate the effect of the CXCR3 axis on the immune profiles of mice treated with VSV and NKT cell immunotherapies. Using the syngeneic B16-F10 melanoma model, responses to NKT cell immunotherapy, alone and in combination with recombinant VSV-ΔM51 constructs (VSV-GFP and VSV-p14), were tested in wild-type and $CXCR3^{-/-}$ C57BL/6 mice. Combined treatments modestly but significantly enhanced survival compared to monotherapies in in both cohorts. $CXCR3^{-/-}$ mice exhibited trends towards improved tumor regression and survival in response to VSV; however, survival and tumor growth were ultimately not significantly different between wild-type and $CXCR3^{-/-}$ mice across treatment groups. These results demonstrate that oncolytic VSV in combination with NKT cell immunotherapy provides superior survival benefit compared to monotherapies. The CXCR3 axis ultimately appeared dispensable in our combined therapy; however,

other factors such as reduced viral clearance and enhanced oncolytic activity may compensate for the loss of CXCR3.

CHAPTER 2: MATERIALS AND METHODS

2.1 *In vitro* work

2.1.1 Cell lines and culture

B16-F10 melanoma cells (RRID: CVCL_0159) and Vero kidney epithelial cells (RRID: CVCL_0059) were acquired from ATCC (Manassas, VA) and cultured at 37°C and 5% CO_2 in complete Dulbecco's Modified Eagle Medium (DMEM) (Corning, New York City, NY) supplemented with 10% fetal bovine serum (FBS) (Fisher-HyClone, Ottawa, ON) and 5% Penicillin-Streptomycin (100 μg/ml streptomycin, 100 units/ml penicillin) (Corning). For passaging and experimental preparation, cells were collected using trypsin-ethylenediamine-tetra acetic acid (EDTA) (Corning). Cells were resuspended in 1X phosphate-buffered saline (PBS) (Corning) for *in vivo* use.

2.1.2 VSV production

VSV-ΔM51 engineered to express green fluorescent protein (GFP) (VSV-GFP), VSV-p14, VSV-p15, VSV-p14endop15, and VSV-p14Δ were provided by Dr. Roy Duncan (Department of Microbiology and Immunology, Dalhousie University, Halifax, NS). Viruses were propagated and used until passage 4. To propagate virus, Vero cells were seeded in T175 flasks (Grenier Bio-One, Monroe, NC) and cultured at 37°C in 5% CO_2. Cells at 90% confluency were infected with VSV at multiplicity of infection (MOI) = ~0.1 for 2 hours followed by the addition of complete DMEM. After 48 hours, flasks were frozen at -80°C and then thawed at 37°C for two freeze-thaw cycles. After the second thaw, supernatant was collected and centrifuged at 300 g for 10 minutes to separate the cell pellet. Supernatant was then layered on a 20% sucrose (Fisher Scientific, Hampton, NH) cushion in ultracentrifuge tubes (Beckman Coulter, Brea, CA).

Ultracentrifuge tubes were balanced in a SW32 rotor (Beckman Coulter) and then spun in an Optima L-90K ultracentrifuge (Beckman Coulter) at 29000 rpm for 2 hours at 4°C. Pelleted virus was resuspended in 15% glucose (Fisher Scientific) and stored at -80°C. Viral titres were determined via plaque assay. UV-inactivated VSV (UV-VSV) was generated using a HL 2000 Hybrilinker (UVP Laboratory Products, Upland, CA) at 100 μJ/ cm^2 for 15 min. UV-VSV aliquots were subsequently stored at 4°C.

2.1.3 VSV plaque assays

Vero cells were seeded at $2x10^5$ cells per well in 12-well plates and infected 24 hours later once they reached ~100% confluency. Media was removed and 200 μL of serially diluted virus stock (10^{-7} to 10^{-12}) was added to individual wells in duplicate. After a 2-hour infection period, infection media was removed and 1 ml of 1% agarose overlay (4% agarose (Fisher Scientific) in complete DMEM) was added to each well. Plates were incubated upside-down at 37°C in 5% CO_2. After 48 hours, cells were fixed in 10% formaldehyde (Fisher Scientific) for 1 hour, followed by removal of the agarose overlay and staining with 1% crystal violet (Sigma Aldrich, St. Louis, MO). Plaques were counted and viral titre was determined using the following formula: viral titre = (average plaques in duplicate wells)/(inoculum volume x dilution factor).

2.1.4 *In vitro* infection assay

B16 melanoma cells were seeded in 100x20mm petri dishes at $2x10^6$ cells per dish in complete DMEM and cultured at 37°C in 5% CO_2. After 24 hours, B16 cells at ~95% confluency were infected at a MOI of ~1 in serum-free DMEM using UV-VSV, VSV-GFP, VSV-p14, VSV-p15, VSV-p14endop15, or VSV-p14 Δ. Infections were stopped

after 2 hours by the addition of complete DMEM, and cells and supernatant were collected after 24 hours for downstream analysis.

2.1.5 Quantitative PCR

B16 melanoma cells were collected 24 hours after infection with UV-VSV, VSV-GFP, VSV-p14, VSV-p15, VSV-p14endop15, orVSV-p14Δ. RNA extraction was performed using TRIzol (Fisher Scientific) and chloroform (Fisher Scientific) for phase separation followed by use of an RNeasy Plus Mini Kit (Qiagen, Dusseldorf, Germany) to precipitate the RNA according to the manufacturer's instructions. RNA concentration and purity were measured using an Epoch Plate Reader (BioTek, Winooski, VT). Prior to reverse transcription, the RNA was confirmed to not be degraded by loading 500 ng samples into a 1% agarose (VWR Life Sciences, Mississauga, ON) ethidium bromide (Fisher Scientific) gel (run at 93 V for 50 minutes). One microgram of RNA was reverse transcribed using the Advanced cDNA Synthesis Kit (Wisent Bio Products, Saint-Jean-Baptiste, QC) using a Mastercycler X50 (Eppendorf, Hamburg, Germany) thermocycler. The resulting cDNA was analyzed by real-time quantitative polymerase chain reaction (RT-qPCR), performed on a CFX96 Real Time System C1000 Touch Thermocycler (Bio-Rad, Hercules, CA) using 4 μL cDNA and PowerTrack SYBRGreen (Applied Biosystems, Waltham, MA). Primers were purchased from Invitrogen (Waltham, MA). Primers used were as follows:

Table 1. Primers used for quantitative PCR

Gene	Forward Primer	Reverse Primer
gapdh	5'-TGCACCAACTGCTTAG-3'	5'-GGATGCTGGGATGATGTTC-3'
actβ	5'-CATTGCTGACAGGATGCAGAAGG-3'	5'-TGCTGGAAGGTGGACAGTGAGG-3'

Gene	Forward Primer	Reverse Primer
ppia	5'-CATACAGGTCCTGGGATCTTGTC-3'	5'-AGACCACATGCTTGCCATCCAG-3'
cxcl9	5'-TGGGCATCATCTTCCTGGAG-3'	5'-CCGGATCTAGGCAGGTTTGA-3'
cxcl10	5'-CCTCATCCTGCTGGGTCTG-3'	5'-CTCAACACGTGGGCAGGA-3'
cxcl11	5'-CGAGATGAAAGCCGTCAA-3'	5'-TATGAGGCGAGCTTGCTTGG-3'
cxcl16	5'-CAACCCTGGGAGATGACCAC-3'	5'-CTGTGTCGCTCTCCTGTTGC-3'
cxcl2	5'-GGCTGTTGTGGCCAGTGAA-3'	5'-GCTTCAGGGTCAAGGCAAA-3'
ifn-α2	5'-CCCTATGGAGATGACGGAGA-3'	5'-GCTGCATCAGACAGCCCTGCAGG T C-3'
tnf	5'-CACGTCGTAGCAAACCACCA AGTGGA-3'	5'-TGGGAGTAGACAAGGTACAACCC-3'
tgf-β2	5'-TAAAATCGACATGCCGTCC-3'	5'-GAGACATCAAAGCGGACGA-3'

Primer pairs were optimized by temperature gradient and standard curve analysis, and reference gene stability was calculated using the CFX Maestro Reference Gene Selection Tool (Bio-Rad). Primer performance was validated by melting curve analysis. RT-qPCR was run at 60°C (*gapdh, ppia, actβ, cxcl9, cxcl10, cxcl11, cxcl2, tnf*), 62.5°C (*cxcl16, ifn-α2*), or 56°C (*tgf-β*) for 40 cycles. Results were analyzed using CFX Maestro software. Relative gene expression was calculated using the Pfaffl method [204] and normalized to *gapdh, actβ,* and *ppia* reference genes.

2.1.6 ELISA

Culture supernatant was collected 24 hours after B16 cell infection with UV-VSV, VSV-GFP, VSV-p14, VSV-p15, VSV-p14endop15, or VSV-p14 Δ. CXCL9 and CXCL10

production were measured using DuoSet Mouse CXCL9 and Mouse CXCL10 enzyme-linked immunosorbent assay (ELISA) kits (R&D Biosciences, Minneapolis, MN) as per manufacturer instructions. 96-well ELISA plates were coated with CXCL9 or CXCL10 capture antibodies diluted in PBS overnight at 4°C. Plates were washed in 1X Wash Buffer (R&D Biosciences) in PBS and blocked with 1X reagent diluent (1% BSA solution in PBS) for 2 hours at room temperature before addition of experimental samples and CXCL9 or CXCL10 standard (1:2 serial dilution in 1X reagent diluent) in duplicate. The CXCL10 standard in the kit was substituted with recombinant murine CXCL10 protein (PeproTech, Rocky Hill, NJ) due to poor performance. Following an overnight incubation at 4°C, plates were washed again, followed by addition of CXCL9 or CXCL10 detection antibodies (in 1X reagent diluent). After a 2-hour incubation, plates were washed, and 1X streptavidin-horseradish peroxidase (in reagent diluent) was added and incubated for 20 minutes in the dark. Plates were washed and substrate solution (o-phenylenediamine dihydrochloride) was added for 15 mins followed by 2N sulfuric acid stop solution. Absorbance was measured at 450nm using an Epoch microplate spectrophotometer (BioTek) and concentration of experimental samples was quantified relative to standard curves.

2.2 *In vivo* work

2.2.1 Mouse strains

Male and female C57BL/6 mice were purchased from Charles River Laboratories (Wilmington, MA). CXCR3$^{-/-}$ mice (RRID:IMSR JAX:005796) were obtained from the Jackson Laboratory (Bar Harbor, ME) and bred at the Carleton Animal Care Facility at Dalhousie University. Mice were enrolled in experiments from 8 to 12 weeks of age.

Experimental protocols were approved by the University Committee on Laboratory Animals following the guidelines of the Canadian Council on Animal Care.

2.2.2 Subcutaneous B16 melanoma model

B16 cells ($2.5x10^5$ in 100 µL PBS) were implanted subcutaneously into the lower abdomen of 8- to 12-week-old WT or $CXCR3^{-/-}$ C57BL/6 mice. Tumors were measured every other day using electronic calipers and tumor volume was calculated using the formula ($width^2$ x length)/2. Mice received intratumoral (i.t.) or intravenous (i.v.) injections of VSV-GFP or VSV-p14 ($5x10^8$ plaque forming units (PFU) in 50 µL PBS) on days 9, 11, and 13 following tumor inoculation. Mice received free αGalCer (KRN7000; DiagnoCine, Hackensack, NJ) (4 ug in 30 µL PBS delivered intraperitoneally (i.p.)) or αGalCer loaded on bone-marrow derived DCs ($6x10^5$ cells in 100 µL PBS delivered i.v.) on day 14 to activate and expand NKT cells *in vivo*. For tumor growth experiments, mice were monitored for tumor volume and survival until humane endpoints (tumor volume exceeding $1500mm^3$ or other signs of morbidity such as lethargy, weight loss, dehydration status, and lowered body temperature) were reached. For immune profiling experiments, mice were sacrificed on day 19 for tissue harvest. To assay VSV via plaque assays, mice were sacrificed following VSV treatment on days 14, 15, and 16.

2.2.3 Generation and αGalCer-loading of bone marrow-derived DCs

WT and $CXCR3^{-/-}$ C57BL/6 mice were anesthetized with inhaled isoflurane (Fresenius Kabi, Bad Homburg, Germany) and sacrificed via cervical dislocation. Under sterile conditions, bone marrow was extracted from the femurs and tibias of mice, flushed through a 40-micron cell strainer (Corning) and pelleted by centrifugation at 300 g for 10

minutes. Cells were resuspended in complete Roswell Park Memorial Institute (RPMI)-1640 (Corning) (10% FBS, 50 μM beta-mercaptoethanol, 2 mM L-glutamine, 1X non-essential amino acids, 1mM sodium pyruvate, 100 μg/mL streptomycin, and 100 units/mL penicillin) with 40ng/mL of murine GM-CSF (PeproTech) and 10ng/mL of murine IL-4 (Peprotech) and cultured in 6-well plates at 37°C and 5% CO_2. Fresh complete RPMI-1640 with 40 ng/mL GM-CSF and 10 ng/mL IL-4 was added on day 3. On day 6, non-adherent cells were collected and re-suspended in complete RPMI-1640 with 20 ng/mL GM-CSF. On day 7, αGalCer was sonicated for 20 minutes at 50°C in a Branson 2510 Ultrasonic Cleaner and then added to each well at a concentration of 0.4 μg/mL. On day 8, adherent and non-adherent DCs were collected and resuspended in PBS at a concentration of $6x10^5$ cells/100 μL for i.v. delivery into mice to induce NKT cell activation.

2.2.4 Cell isolation

On day 19 following B16 tumor implantation, mice were sacrificed for immune profiling. Spleens and tumors were harvested and cells were isolated by mechanical dispersion through 70-micron wire mesh with 2% FBS in PBS. Splenic red blood cells were lysed in 5 ml of lysis buffer (150 mM NH_4Cl (Sigma-Aldrich), 10 mM $KHCO_3$ (J.T. Baker, Montreal, QC), and 0.1 mM EDTA (Sigma-Aldrich)) for 5 minutes, followed by addition of an equal volume of 2% FBS in PBS to inhibit further lysis. Spleen and tumor cells were pelleted by centrifugation at 300 g for 10 minutes at 4°C. Tumor lymphocytes were isolated by density centrifugation through a 33% Percoll gradient (GE Healthcare, Baie d'Urfe, QC) at 700 g for 20 minutes. Cells were resuspended in 2% FBS in PBS and counted using a hemocytometer.

2.2.5 Antibodies and flow cytometry

The following antibodies were purchased from Biolegend (San Diego, CA) or eBioscience (San Diego, CA): Brilliant Violet 450 conjugate-labeled fixable viability dye; Brilliant Violet 510 conjugate-labeled CD19 (clone 6D5); Brilliant Violet 605 conjugate-labeled CD8α (clone 53-6.7); Brilliant Violet 650 conjugate-labeled CD25 (clone PC61) and CD11b (clone M1/70); Brilliant Violet 785 conjugate-labeled PD-1 (clone 29F.1.A12) and CD44 (clone IM7); fluorescein isothiocyanate-labeled TCRβ (clone H57-597) and Ly6C (clone HK1.4); phycoerythrin-labeled Ly6G (clone 1A8) and FoxP3 (clone FJK-16s); peridinin-chlorophyll-protein complex: Cy5.5 conjugate-labeled NK1.1 (clone PK136) and F4/80 (clone BM8); phycoerythrin Cy-7 tandem conjugate-labeled CD45 (clone 30-F11); allophycocyanin-labelled CD80 (clone 16-10A1), CD69 (clone H1.2F3), and CD62L (clone MEL-14); Alexa Fluor 700-labelled CD4 (clone RM4-5) and MHC II (clone M5/114.15.2); allophycocyanin-eFluor 780-labelled CD69 (clone H1.2F3) and CD11c (clone N418). The NIH Tetramer Core Facility (Atlanta, GA) provided allophycocyanin-labeled and phycoerythrin-labeled CD1d tetramers loaded with the synthetic glycolipid PBS57.

Tumor or spleen cells were added to 5 mL polystyrene tubes (10^6/tube). Cells were washed in 2% FBS in PBS and stained for 30 minutes at 4°C with Brilliant Violet 450 conjugate-labelled fixable viability dye (1:1000 in PBS). Cell surface antibody panels were diluted 1:300 in Super Bright Complete Staining Buffer (Invitrogen). After additional washes with 2% FBS in PBS, cells were stained with cell surface antibody panels for 30 minutes at 4°C in the dark. Cells were then washed, fixed in 2% paraformaldehyde (Fisher Scientific) for 20 minutes, rinsed in 2% FBS in PBS, and

resuspended in a final volume of 300 μL 2% FBS in PBS. Cells were stored at 4°C in the dark for up to two days before analysis. Acquisition was performed with the FACSCelesta using FACSDiva software (BD Biosciences, San Jose, CA). Analysis was performed using FloJo (v10.6) software (BD Biosciences).

2.2.6 Intracellular staining

Cells receiving intracellular staining with phycoerythrin-labeled FoxP3 (clone FJK-16s) were washed three times in Fixation/Permeabilization buffer (Invitrogen) following cell surface antibody staining, and then permeabilized in Fixation/Permeabilization buffer for 40 minutes. Cells were then washed in 1X Permeabilization buffer (Invitrogen) and incubated for 1 hour at 4°C with phycoerythrin-labeled FoxP3 (clone FJK-16s) diluted 1:200 in in 1X Permeabilization buffer. Samples were then fixed and analyzed as described above.

2.2.7 VSV plaque assays from tumor lysates

Wild-type and CXCR3$^{-/-}$ C57BL/6 mice were implanted with B16 cells and either left untreated or treated with VSV-p14 as described above. On days 14, 15, and 16, B16 tumors were harvested under sterile conditions and weighed. Tumor cells were then isolated by mechanical dispersion through 70-micron wire mesh (Gerard Daniel Worldwide Ltd., Mississauga, ON) and pelleted by centrifugation at 300 g for 10 minutes at 4°C. Tumor cells were then lysed by homogenization with a Fisher Scientific PowerGen 125 homogenizer for 2 minutes. Tumor lysates were filtered through a 40-micron filter and resuspended in 1 mL PBS. Vero cells were seeded at 2x10^5 cells per well in 12-well plates and grown overnight to~100% confluency. Cells were infected with 200 μL of tumor lysate (10^{-1} and 10^{-2} dilutions in PBS). After a 2-hour infection

period, the infection media was removed and 1ml of 1% agarose overlay (4% agarose in complete DMEM) was added to each well. Plates were incubated upside-down at 37°C in 5% CO_2. After 48 hours, cells were fixed and stained with crystal violet to visualize plaques as described above. Plaques were counted and viral titre/tumor weight (g) was determined using the following formula: viral titre/g = (average plaques in duplicate wells/(inoculum volume x dilution factor))/tumor weight.

2.3 Statistical tests

Data analysis and statistical tests were carried out using GraphPad Prism (version 8.4.3). Data are expressed as mean ± standard error of the mean (SEM). Statistical significance is set at $p<0.05$. Survival data were analyzed by a log-rank (Mantel-Cox) significance test. All other data was tested for normality using the Shapiro-Wilk test. Tumor flow cytometry data met the assumption of normality (Shapiro-Wilk Test $p>0.05$) and was analyzed using a 2-way analyses of variances (ANOVA) with mouse strain (WT, $CXCR3^{-/-}$) and treatment (untreated, VSV-p14, αGalCer-loaded DCs, free αGalCer, VSV-p14 + αGalCer-loaded DCs, VSV-p14 + free αGalCer) as the between-group factors. Tumor plaque assay data also met the assumption of normality and was analyzed using a 2-way ANOVA, with mouse strain (WT, $CXCR3^{-/-}$) and treatment (untreated, VSV-p14) as the between-group factors. If the 2-way ANOVA was significant ($p<0.05$), Tukey's multiple comparisons test was performed to maintain the alpha error rate at 0.05. qPCR and ELISA data did not meet the assumption of normality (Shapiro-Wilk Test $p<0.05$) and were analyzed using the nonparametric Kruskal-Wallis test. A non-parametric two-tailed Mann-Whitney U test was used to compare between two data

groups, whereas comparisons between more than two data groups were made using a Kruskal-Wallis non-parametric analysis of variance with Dunn's post-test.

CHAPTER 3: RESULTS

3.1 Oncolytic VSV stimulates tumor cells to produce CXCR3 ligands

3.1.1 VSV infection upregulates production of CXCR3 ligands by B16 melanoma cells *in vitro*

Previous work has established that VSV-ΔM51 infection can upregulate production of CXCR3 ligands CXCL9, -10, and -11 in a mouse model of breast cancer [128]. Given the importance of immune cell infiltration into tumors for prognosis, and the fact that many key anti-tumor immune cell subsets, including CD8 + T cells, NK cells, and NKT cells, express CXCR3 on their surface and migrate towards sites where CXCL9, -10, and -11 are produced [163,164], we sought to determine whether infection with oncolytic VSV-ΔM51 expressing GFP (VSV-GFP) and various VSV-FAST constructs (VSV-p14, VSV-p15, VSV-p14endop15, VSV-p14Δ) would stimulate murine B16-F10 melanoma cells to produce these CXCR3 ligands. This could potentially improve tumor immune infiltration to make B16 tumors "hotter" [98,163,164].

As a reminder, B16 melanoma cells are derived from the C57BL/6 mouse background, which carries a mutation in the CXCL11 gene that results in a single-nucleotide deletion targeting the mRNA for nonsense-mediated decay [202]. Therefore, CXCL11 mRNA should be detectable in B16 melanoma cells but there will be no translation of a protein product.

To establish the ability of VSV to induce CXCR3 ligand expression in this tumor model, B16 cells were cultured *in vitro* with media alone, UV-VSV, or the different VSV-FAST constructs described above at a multiplicity of infection (MOI) of 1. Cells and

supernatant were harvested 24-hours post-infection for gene expression analysis by RT-qPCR and protein expression analysis by ELISA.

Messenger RNA (mRNA) expression of CXCL9, -10, and -11 was significantly upregulated in B16 cells at 24 hours by VSV-GFP, VSV-p14, VSV-p15, VSV-p14endop15, and VSV-p14Δ infection relative to UV-VSV and media controls (Figure 4A). Protein secretion of CXCL9 and CXCL10 were also significantly upregulated at 24 hours by B16 cells infected with each of these VSV constructs (Figure 4B). The inability of UV-VSV to induce comparable levels of CXCR3 ligands suggests that active infection is required to drive this expression rather than simply exposure to potential viral PAMPs, in line with previous reports [128]. There were differences between VSV constructs in terms of their capacity to induce each CXCR3 ligand; however, no clear patterns were observed across chemokines, and the variation between constructs did not exceed a log difference. Ultimately, active infection with VSV-GFP and VSV-FAST constructs resulted in significant upregulation of both CXCL9, -10, and -11 mRNA expression as well as secretion of high levels of CXCL9 and CXCL10 by B16 cells, in line with results previously generated in a model of 4T1 breast carcinoma [128]. These results indicate a potential axis by which VSV infection of B16 tumor cells may improve subsequent anti-tumor immune responses.

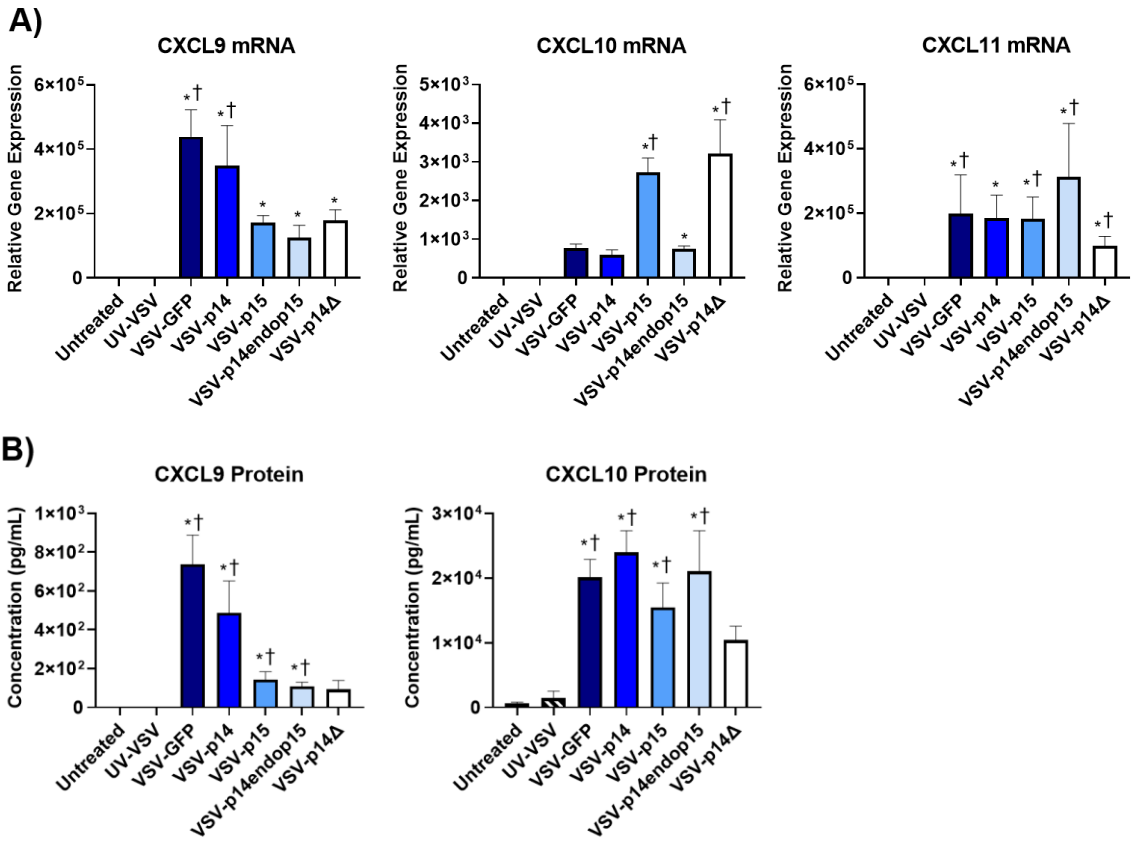

Figure 4. Oncolytic VSV infection increases expression and production of CXCL9, CXCL10, and CXCL11 by B16 melanoma cells *in vitro*. $2x10^6$ B16 cells were infected at MOI=1 for 2 hours. Cells and supernatant were harvested at 24-hours post-infection for downstream RT-qPCR and ELISA. A) Relative mRNA expression of *cxcl9*, *cxcl10*, and *cxcl11* from B16 melanoma cells infected with UV-VSV, VSV-GFP, VSV-p14, VSV-p15, VSV-p14endop15, or VSV-p14Δ. Relative gene expression is normalized to media-only untreated control. Gene expression was calculated using the Pfaffl method and normalized to *gapdh*, *actb*, and *ppia* reference genes. B) Protein expression of CXCL9 and CXCL10 from B16 melanoma cells infected with UV-VSV, VSV-GFP, VSV-p14, VSV-p15, VSV-p14endop15, or VSV-p14Δ. Error bars represent mean ± SEM for n=7-12. *p<0.05 vs. untreated, †p<0.05 vs. UV-VSV.

3.1.2 VSV infection upregulates expression of additional cytokines and chemokines by B16 melanoma cells *in vitro*

I also assessed whether VSV infection of B16 melanoma cells increased their expression of additional chemokines CXCL2 and CXCL16, as well as cytokines TNF, IFNα, and TGFβ. These chemokines and cytokines were chosen for their important roles in cancer and immune cell recruitment. CXCL2, which binds CXCR2, is important for neutrophil chemotaxis and has also been implicated in cancer cell proliferation and metastasis [205,206]. CXCL16 binds CXCR6 and mediates recruitment of NKT cells in various contexts, including cancer, but has also been implicated in pro-tumorigenic effects including driving angiogenesis, tumor cell metastasis, and recruitment of immunosuppressive subsets including TAMs, MDSCs, and Tregs [207]. TNF is an important pro-inflammatory cytokine in many contexts – initially named for its ability to directly induce tumor necrosis when administered in high amounts, it has since been revealed to have a more complex role in cancer, including constitutive production by tumor cells to drive pro-tumorigenic inflammation [208]. IFNα is another pro-inflammatory cytokine which plays a key role in antiviral responses and can drive production of CXCL9, -10, and -11 [209]. Finally, TGFβ is an anti-inflammatory and fibrotic cytokine which can be produced by tumor cells as well as regulatory immune cells to induce an immunosuppressive tumor microenvironment [210].

B16 melanoma cells were infected with VSV constructs and harvested 24 hours post-infection for gene expression analysis by RT-qPCR. Of the cytokines assessed, TNF mRNA was highly upregulated at 24 hours (>1000-fold expression relative to media control) in response to infection with VSV-GFP, VSV-p14, VSV-p15, VSV-p14endop15,

or VSV-p14Δ, although this upregulation was not significant relative to media or UV-VSV controls for VSV-p14, and only significant relative to both media and UV-VSV for VSV-p15 and VSV-p14Δ (Figure 5). TGFβ, CXCL2, and CXCL16 were also upregulated (<1000-fold expression) (Figure 5) For TGFβ, this upregulation was only significant (relative to media and UV-VSV controls) for VSV-p15. For CXCL2, upregulation was only significant relative to controls for VSV-p15and VSV-p14Δ. For CXCL16, only VSV-p15 and VSV-p14endop15 significantly upregulated expression. IFNα mRNA was increased significantly only in response to VSV-p15 and VSV-p14 Δ (Figure 5). Overall, VSV constructs induced variable expression of immune-modulating cytokines and chemokines by B16 cells *in vitro*.

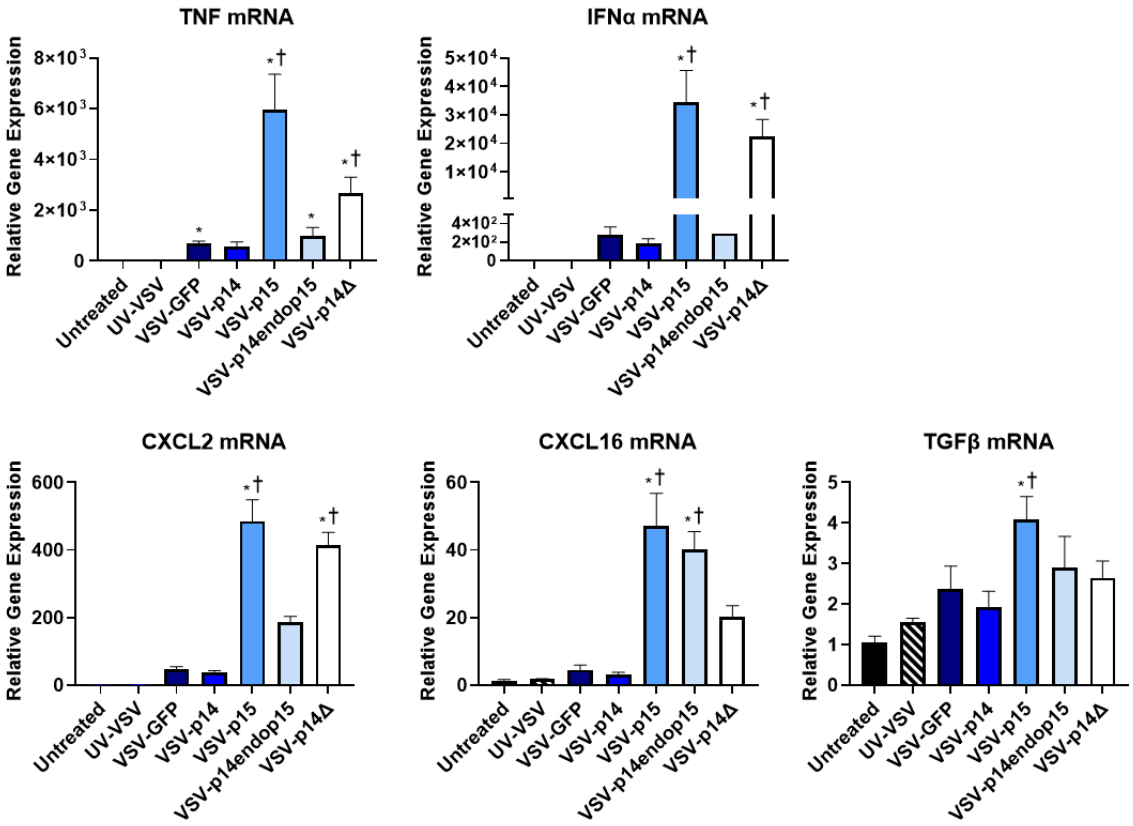

Figure 5. Oncolytic VSV infection increases expression of additional cytokines and chemokines by B16 melanoma cells *in vitro*. 2x10^6 B16 cells were infected at MOI=1 for 2 hours. Cells and supernatant were harvested at 24-hours post-infection for downstream RT-qPCR. Relative mRNA expression of *tnf, ifnα, tgf-β, cxcl16, and cxcl2* from B16 melanoma cells infected with UV-VSV, VSV-GFP, VSV-p14, VSV-p15, VSV-p14endop15, or VSV-p14Δ. Relative gene expression is normalized to media-only untreated control. Gene expression was calculated using the Pfaffl method and normalized to *gapdh*, *actb*, and *ppia* reference genes. Error bars represent mean ± SEM for n=3-8. *p<0.05 vs. untreated, †p<0.05 vs. UV-VSV.

3.2 CXCR3 is dispensable for responses to VSV and NKT cell activation therapies

3.2.1 Combined VSV-GFP and NKT cell activation cause greater tumor regression and increased survival than monotherapies in both WT and CXCR3$^{-/-}$ mice

Given the ability of VSV to upregulate expression of CXCR3 ligands in B16 melanoma cells *in vitro*, as well as the importance of CXCR3 for migration of anti-tumor immune populations into tumors, I investigated the impact of CXCR3 on responsiveness to VSV and αGalCer-loaded DC therapies both separately and in combination in mice harbouring B16 melanoma tumors. Wild-type (WT) and CXCR3$^{-/-}$ C57BL/6 mice were inoculated subcutaneously (sc.) with 2.5x10^5 B16 cells to establish tumors. Mice were then treated with intratumoral VSV-GFP 9, 11, and 13 days after tumor inoculation. NKT cells were activated on day 14 by intravenous administration of 6x10^5 αGalCer-loaded DCs (Figure 6A). Mice were monitored for tumor growth and survival.

Combination VSV-GFP and αGalCer-loaded DC therapy was the most effective at inducing temporary tumor regression, slowing tumor growth, and prolonging median survival duration in both WT and CXCR3$^{-/-}$ cohorts (Figure 6B-C). VSV-GFP was the second-most effective, and one VSV-GFP treated mouse in each of the WT and CXCR3$^{-/-}$ cohorts experienced complete tumor regression and survived past the study endpoint without tumor regrowth (Figure 6B-C). Despite this robust response in one mouse in each cohort, overall responses to VSV-GFP monotherapy were more variable in both WT and CXCR3$^{-/-}$ mice compared to combination therapy, which induced the most consistent responses and greatest overall increase in median survival duration (Figure 6B-C). αGalCer-loaded DCs were least effective as a monotherapy, although they still induced some tumor regression and improved survival duration relative to the untreated cohorts

(Figure 6B-C). CXCR3$^{-/-}$ mice displayed modestly reduced responsiveness to αGalCer-loaded DC monotherapy compared to the WT cohort, as well as more variable responses to VSV-GFP monotherapy (Figure 6B-C). But, overall, comparable therapeutic responses, including robust responses to combination therapy, were observed in both the WT and CXCR3$^{-/-}$ cohorts, indicating that CXCR3 may be dispensable for the efficacy of one or both therapies.

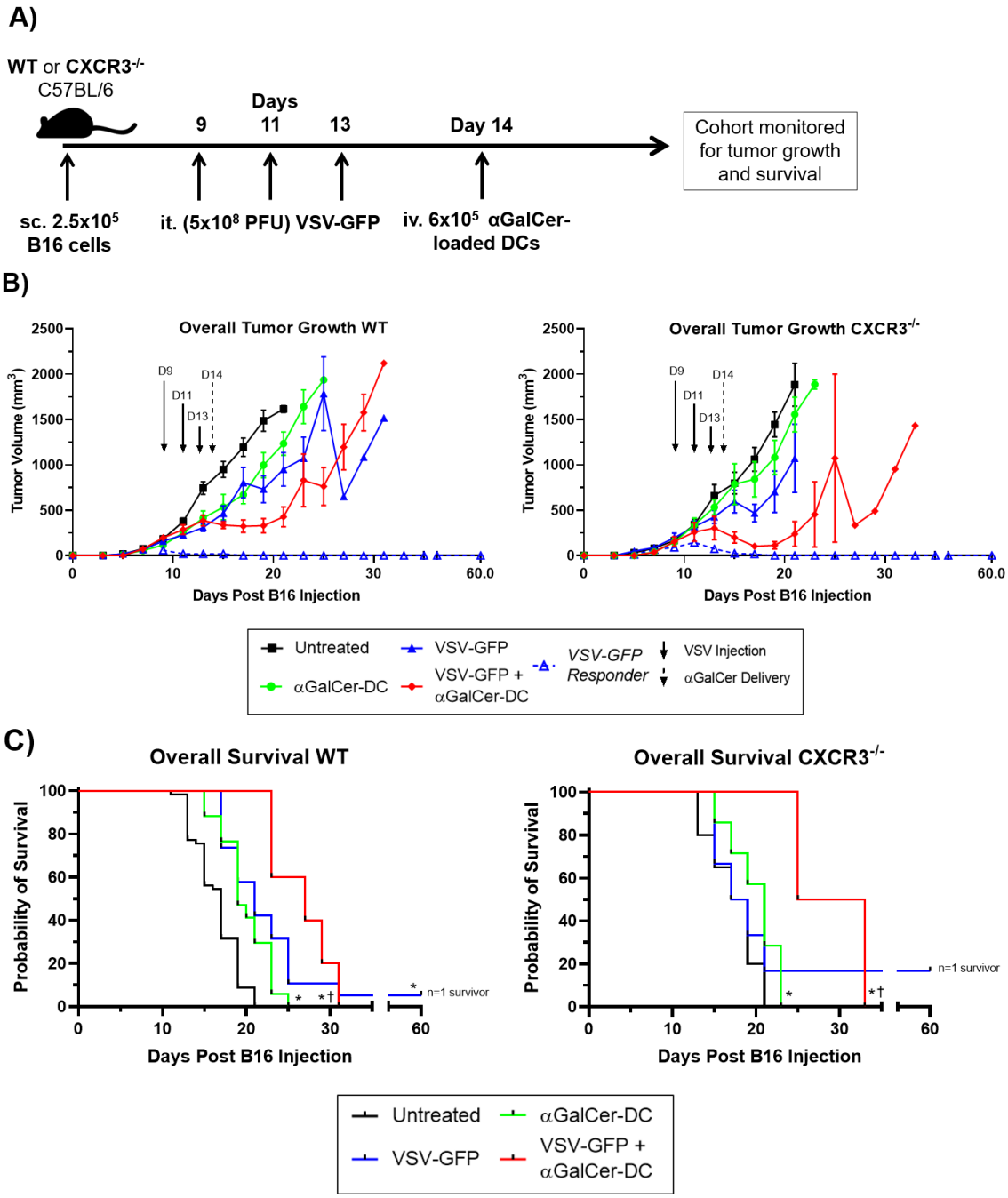

Figure 6. Combined VSV-GFP and NKT cell activation cause greater tumor regression and increased survival than monotherapies in both WT and CXCR3$^{-/-}$ mice. A) Schematic of B16 tumor induction and treatment timeline. WT and CXCR3$^{-/-}$ C57BL/6 mice were subcutaneously inoculated with 2.5x10^5 B16 cells on day 0. Mice received intratumoral VSV-GFP (5x10^8 PFU) on days 9, 11, and 13. Mice receiving NKT cell activation treatment received 6x10^5 αGalCer-loaded DCs intravenously on day 14. B) B16 tumor volume and C) overall survival were assessed in WT and CXCR3$^{-/-}$ untreated mice, those receiving VSV-GFP alone, NKT cell activation treatment alone, or VSV-GFP + NKT cell activation (n=5-50 per group for WT cohort, 4-30 for CXCR3$^{-/-}$ cohort). *p<0.05 vs. untreated, †p<0.05 vs. αGalCer-loaded DCs.

3.2.2 CXCR3$^{-/-}$ mice have modestly improved responsiveness to VSV-p14, both alone and in combination with αGalCer-DCs

To determine whether addition of a FAST protein would improve responses to VSV monotherapy or combination therapy, VSV-p14 (i.t. at $5x10^8$ PFU/mL) was substituted for VSV-GFP (Figure 7A).

VSV-p14 also induced tumor regression and prolonged survival in both WT and CXCR3$^{-/-}$ cohorts, alone and in combination therapy. Combination therapy again led to the greatest tumor regression and survival duration relative to monotherapies in both cohorts (Figure 7B-C). Surprisingly, CXCR3$^{-/-}$ mice responded better than WT mice to VSV-p14, both alone and in combination therapy, with CXCR3$^{-/-}$ mice experiencing greater tumor regression and prolonged survival in response to both VSV-p14 monotherapy and combination therapy compared to the WT cohort (Figure 7B-C). Furthermore, one CXCR3$^{-/-}$ mouse in each of the VSV-p14 monotherapy and combination therapy groups exhibited complete tumor clearance (Figure 7B-C).

The increased efficacy of combination therapy in both cohorts again suggests that loss of CXCR3 may not negatively impact responses to treatment. In fact, the CXCR3$^{-/-}$ cohort exhibited more robust responses to VSV-p14 than the WT cohort, as demonstrated by the improved magnitude and duration of delayed tumor outgrowth, as well as complete tumor regression in two CXCR3$^{-/-}$ mice, suggesting that improved responses to oncolytic VSV may be compensating for the loss of CXCR3 in this model.

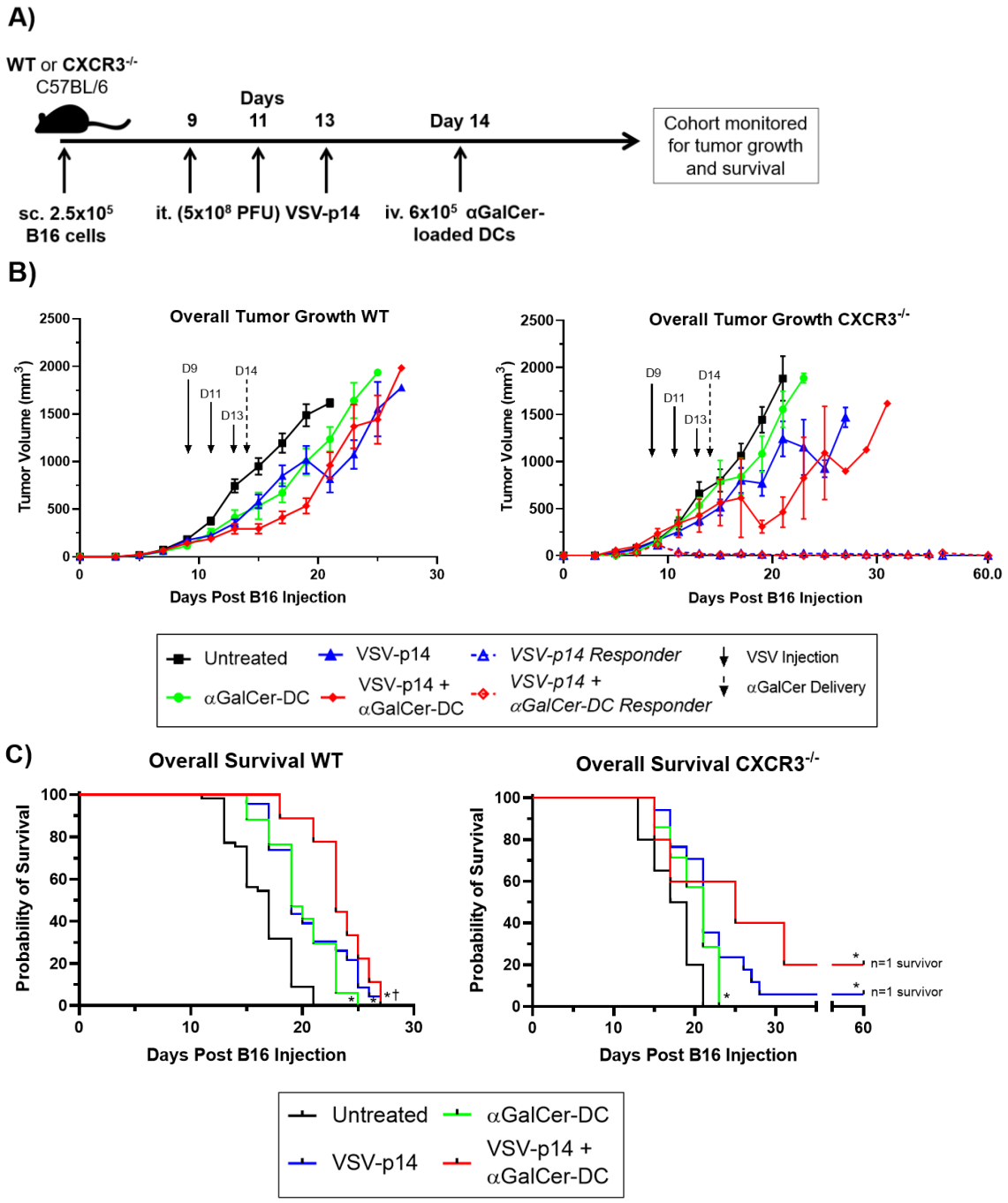

Figure 7. Combined VSV-p14 and NKT cell activation cause greater tumor regression and increased survival than monotherapies in both WT and CXCR3$^{-/-}$ mice. A) Schematic of B16 tumor induction and treatment timeline. WT and CXCR3$^{-/-}$ C57BL/6 mice were subcutaneously inoculated with 2.5x10^5 B16 cells on day 0. Mice received intratumoral VSV-p14 (5x10^8 PFU) on days 9, 11, and 13. Mice receiving NKT cell activation treatment received 6x10^5 αGalCer-loaded DCs intravenously on day 14. B) B16 tumor volume and C) overall survival were assessed in WT and CXCR3$^{-/-}$ untreated mice, those receiving VSV-p14 alone, NKT cell activation treatment alone, or VSV-p14 + NKT cell activation (n=14-50 per group for WT cohort, 7-30 for CXCR3$^{-/-}$ cohort). *p<0.05 vs. untreated, †p<0.05 vs. αGalCer-loaded DCs.

3.2.3 Tumor rechallenge in CXCR3$^{-/-}$ complete responders

The two CXCR3$^{-/-}$ complete responders were subsequently re-challenged with B16 melanoma cells 60 days after initial inoculation to assess potential immune memory responses (Figure 8A). The complete responder to VSV-p14 monotherapy experienced tumor regrowth and had to be sacrificed for endpoint volume 20 days post-re-challenge (data not shown), comparable to the naïve untreated challenge group, who survived a median of 17 days post-inoculation, and a maximum of 21 days post-inoculation (Figure 7C). The mouse that had cleared its B16 tumor following combination VSV-p14 plus αGalCer-loaded DC therapy experienced no tumor regrowth, indicating the formation of persistent anti-tumor immune memory.

The spleen and inguinal lymph nodes (LNs) of this mouse were therefore harvested 120 days following initial challenge for immune memory profiling, along with those of two tumor-naïve CXCR3$^{-/-}$ controls (Figure 8A). Overall levels of NKT, CD4+, and CD8+ T cells were comparable between naïve controls and the rechallenged CXCR3$^{-/-}$ responder (Figure 8B-G). Compared to naïve controls, the rechallenged CXCR3$^{-/-}$ responder exhibited few differences in NKT cells, with an apparent decease in PD-1+ NKT cells in the inguinal lymph node (Figure 8B-C). Activated (CD69+) and effector memory (CD44+) CD8+ T cell populations in the spleen and lymph nodes appeared increased in the responder (Figure 8D-E), with a decrease in central memory (CD44+ CD62L+) CD8+ T cells in the lymph node (Figure 8D) and naïve (CD62L+) CD8+ T cells in the spleen (Figure 5E). Expression of PD-1 on CD8+ T cells was variable (Figure 8D-E). Effector memory (CD44+) CD4+ T cells were increased in the spleen of the responder, whereas naïve (CD62L+) CD4+ T cells were decreased (Figure 8G). PD-1+ CD4+ T cells were

increased only in the spleen (Figure 8F-G). Overall, this data suggests that this CXCR3$^{-/-}$ complete responder was able to develop protective anti-tumor immune memory in response to combination VSV-p14 plus αGalCer-loaded DC therapy.

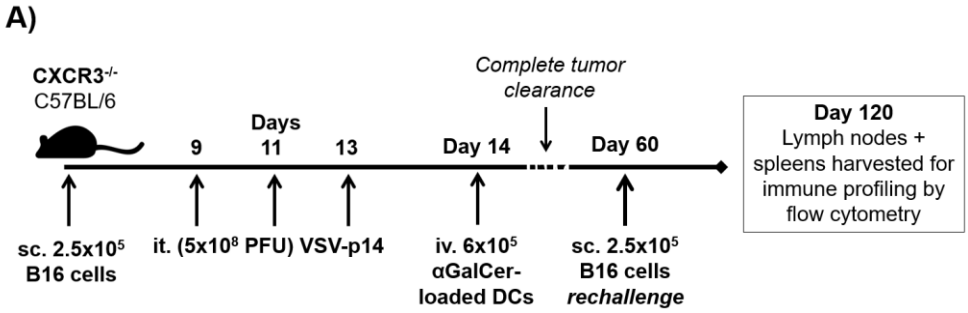
A)
CXCR3-/-
C57BL/6
Days
9
11
13
Day 14
Complete tumor clearance
Day 60
Day 120
Lymph nodes + spleens harvested for immune profiling by flow cytometry
sc. 2.5x10^5 B16 cells
it. (5x10^8 PFU) VSV-p14
iv. 6x10^5 αGalCer-loaded DCs
sc. 2.5x10^5 B16 cells rechallenge

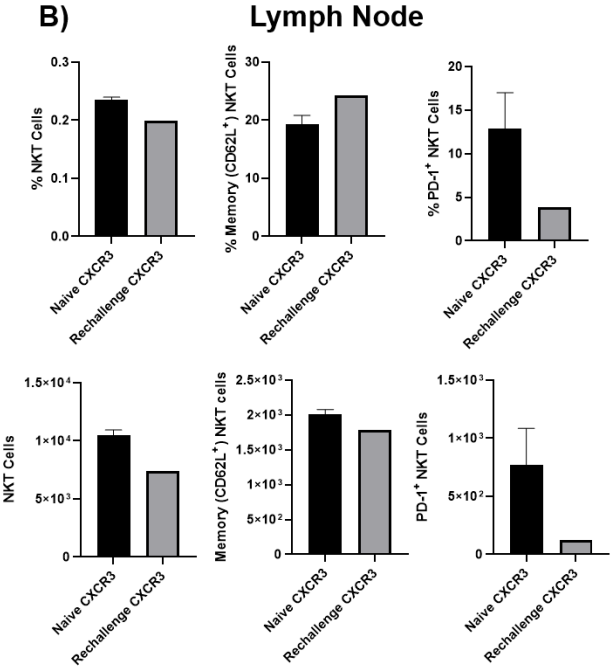
B)
Lymph Node
% NKT Cells
% Memory (CD62L+) NKT Cells
% PD-1+ NKT Cells
NKT Cells
Memory (CD62L+) NKT cells
PD-1+ NKT Cells
Naive CXCR3
Rechallenge CXCR3

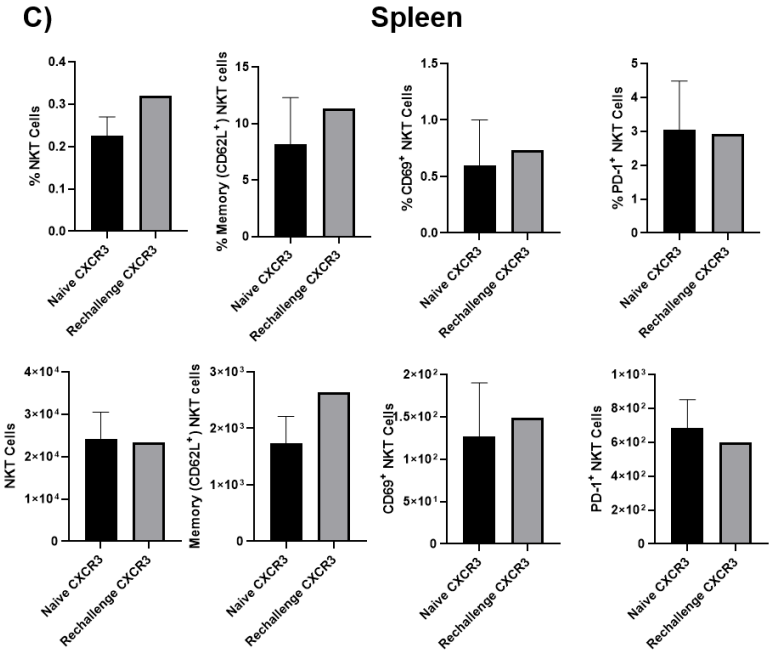
C)
Spleen
% NKT Cells
% Memory (CD62L+) NKT cells
% CD69+ NKT Cells
% PD-1+ NKT Cells
NKT Cells
Memory (CD62L+) NKT cells
CD69+ NKT Cells
PD-1+ NKT Cells
Naive CXCR3
Rechallenge CXCR3

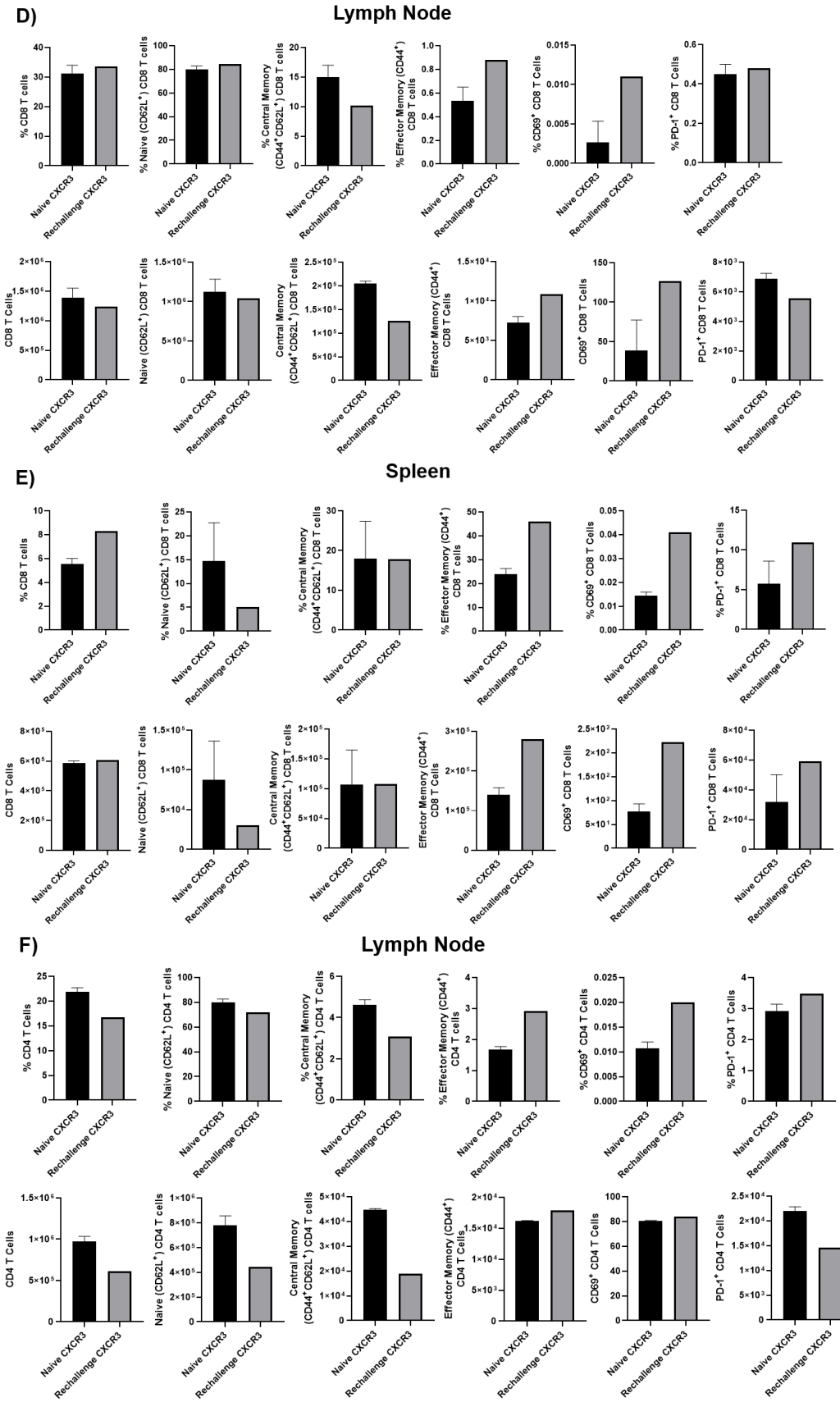
D)
Lymph Node
% CD8 T cells
% Naive (CD62L+) CD8 T cells
% Central Memory (CD44+CD62L+) CD8 T cells
% Effector Memory (CD44+) CD8 T cells
% CD69+ CD8 T Cells
% PD-1+ CD8 T Cells
CD8 T Cells
Naive (CD62L+) CD8 T cells
Central Memory (CD44+CD62L+) CD8 T cells
Effector Memory (CD44+) CD8 T Cells
CD69+ CD8 T Cells
PD-1+ CD8 T Cells
Naive CXCR3
Rechallenge CXCR3
E)
Spleen
% CD8 T cells
% Naive (CD62L+) CD8 T cells
% Central Memory (CD44+CD62L+) CD8 T cells
% Effector Memory (CD44+) CD8 T cells
% CD69+ CD8 T Cells
% PD-1+ CD8 T Cells
CD8 T Cells
Naive (CD62L+) CD8 T cells
Central Memory (CD44+CD62L+) CD8 T cells
Effector Memory (CD44+) CD8 T Cells
CD69+ CD8 T Cells
PD-1+ CD8 T Cells
Naive CXCR3
Rechallenge CXCR3
F)
Lymph Node
% CD4 T Cells
% Naive (CD62L+) CD4 T cells
% Central Memory (CD44+CD62L+) CD4 T cells
% Effector Memory (CD44+) CD4 T cells
% CD69+ CD4 T Cells
% PD-1+ CD4 T Cells
CD4 T Cells
Naive (CD62L+) CD4 T cells
Central Memory (CD44+CD62L+) CD4 T cells
Effector Memory (CD44+) CD4 T Cells
CD69+ CD4 T Cells
PD-1+ CD4 T Cells
Naive CXCR3
Rechallenge CXCR3

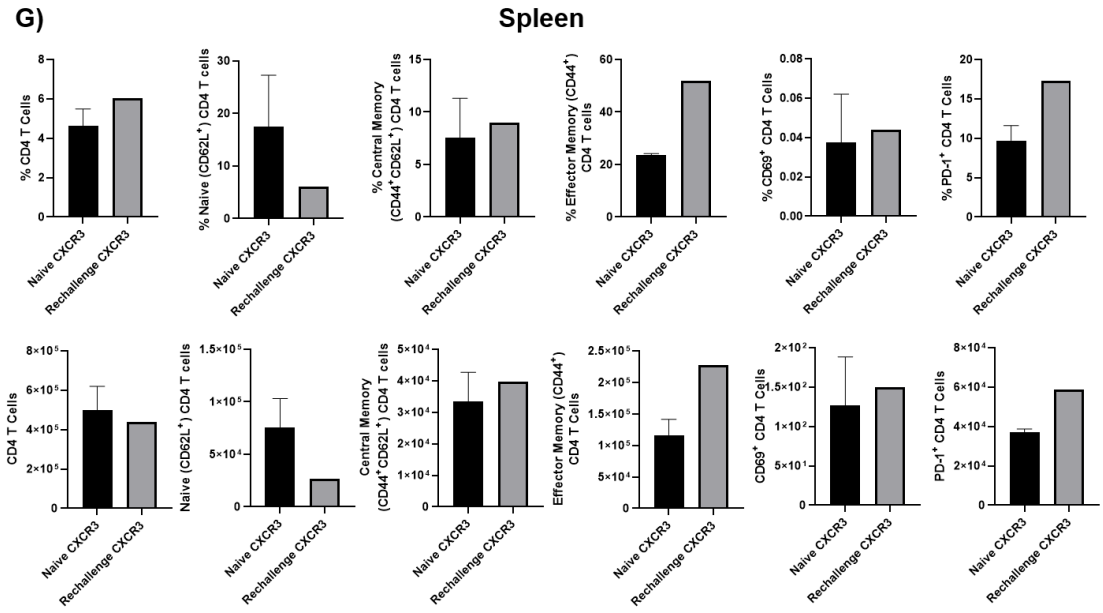

Figure 8. Immune memory populations in lymph nodes and spleen of re-challenged CXCR3$^{-/-}$ complete responder. A) Schematic of B16 tumor induction and treatment timeline. CXCR3$^{-/-}$ C57BL/6 mouse was subcutaneously inoculated with 2.5x10^5 B16 cells on day 0. Mouse received intratumoral VSV-p14 (5x10^8 PFU) on days 9, 11, and 13. Mice receiving NKT cell activation treatment received 6x10^5 αGalCer-loaded DCs intravenously on day 14. Mouse cleared tumor completely and was rechallenged on day 60 following initial tumor inoculation. Mouse did not regrow tumor and was harvested on day 120 following initial tumor inoculation. Spleens and inguinal lymph nodes were isolated and homogenized. Spleens and inguinal lymph nodes were also harvested from 2 tumor-naïve CXCR3$^{-/-}$ control mice. Flow cytometry was used to assess B-C) NKT cells (CD1d-tetramer+ TCRβ+), D-E) CD8+ T cells (TCRβ+ CD8a+), and F-G) CD4+ T cells (TCRβ+ CD4+), as well as activation (CD69+), and exhaustion (PD-1+). Memory NKT cells (CD62L+), naïve T cells (CD62L+CD44-), effector memory T cells (CD44+CD62L-), and central memory T cells (CD44+CD62L+) were also assessed. Error bars represent variance (n=2 for naïve CXCR3$^{-/-}$ controls, n=1 for rechallenged CXCR3$^{-/-}$ complete responder).

3.2.4 NKT cell activation therapy differentially increases NKT cell levels in spleens and tumors of WT and CXCR3$^{-/-}$ mice

I then assessed the effect of the CXCR3 axis on immune responses to treatment by characterizing immune populations in the tumors and spleens of WT and CXCR3$^{-/-}$ mice treated with VSV-p14 and αGalCer-loaded DCs (Figure 9A). Spleens and tumors were harvested 19 days after initial B16 tumor inoculation for assessment via flow cytometry.

αGalCer-loaded DC monotherapy and combination therapy generated the greatest decreases in tumor size at day 19, with combination therapy inducing the most significant control of tumor weight, particularly in the WT cohort (Figure 9B). Given that NKT cell activation is the direct target of αGalCer-loaded DCs, and that NKT cells express CXCR3 and are known to migrate via this axis, we first assessed the impact of CXCR3-deficiency on NKT cell populations.

NKT cell frequency and number were comparable in the spleens of tumor-bearing untreated WT and CXCR3$^{-/-}$ mice (Figure 9C). VSV-p14 treatment alone did not affect NKT cell levels within the spleens of WT or CXCR3$^{-/-}$ mice (Figure 9C). In contrast, NKT cells significantly expanded in the spleen following delivery of αGalCer-DCs, as has been shown previously (Figure 9C). This accumulation was significantly greater in CXCR3$^{-/-}$ mice compared to the WT cohort (Figure 9C). Additionally, when overall cell numbers were taken into account, combination VSV-p14 plus αGalCer-loaded DC treatment increased splenic NKT cells to a significantly greater extent than αGalCer-DC monotherapy, specifically in the CXCR3$^{-/-}$ cohort (Figure 9C). Even more strikingly, αGalCer-loaded DC treatment also significantly increased NKT cell levels within tumors,

and this effect was reduced in CXCR3$^{-/-}$ mice, significantly with αGalCer-loaded DC treatment and trending toward significance (p=0.0747) with combination treatment, indicating that CXCR3 may play a role in mediating NKT cell accumulation in tumors upon αGalCer activation (Figure 9D). Untreated and VSV-p14 monotherapy-treated CXCR3$^{-/-}$ mice also had lower numbers of intratumoral NKT cells than their WT counterparts, although these observations did not reach significance, suggesting that CXCR3 deficiency may possibly impair NKT cell recruitment into tumors at baseline as well (Figure 9D). In the tumors, αGalCer-loaded DCs and combination therapy increased NKT cell infiltration to the same extent (Figure 9D). Overall, these results suggest that loss of CXCR3 may impair recruitment and/or activation of NKT cells in tumors, potentially resulting in increased NKT cell accumulation within the spleen. Additionally, VSV-p14 therapy, alone or in combination with NKT cell therapy, does not appear to substantially impact NKT cell accumulation in tumors.

I also assessed expression of CD69, a marker of early immune cell activation, as well as PD-1, a co-inhibitory receptor associated with immune cell activation and subsequent exhaustion. NKT cell expression of both CD69 and PD-1 was more variable in response to treatment. In the spleen, the frequency of CD69+ NKT cells increased upon VSV-p14 treatment in the WT cohort (Figure 9C). By contrast, αGalCer-loaded DC monotherapy and combination therapy significantly decreased the frequency of CD69 expression on CXCR3$^{-/-}$ NKT cells relative to the untreated group (Figure 9C). VSV-p14 treatment also increased the frequency of splenic PD-1+ NKT cells, again only in the WT cohort (Figure 9C). Lack of correlation between splenic frequency and cell number may be influenced by factors including higher overall cell counts and specifically increased splenic NKT

cells in the CXCR3$^{-/-}$ cohort. In tumors, αGalCer-loaded DC monotherapy and combination therapy increased levels of CD69+ NKT cells significantly only in the WT cohort, whereas VSV-p14 monotherapy instead appeared to decrease CD69+ NKT cells below the untreated baseline (Figure 9D). Expression of PD-1 on intratumoral NKT cells was more variable, although there was a non-significant trend towards increased PD-1+ NKT cell frequency again upon VSV-p14 treatment (Figure 9D).

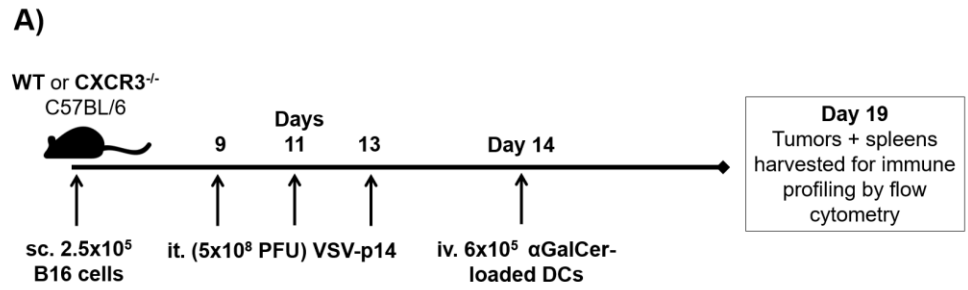
A)
WT or CXCR3-/-
C57BL/6
Days
9
11
13
Day 14
Day 19
Tumors + spleens harvested for immune profiling by flow cytometry
sc. 2.5x10^5 B16 cells
it. (5x10^8 PFU) VSV-p14
iv. 6x10^5 αGalCer-loaded DCs

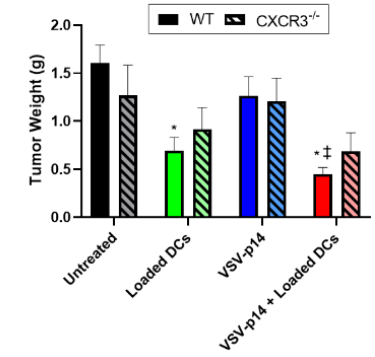
B)
WT
CXCR3-/-
Tumor Weight (g)
Untreated
Loaded DCs
VSV-p14
VSV-p14 + Loaded DCs

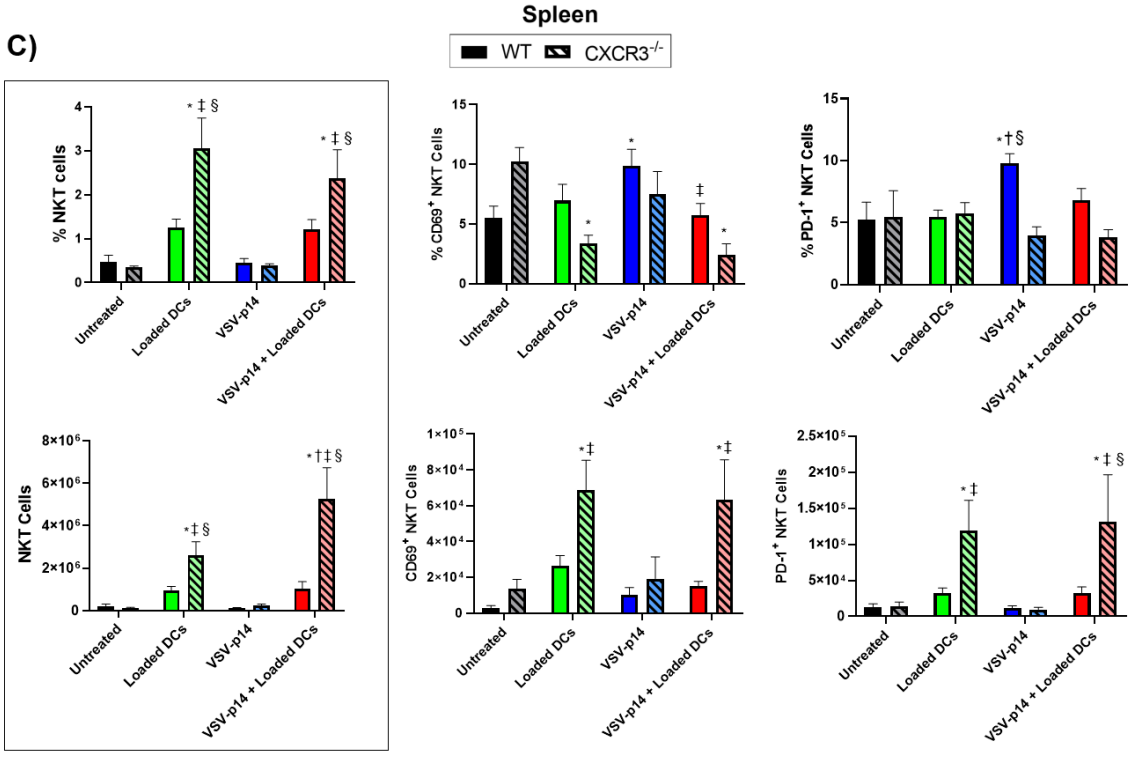
C)
Spleen
WT
CXCR3-/-
% NKT cells
NKT Cells
% CD69+ NKT Cells
CD69+ NKT Cells
% PD-1+ NKT Cells
PD-1+ NKT Cells
Untreated
Loaded DCs
VSV-p14
VSV-p14 + Loaded DCs

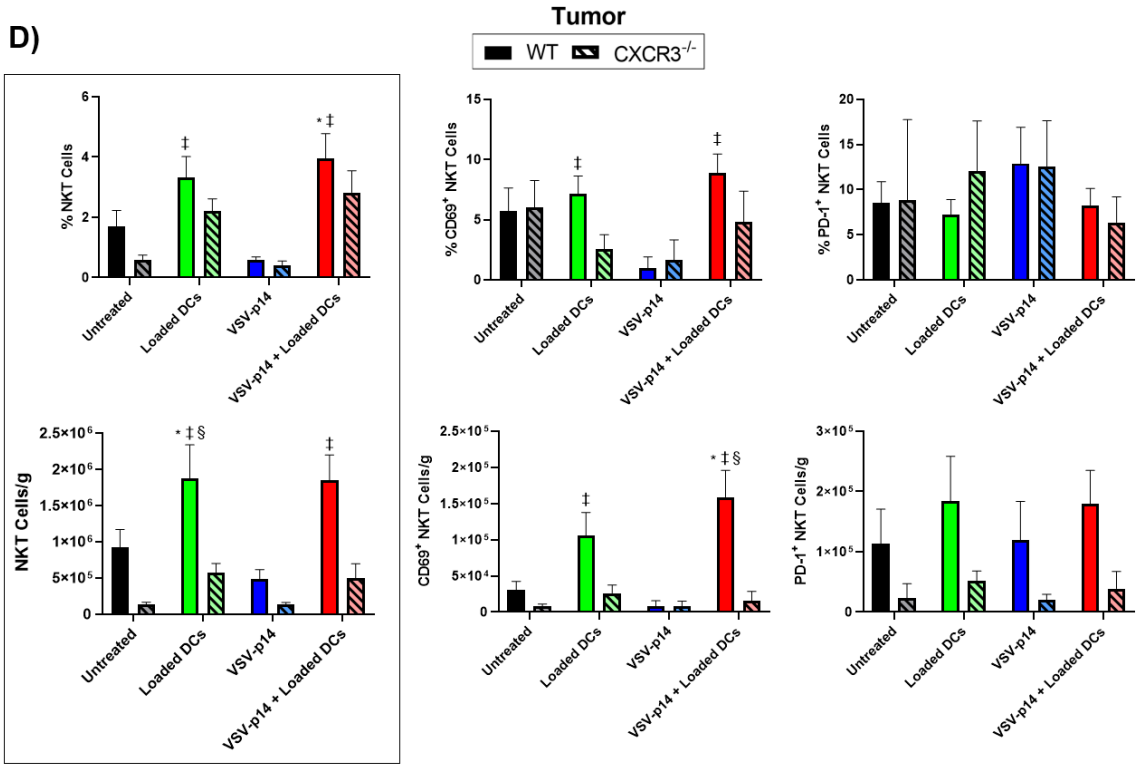

Figure 9. NKT cell activation therapy differentially increases NKT cell levels in spleens and tumors of WT and CXCR3$^{-/-}$ mice. A) Schematic of B16 tumor induction and treatment timeline. WT and CXCR3$^{-/-}$ C57BL/6 mice were subcutaneously inoculated with 2.5x10^{5} B16 cells on day 0. Mice received intratumoral VSV-p14 (5x10^{8} PFU) on days 9, 11, and 13. Mice receiving NKT cell activation treatment received 6x10^{5} αGalCer-loaded DCs intravenously on day 14. Mice were harvested on day 19. B) Tumors were weighed. C) Spleens and D) tumors of WT and CXCR3$^{-/-}$ mice were isolated and homogenized. Flow cytometry was used to assess NKT cells (CD1d-tetramer+ TCRβ+), activation (CD69+), and exhaustion (PD-1+). Tumor cell counts were normalized to tumor weights. *p<0.05 vs. untreated, †p<0.05 vs. αGalCer-loaded DCs, ‡p<0.05 vs. VSV-p14, §p<0.05 WT vs. CXCR3$^{-/-}$ (n=14-18 for WT cohort, n=7-9 for CXCR3$^{-/-}$ cohort).

3.2.5 Lymphoid immune populations in spleens and tumors of WT and CXCR3$^{-/-}$ mice respond variably to treatment

I also assessed accumulation of other immune populations implicated in the anti-tumor immune response, including NK cells, CD8+ T cells, CD4+ T cells, and B cells (Figure 10A). Overall, these populations were less affected by treatment or CXCR3 deficiency than NKT cells, although there were notable shifts in some populations. Somewhat surprisingly, levels of intratumoral NK cells and CD8+ T cells were minimally affected by loss of CXCR3, suggesting that CXCR3 may not be essential for their recruitment into tumors in this model (Figure 10C, E). Overall CD4+ T cell levels within tumors were also not strongly affected by loss of CXCR3 (Figure 10G). However, FoxP3+ CD4+ Treg frequencies trended higher in WT compared to CXCR3$^{-/-}$ tumors, although this trend did not reach significance. This trend was also observed in the spleen, where it was statistically significant in untreated mice (Figure 10H). VSV-p14 treatment, alone and in combination with αGalCer-loaded DCs, increased splenic CD8+ T cell levels significantly in the CXCR3$^{-/-}$ cohort (Figure 10D), in line with previous observations in a 4T1 breast cancer model [154]. However, this increase did not translate to tumors (Figure 10E). Both splenic and intratumoral levels of NK cells were also not strongly affected by treatments (Figure 10B-C).

However, VSV-p14 and αGalCer-loaded DC treatments did impact patterns of PD-1 expression on several subsets. In spleens, the frequency of PD-1+ CD8+ T, CD4+ T, and NK cells was high (~40%) in untreated and VSV-p14 monotherapy groups across WT and CXCR3$^{-/-}$ cohorts, but αGalCer-loaded DC monotherapy and combination therapy decreased PD-1 expression by at least half in both cohorts (Figure 10B, D, F). When

looking at tumors, this trend remained only in CD4+ T cells (Figure 10G). PD-1 expression on intratumoral CD8+ T cells was uniformly high (>50%), suggestive of activation but also an immunosuppressive tumor environment that would likely benefit from anti-PD-1 therapy (Figure 10E). Overall patterns of CD69 expression were less clear, although frequencies of CD69 expression on CD4+ T cells following treatment were significantly lower in $CXCR3^{-/-}$ mice (Figure 10F). But, higher overall cell counts for $CXCR3^{-/-}$ spleens appear to cause discrepancies between patterns in frequency and cell number for several subsets.

Spleens, as expected, had high frequencies of B cells across treatment groups and cohorts, with limited CD69 and PD-1 expression (Figure 10I). In tumors, B cell levels were highest in untreated mice, and overall greater in the WT cohort than the $CXCR3^{-/-}$ cohort (Figure 10J). No clear patterns of CD69 and PD-1 expression were observed on B cells (Figure 10J).

Overall, neither loss of CXCR3 nor VSV-p14 and αGalCer-loaded DC therapy significantly affected levels of other lymphoid populations, such as CD8+ T cells, CD4+ T cells, or NK cells, in tumors. Some trends were observed in the spleen, but overall there were difficulties in achieving significance. Trends in activation markers were less clear in general, although αGalCer-loaded DCs did notably reduce PD-1 expression on CD8+ T cells, CD4+ T cells, and NK cells within spleens.

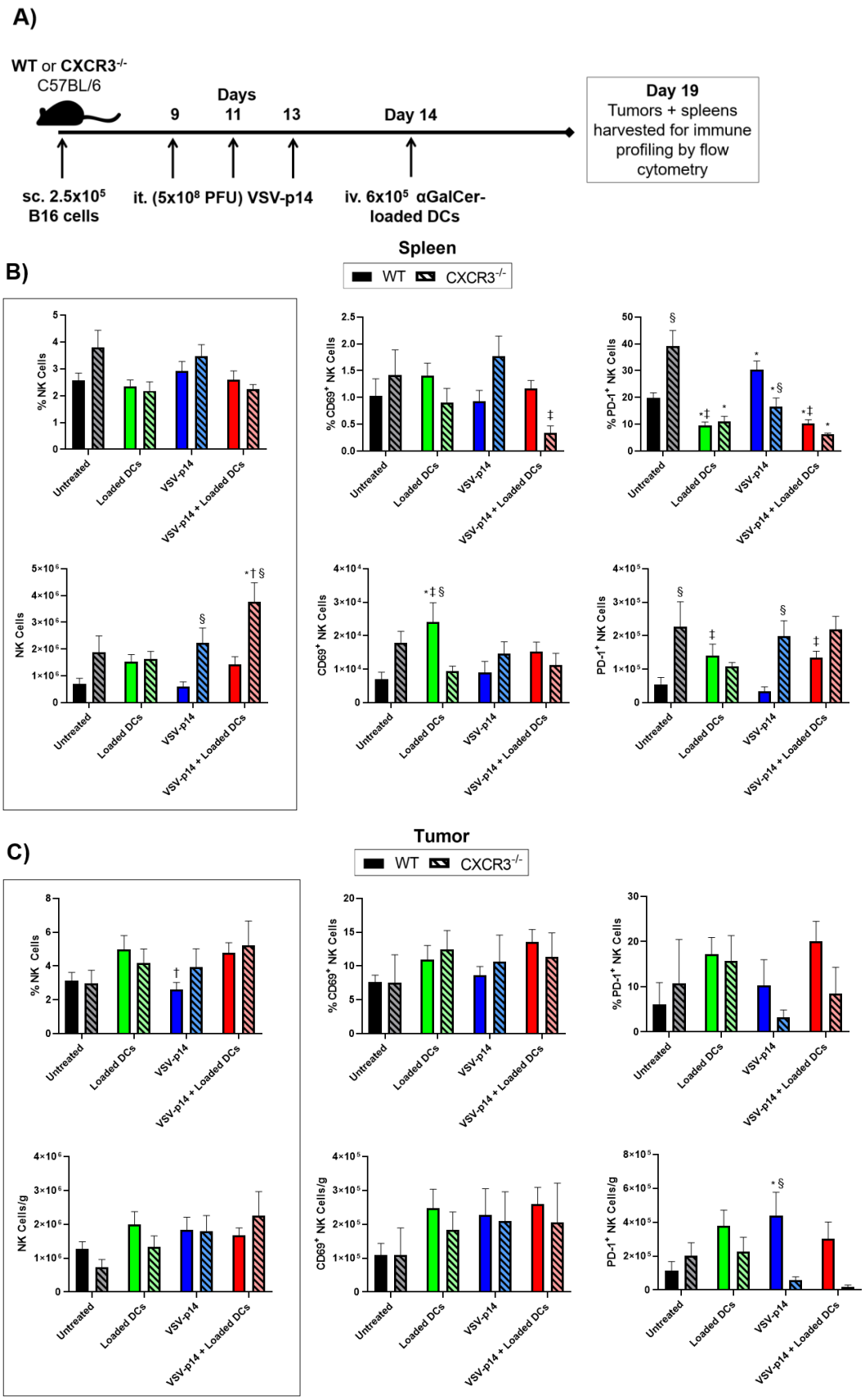
A)
WT or CXCR3-/-
C57BL/6
Days
9
11
13
Day 14
Day 19
Tumors + spleens harvested for immune profiling by flow cytometry
sc. 2.5x10^5 B16 cells
it. (5x10^8 PFU) VSV-p14
iv. 6x10^5 αGalCer-loaded DCs
B)
Spleen
WT
CXCR3-/-
% NK Cells
% CD69+ NK Cells
% PD-1+ NK Cells
NK Cells
CD69+ NK Cells
PD-1+ NK Cells
Untreated
Loaded DCs
VSV-p14
VSV-p14 + Loaded DCs
C)
Tumor
WT
CXCR3-/-
% NK Cells
% CD69+ NK Cells
% PD-1+ NK Cells
NK Cells/g
CD69+ NK Cells/g
PD-1+ NK Cells/g
Untreated
Loaded DCs
VSV-p14
VSV-p14 + Loaded DCs

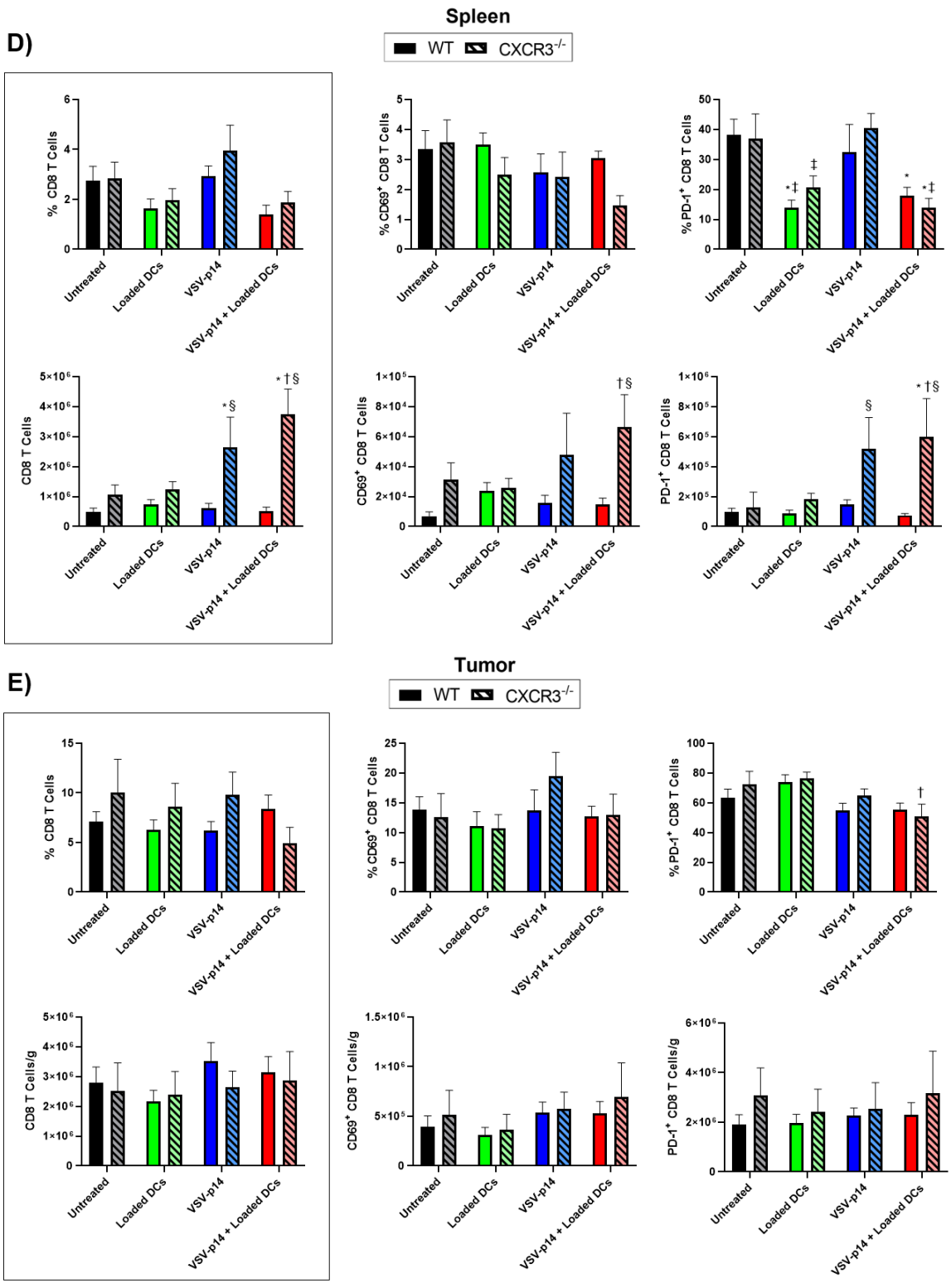
D)
Spleen
WT
CXCR3-/-
% CD8 T Cells
% CD69+ CD8 T Cells
% PD-1+ CD8 T Cells
CD8 T Cells
CD69+ CD8 T Cells
PD-1+ CD8 T Cells
Untreated
Loaded DCs
VSV-p14
VSV-p14 + Loaded DCs
E)
Tumor
WT
CXCR3-/-
% CD8 T Cells
% CD69+ CD8 T Cells
% PD-1+ CD8 T Cells
CD8 T Cells/g
CD69+ CD8 T Cells/g
PD-1+ CD8 T Cells/g
Untreated
Loaded DCs
VSV-p14
VSV-p14 + Loaded DCs

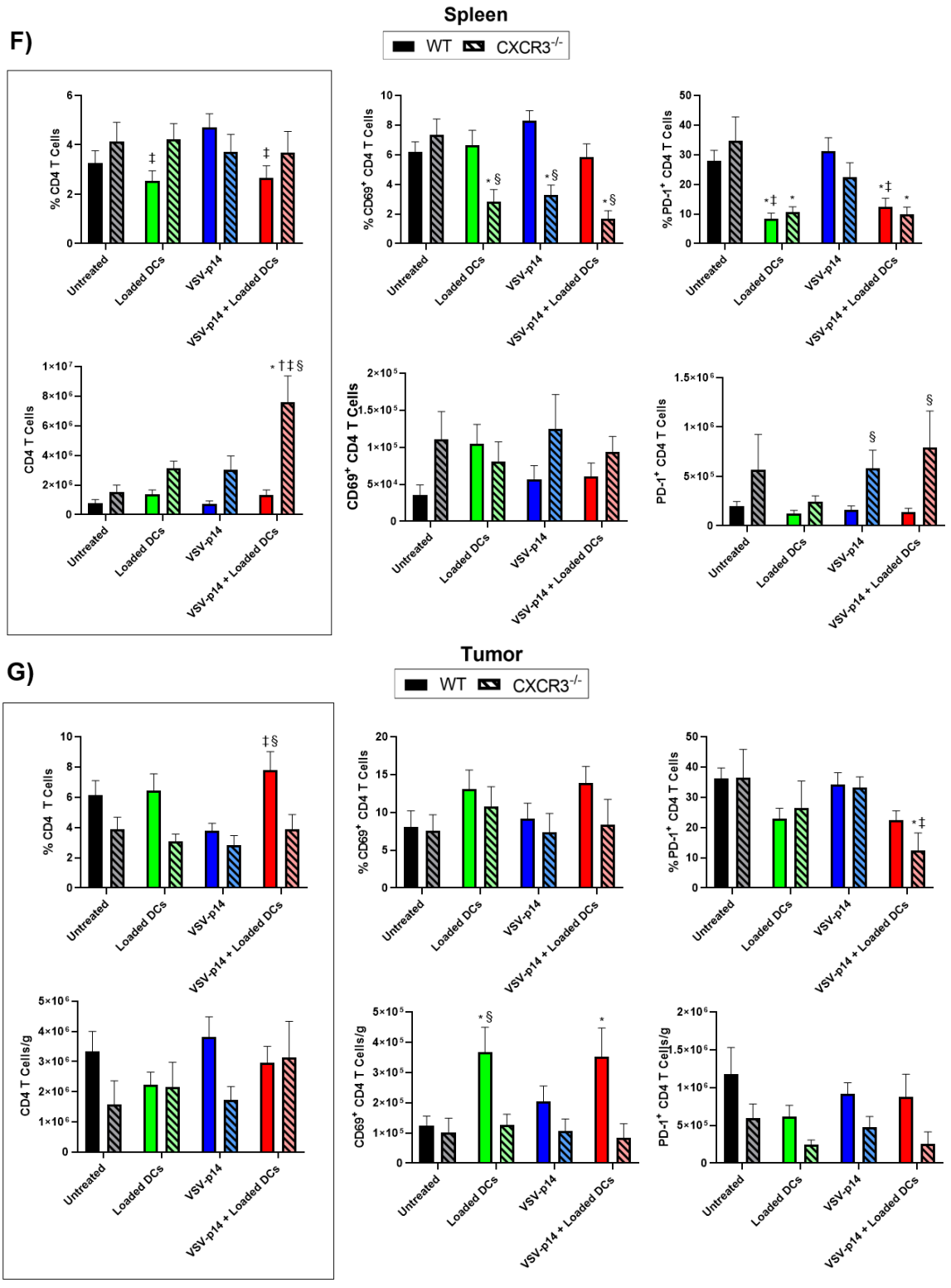
F)
Spleen
WT
CXCR3-/-
% CD4 T Cells
% CD69+ CD4 T Cells
% PD-1+ CD4 T Cells
CD4 T Cells
CD69+ CD4 T Cells
PD-1+ CD4 T Cells
Untreated
Loaded DCs
VSV-p14
VSV-p14 + Loaded DCs
G)
Tumor
WT
CXCR3-/-
% CD4 T Cells
% CD69+ CD4 T Cells
% PD-1+ CD4 T Cells
CD4 T Cells/g
CD69+ CD4 T Cells/g
PD-1+ CD4 T Cells/g
Untreated
Loaded DCs
VSV-p14
VSV-p14 + Loaded DCs

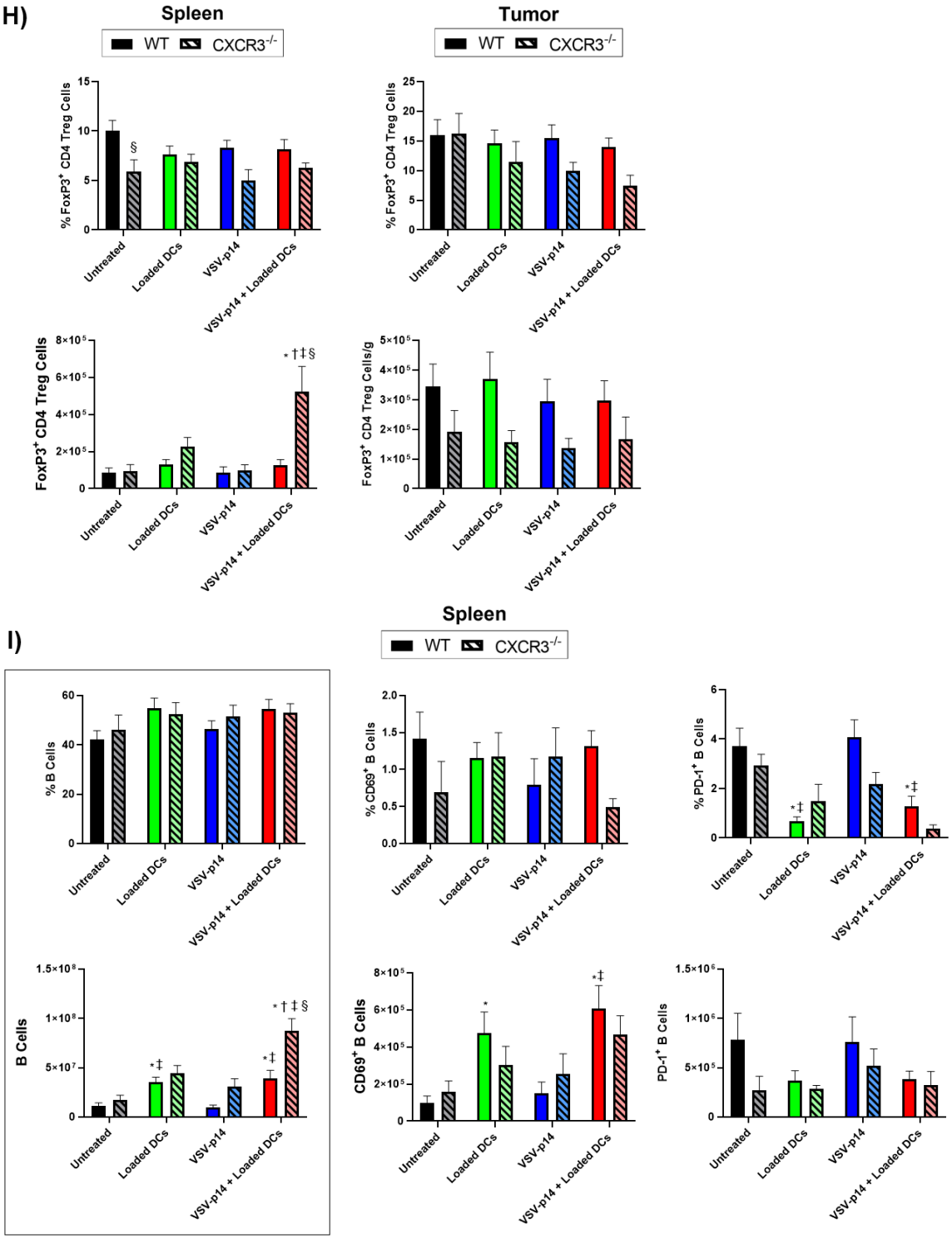
H)
Spleen
WT
CXCR3-/-
% FoxP3+ CD4 Treg Cells
§
Untreated
Loaded DCs
VSV-p14
VSV-p14 + Loaded DCs
Tumor
WT
CXCR3-/-
% FoxP3+ CD4 Treg Cells
FoxP3+ CD4 Treg Cells
*†‡§
FoxP3+ CD4 Treg Cells/g
I)
Spleen
WT
CXCR3-/-
% B Cells
% CD69+ B Cells
% PD-1+ B Cells
B Cells
*†‡§
*‡
CD69+ B Cells
*
*‡
PD-1+ B Cells

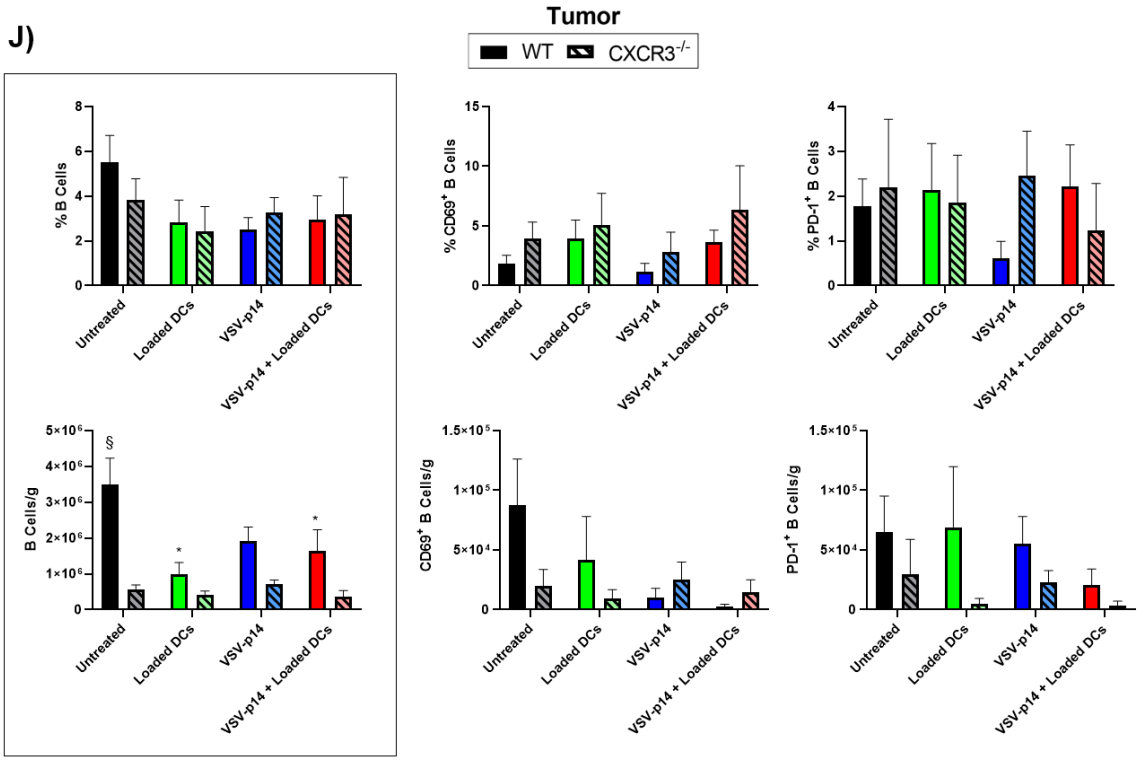

Figure 10. Lymphoid immune populations in spleens and tumors of WT and CXCR3$^{-/-}$ mice respond variably to treatment. A) Schematic of B16 tumor induction and treatment timeline. WT and CXCR3$^{-/-}$ C57BL/6 mice were subcutaneously inoculated with 2.5x10^5 B16 cells on day 0. Mice received intratumoral VSV-p14 (5x10^8 PFU) on days 9, 11, and 13. Mice receiving NKT cell activation treatment received 6x10^5 αGalCer-loaded DCs intravenously on day 14. Mice were harvested on day 19. Spleens and tumors of WT and CXCR3$^{-/-}$ mice were isolated and homogenized. Flow cytometry was used to assess B-C) NK cells (NK1.1+ TCRβ-), D-E) CD8 T cells (TCRβ+ CD8a+), F-G) CD4 T cells (TCRβ+ CD4+), H) CD4 Tregs (FoxP3+), and I-J) B cells (CD19+ TCR β-), as well as activation (CD69+), and exhaustion (PD-1+). Tumor cell counts were normalized to tumor weights. *p<0.05 vs. untreated, †p<0.05 vs. αGalCer-loaded DCs, ‡p<0.05 vs. VSV-p14, §p<0.05 WT vs. CXCR3$^{-/-}$ (n=14-18 for WT cohort, n=7-9 for CXCR3$^{-/-}$ cohort).

3.2.6 Minimal changes in myeloid compartment in response to treatment or loss of CXCR3

Myeloid immune cell populations were also assessed following treatments (Figure 11A). Minimal changes were observed in the myeloid compartment in response to therapy or between WT and CXCR3$^{-/-}$ cohorts (Figure 11B-C). In spleens, the frequency of macrophages significantly decreased in the WT cohort upon αGalCer-loaded DC monotherapy and combination therapy relative to untreated and VSV-p14 groups, although this trend was lost for cell numbers, as αGalCer-loaded DC-driven splenomegaly likely drove up overall spleen counts in αGalCer-loaded DC monotherapy and combination therapy groups (Figure 11B). In tumors, levels of conventional DCs (cDCs) (CD11b- CD19+ MHCII+ CD11c+) increased in response to αGalCer-loaded DC monotherapy and combination therapy, while monocyte-derived DCs (moDCs) (CD11b+ CD11c+) remained relatively unchanged (Figure 11C). The overall granulocyte (CD11b+ Ly6G+) population within tumors trended toward increased levels upon VSV-p14 therapy, particularly in the WT cohort, although granulocytes still made up a small fraction of myeloid cells within the tumor (Figure 11C). Macrophages (CD11b+ F4/80+) dominated the intratumoral myeloid population, with minimal changes in frequency in response to treatment or loss of CXCR3 (Figure 11C).

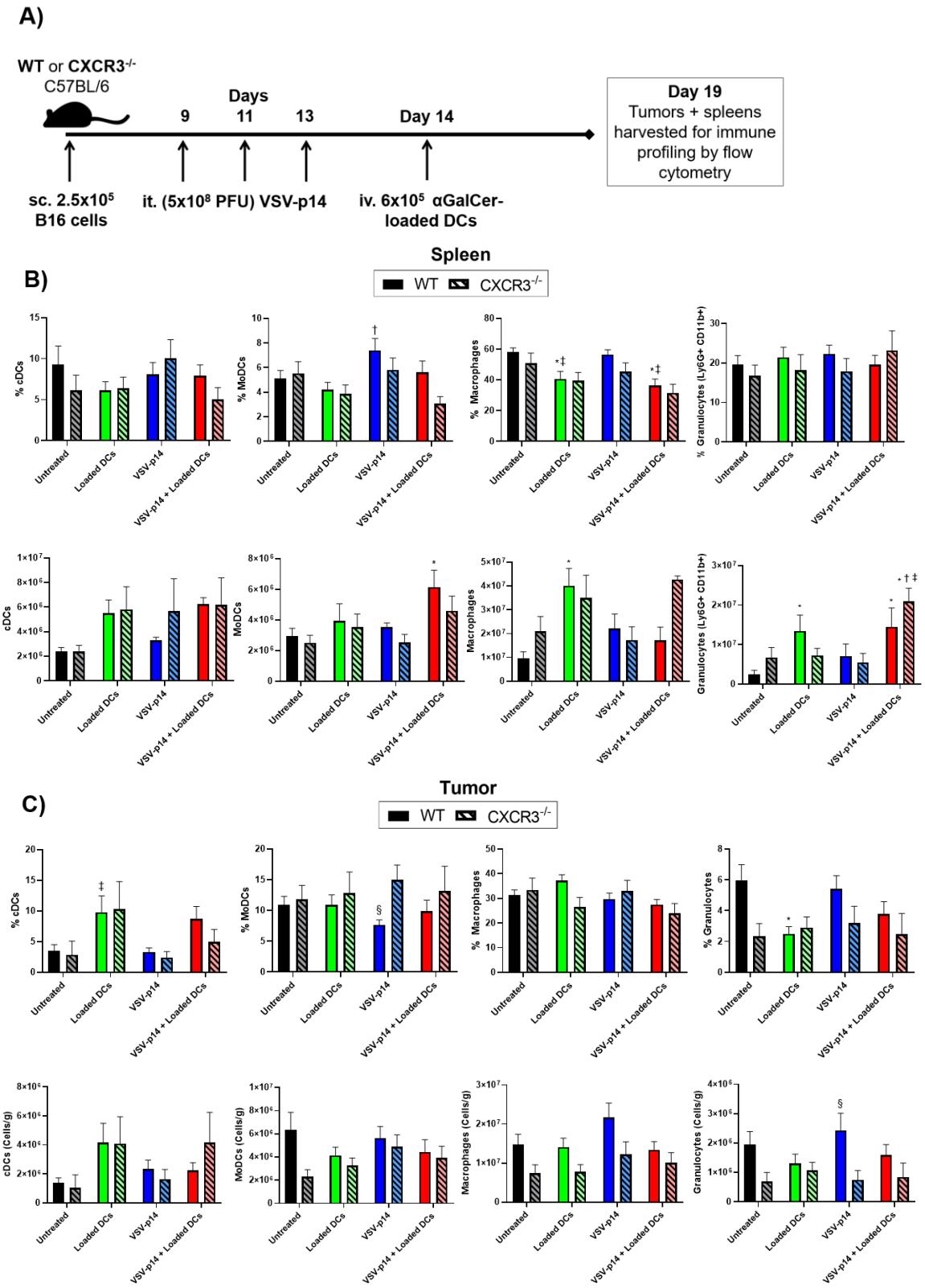

Figure 11. Myeloid populations in spleens and tumors of WT and CXCR3$^{-/-}$ mice shift minimally in response to treatment. A) Schematic of B16 tumor induction and treatment timeline. WT and CXCR3$^{-/-}$ C57BL/6 mice were subcutaneously inoculated

with $2.5x10^5$ B16 cells on day 0. Mice received intratumoral VSV-p14 ($5x10^8$ PFU) on days 9, 11, and 13. Mice receiving NKT cell activation treatment received $6x10^5$ αGalCer-loaded DCs intravenously on day 14. Mice were harvested on day 19. B) Spleens and C) tumors of WT and $CXCR3^{-/-}$ mice were isolated and homogenized. Flow cytometry was used to assess conventional DCs (cDCs) (CD11b- CD11c+ CD19+ MHCII+), monocyte-derived DCs (moDCs) (CD11b+ CD11c+), macrophages (CD11b+ F4/80+), and granulocytes (CD11b+ Ly6G+). Tumor cell counts were normalized to tumor weights. *p<0.05 vs. untreated, †p<0.05 vs. αGalCer-loaded DCs, ‡p<0.05 vs. VSV-p14, §p<0.05 WT vs. $CXCR3^{-/-}$ (n=14-18 for WT cohort, n=7-9 for $CXCR3^{-/-}$ cohort).

Overall, this data suggests that VSV-p14 and αGalCer-DCs have modest to limited effects on the immune populations of mice ten days after the initiation of VSV-p14 treatment and five days after αGalCer-DC delivery, with the exception of the NKT cell population, which was significantly increased in response to αGalCer-DC therapy, as expected. In contrast to previous reports [154], VSV-p14 treatment did not substantially increase other anti-tumor immune subsets, suggesting that it is likely driving minimal immune activation at this timepoint in this model. In addition, loss of CXCR3 reduced frequency and number of NKT cells within B16 tumors, but did not significantly impact intratumoral levels of other key anti-tumor immune populations, including CD8+ T cells and NK cells, suggesting that there may be some level of redundancy in place compensating for the loss of CXCR3 in this model.

3.3 Justifying treatment strategy

Alongside this characterization of functional responsiveness to treatment, I conducted experiments to confirm whether the strategies chosen for delivery of both oncolytic VSV and NKT cell activation by αGalCer were the most effective choices for this model.

3.3.1 Intratumoral VSV delivery is more effective than intravenous VSV injection in both WT and CXCR3$^{-/-}$ mice

To assess the delivery strategy for oncolytic VSV in our model, I compared intravenous and intratumoral delivery of virus. WT and CXCR3$^{-/-}$ mice were inoculated with B16 cells, and then treated with intravenous or intratumoral VSV-GFP or VSV-p14 on days 9, 11, and 13 post-tumor inoculation (Figure 12A). Mice were then monitored for tumor growth and survival. Both intravenous and intratumoral delivery of VSV-GFP modestly slowed tumor growth and improved survival duration relative to untreated mice, but

intratumoral delivery exhibited greater efficacy as it led to complete cures in one mouse in each of the WT and CXCR3$^{-/-}$ cohorts (Figure 12B). Similar results were observed for intravenous and intratumoral delivery of VSV-p14, with both delivery strategies exhibiting roughly comparable efficacy in the WT cohort, and intratumoral VSV-p14 performing better in the CXCR3$^{-/-}$ cohort, leading to a complete cure in one CXCR3$^{-/-}$ mouse (Figure 12C). These results indicate that intratumoral delivery of VSV constructs is modestly more effective than intravenous delivery.

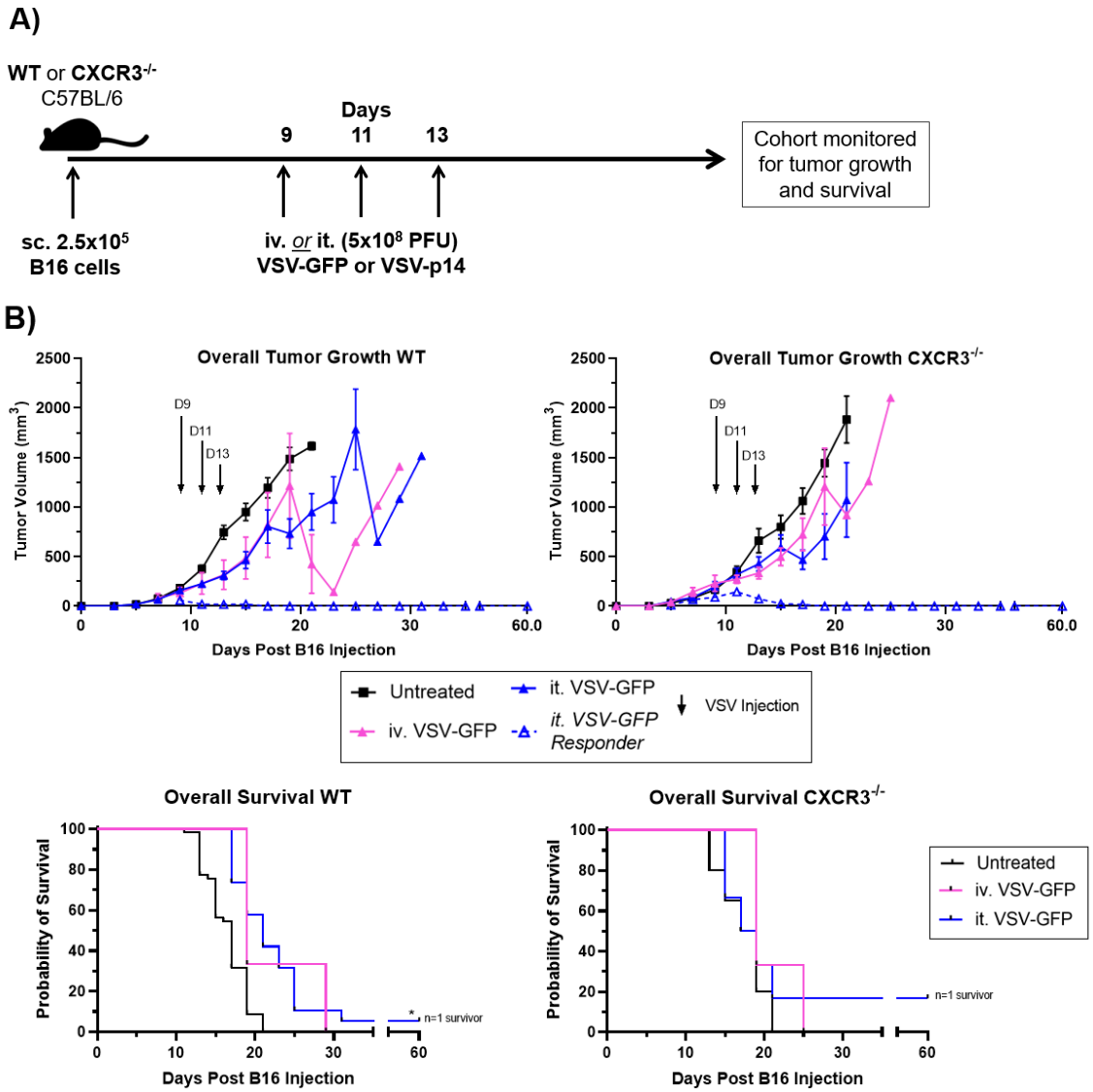
A)
WT or CXCR3-/-
C57BL/6
Days
9
11
13
Cohort monitored for tumor growth and survival
sc. 2.5x10^5 B16 cells
iv. or it. (5x10^8 PFU) VSV-GFP or VSV-p14
B)
Overall Tumor Growth WT
Overall Tumor Growth CXCR3-/-
Tumor Volume (mm3)
Days Post B16 Injection
D9
D11
D13
Untreated
iv. VSV-GFP
it. VSV-GFP
it. VSV-GFP Responder
VSV Injection
Overall Survival WT
Overall Survival CXCR3-/-
Probability of Survival
n=1 survivor

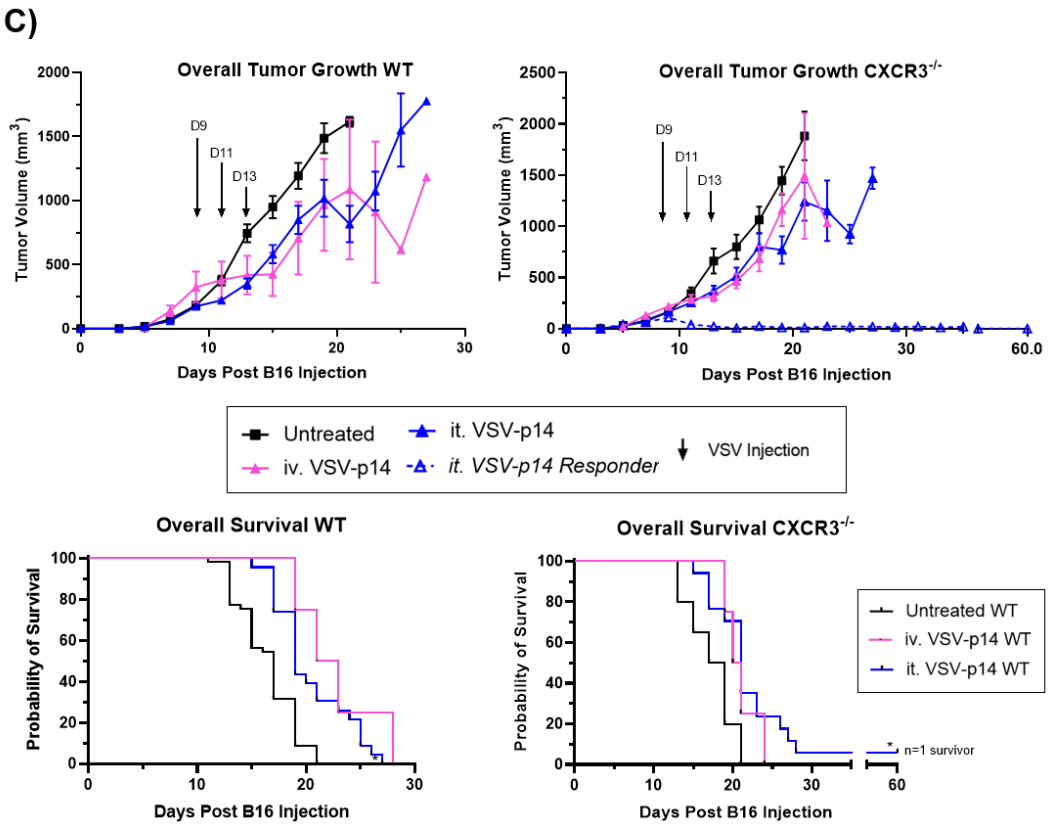

Figure 12. Intratumoral delivery of VSV-GFP and VSV-p14 is more effective than intravenous delivery in WT and CXCR3$^{-/-}$ mice. A) Schematic of B16 tumor induction and treatment timeline. WT and CXCR3$^{-/-}$ C57BL/6 mice were subcutaneously inoculated with 2.5x10^{5} B16 cells on day 0. Mice received intratumoral or intravenous B) VSV-GFP or C) VSV-p14 (5x10^{8} PFU) on days 9, 11, and 13. B16 tumor volume and overall survival were assessed. *p<0.05 vs. untreated (n=4-50 per group for WT cohort, 5-30 for CXCR3$^{-/-}$ cohort).

3.3.2 Delivery of αGalCer-loaded DCs is more effective than free αGalCer in both WT and CXCR3$^{-/-}$ mice

I also compared delivery of free αGalCer to αGalCer loaded on DCs derived from WT C57BL/6 donors. WT and CXCR3$^{-/-}$ mice were inoculated with B16 tumors and received intraperitoneal delivery of 4 μg αGalCer or intravenous delivery of $6x10^5$ αGalCer-DCs 14 days later (Figure 13A). Combination therapy groups also received VSV-GFP or VSV-p14 on days 9, 11, and 13, prior to NKT cell activation therapy (Figure 13A). Free αGalCer and αGalCer-loaded DC monotherapies were surprisingly comparable, inducing the same degree of tumor regression and duration of survival (Figure 13B-C). This roughly equivalent response was observed in both WT and CXCR3$^{-/-}$ cohorts, although, as mentioned previously, the WT cohort responded more robustly to αGalCer than the CXCR3$^{-/-}$ cohort, regardless of whether it was delivered freely or loaded on DCs (Figure 13B-C). However, when free αGalCer was combined with VSV-p14 therapy, this combination appeared modestly less effective than combination with αGalCer-loaded DCs, particularly in the CXCR3$^{-/-}$ cohort (Figure 13B-C). A similar, although weaker, trend was observed with VSV-GFP combination therapy (Figure 13B-C). Overall, free αGalCer delayed tumor outgrowth and prolonged survival to the same extent as αGalCer-loaded DCs as a monotherapy, but was less effective in combination with VSV therapy.

A separate cohort of mice was harvested 19 days after initial tumor inoculation, following treatment with VSV-p14 and either free αGalCer or αGalCer-loaded DCs, for immune profiling of tumors and spleens (Figure 13A). Here, αGalCer-loaded DCs, both alone and in combination therapy, resulted in greater accumulation of NKT cells in tumors and

spleens compared to free αGalCer treatment, suggesting that loading αGalCer on DCs is more effective for NKT cell activation (Figure 13D).

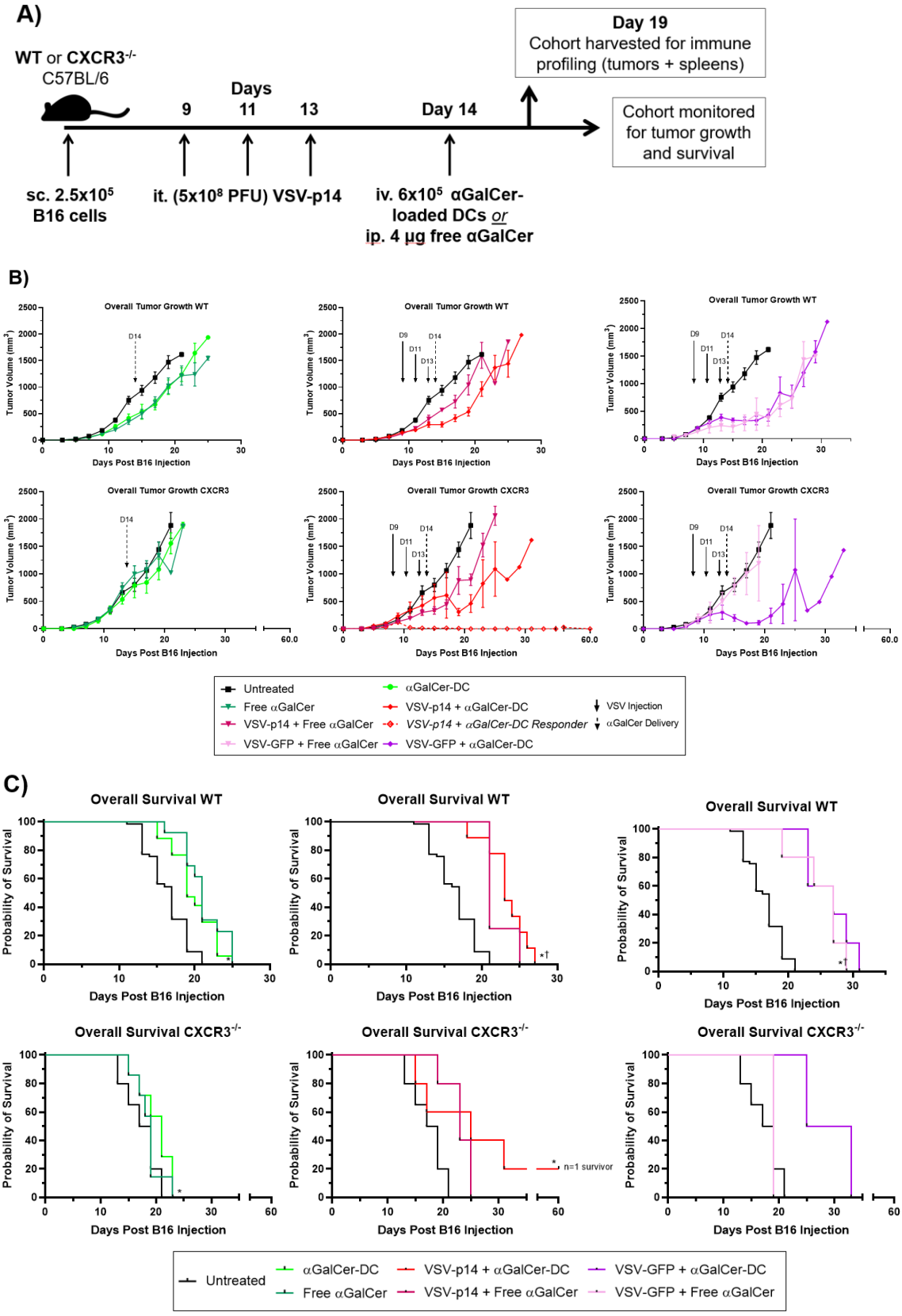
A)
WT or CXCR3-/-
C57BL/6
Days
9
11
13
Day 14
Day 19
Cohort harvested for immune profiling (tumors + spleens)
Cohort monitored for tumor growth and survival
sc. 2.5x10^5 B16 cells
it. (5x10^8 PFU) VSV-p14
iv. 6x10^5 αGalCer-loaded DCs or ip. 4 μg free αGalCer
B)
Overall Tumor Growth WT
Overall Tumor Growth CXCR3
Tumor Volume (mm^3)
Days Post B16 Injection
D9
D11
D13
D14
Untreated
Free αGalCer
VSV-p14 + Free αGalCer
VSV-GFP + Free αGalCer
αGalCer-DC
VSV-p14 + αGalCer-DC
VSV-p14 + αGalCer-DC Responder
VSV-GFP + αGalCer-DC
VSV Injection
αGalCer Delivery
C)
Overall Survival WT
Overall Survival CXCR3-/-
Probability of Survival
Days Post B16 Injection
n=1 survivor
Untreated
αGalCer-DC
Free αGalCer
VSV-p14 + αGalCer-DC
VSV-p14 + Free αGalCer
VSV-GFP + αGalCer-DC
VSV-GFP + Free αGalCer

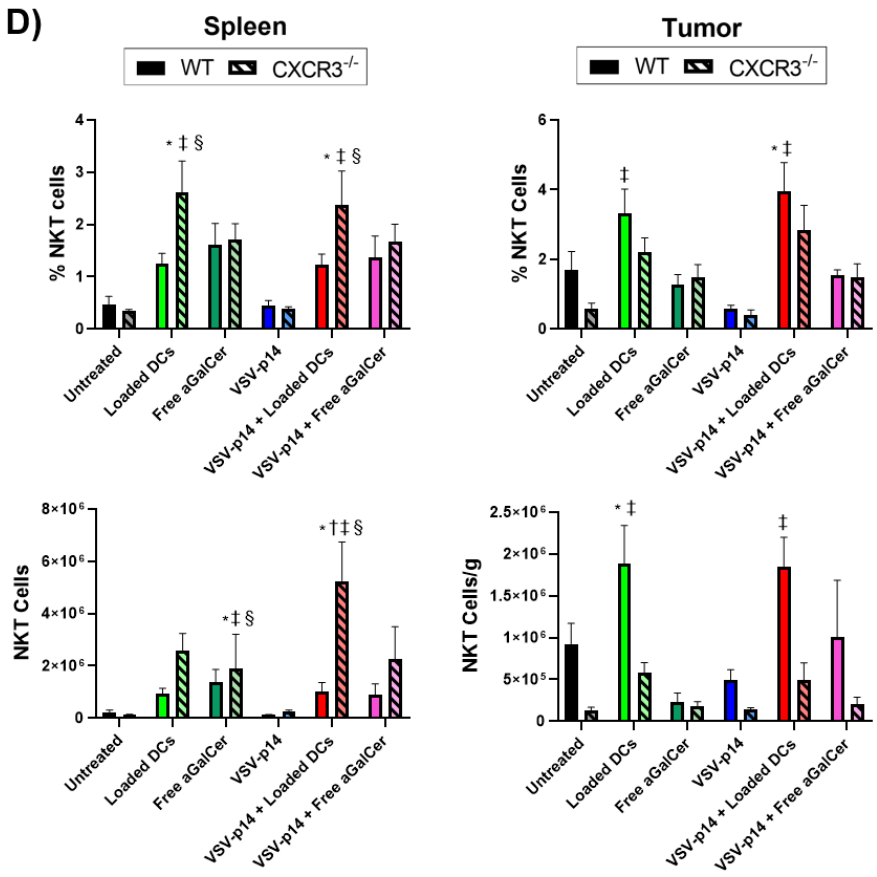

Figure 13. αGalCer-loaded DCs are more effective than free αGalCer alone and in combination with VSV therapy in WT and CXCR3$^{-/-}$ mice. A) Schematic of B16 tumor induction and treatment timeline. WT and CXCR3$^{-/-}$ C57BL/6 mice were subcutaneously inoculated with 2.5x10^5 B16 cells on day 0. Mice received intratumoral VSV-GFP or VSV-p14 (5x10^8 PFU) on days 9, 11, and 13. Mice receiving NKT cell activation treatment received 6x10^5 αGalCer-loaded DCs intravenously or 4 μg free αGalCer intraperitoneally on day 14. B) B16 tumor volume and C) overall survival were assessed in WT and CXCR3$^{-/-}$ untreated mice, those receiving VSV-p14 alone, NKT cell activation treatment alone, or VSV-p14 + NKT cell activation (n=14-50 per group for WT cohort, 7-30 for CXCR3$^{-/-}$ cohort). D) A separate cohort of mice were harvested on day 19. Spleens and tumors of WT and CXCR3$^{-/-}$ mice were isolated and homogenized. Flow cytometry was used to assess NKT cells (CD1d-tetramer$^+$ TCRβ$^+$). Tumor cell counts were normalized to tumor weights. *p<0.05 vs. untreated, †p<0.05 vs. αGalCer-loaded DCs, ‡p<0.05 vs. VSV-p14, §p<0.05 WT vs. CXCR3$^{-/-}$ (n=4-18 for WT cohort, n=3-9 for CXCR3$^{-/-}$ cohort).

3.3.3 DCs derived from CXCR3$^{-/-}$ donors do not exhibit impaired presentation of αGalCer

I also assessed whether the donor source for our *ex vivo*-expanded DCs affected their ability to present αGalCer when transferred back into recipient mice for NKT cell activation therapy. DCs were derived from WT or CXCR3$^{-/-}$ donors and loaded with αGalCer to treat B16 tumor-bearing mice, alone or in combination with VSV-p14 (Figure 14A). No substantial differences were observed between WT and CXCR3$^{-/-}$-derived αGalCer-loaded DCs in their abilities to induce tumor regression and enhance survival duration when they were delivered as a monotherapy (Figure 14B-C). However, CXCR3$^{-/-}$-derived DCs exhibited slightly less efficacy in combination with VSV-p14, particularly in the CXCR3$^{-/-}$ cohort, although this trend may be exaggerated by confounding factors such as tumor ulceration (Figure 14B-C).

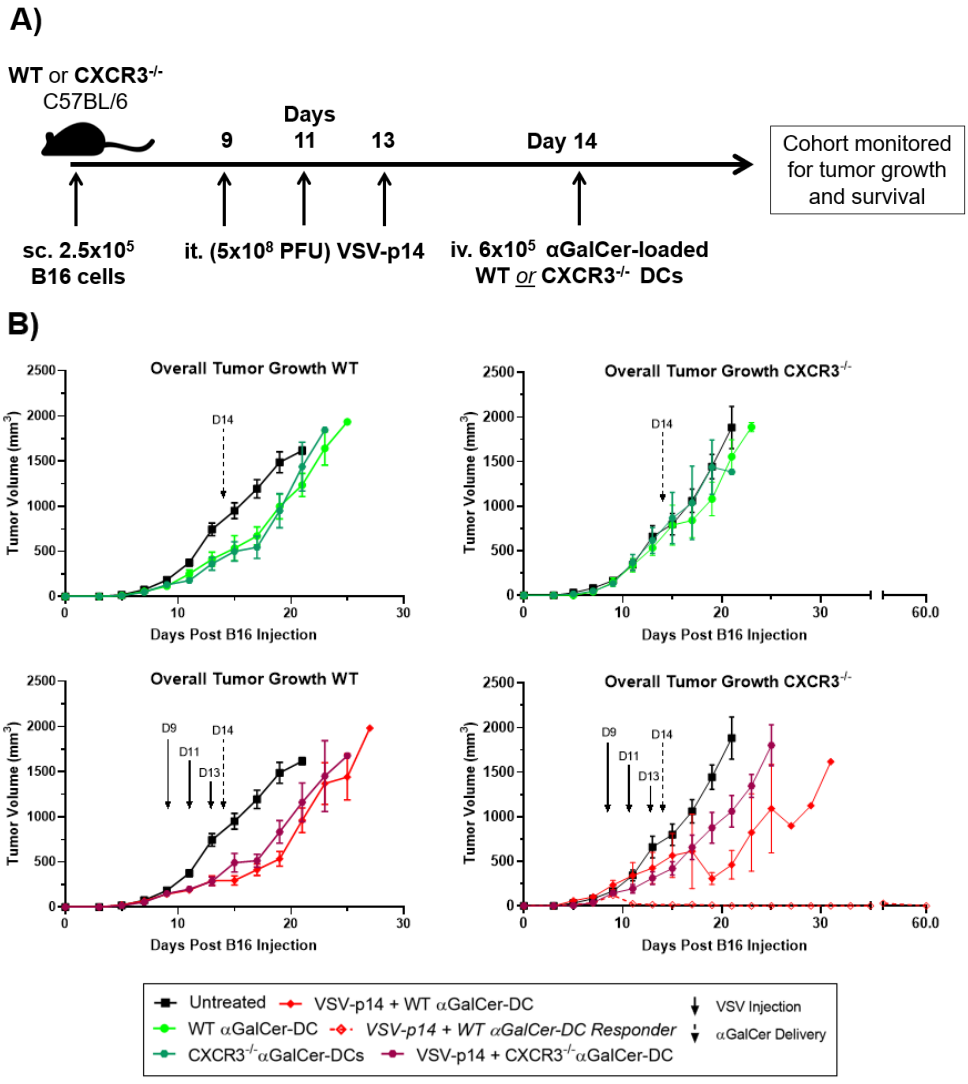
A)
WT or CXCR3-/-
C57BL/6
Days
9
11
13
Day 14
Cohort monitored for tumor growth and survival
sc. 2.5x10^5 B16 cells
it. (5x10^8 PFU) VSV-p14
iv. 6x10^5 αGalCer-loaded WT or CXCR3-/- DCs
B)
Overall Tumor Growth WT
Overall Tumor Growth CXCR3-/-
Tumor Volume (mm3)
Days Post B16 Injection
D9
D11
D13
D14
Untreated
WT αGalCer-DC
CXCR3-/-αGalCer-DCs
VSV-p14 + WT αGalCer-DC
VSV-p14 + WT αGalCer-DC Responder
VSV-p14 + CXCR3-/-αGalCer-DC
VSV Injection
αGalCer Delivery

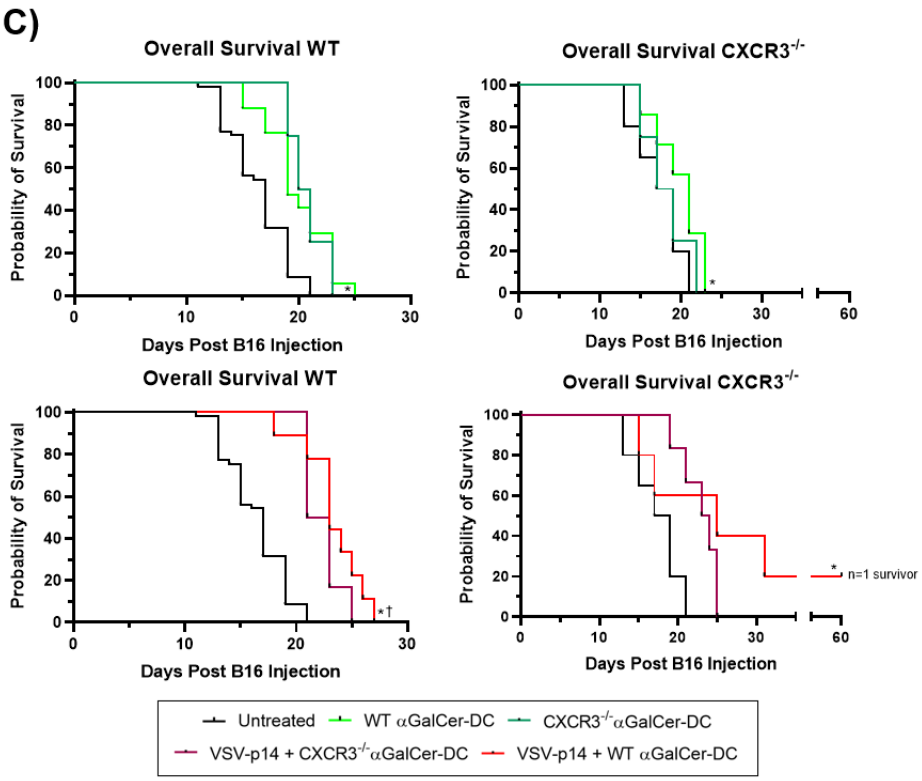

Figure 14. CXCR3$^{-/-}$-derived DCs compared to WT-derived DCs alone and in combination with VSV-p14 in WT and CXCR3$^{-/-}$ mice. A) Schematic of B16 tumor induction and treatment timeline. WT and CXCR3$^{-/-}$ C57BL/6 mice were subcutaneously inoculated with 2.5x10^5 B16 cells on day 0. Mice received intratumoral VSV-p14 (5x10^8 PFU) on days 9, 11, and 13. Mice receiving NKT cell activation treatment received 6x10^5 αGalCer-loaded WT-derived or CXCR3$^{-/-}$-derived DCs intravenously on day 14. B) B16 tumor volume and C) overall survival were assessed in WT and CXCR3$^{-/-}$ untreated mice, those receiving VSV-p14 alone, NKT cell activation treatment alone, or VSV-p14 + NKT cell activation (n=4-50 per group for WT cohort, 5-30 for CXCR3$^{-/-}$ cohort). *p<0.05 vs. untreated, †p<0.05 vs. αGalCer-loaded DCs.

3.3.4 Earlier treatment does not alter efficacy of combined VSV-p14 and NKT cell therapies in WT and CXCR3$^{-/-}$ mice

Given the rapid rate of tumor growth observed in our model, I also tested whether beginning treatment earlier would improve responsiveness. WT and CXCR3$^{-/-}$ mice were inoculated with B16 tumors as described above, but instead of beginning treatment on day 9, mice were treated with VSV-p14 on days 7, 9, and 11, followed by αGalCer-DCs on day 12 (Figure 15A). Day 7 was chosen for earlier treatment initiation because it was the earliest timepoint at which tumors consistently reached an injectable size. Despite issues with ulceration, which will be discussed later, overall responses were similar to those observed with the regular treatment schedule (Figure 15B-C). Combination therapy was consistently most effective in both WT and CXCR3$^{-/-}$ cohorts. Tumor ulceration issues negatively impacted our ability to assess VSV-p14 treatments. αGalCer-loaded DC monotherapy was, as previously described, slightly less effective in the CXCR3$^{-/-}$ cohort (Figure 15B-C). Overall, the comparable duration of responsiveness between timepoints suggest that beginning treatment earlier would not significantly improve therapeutic responses, which underscores the aggressiveness of the B16 melanoma model.

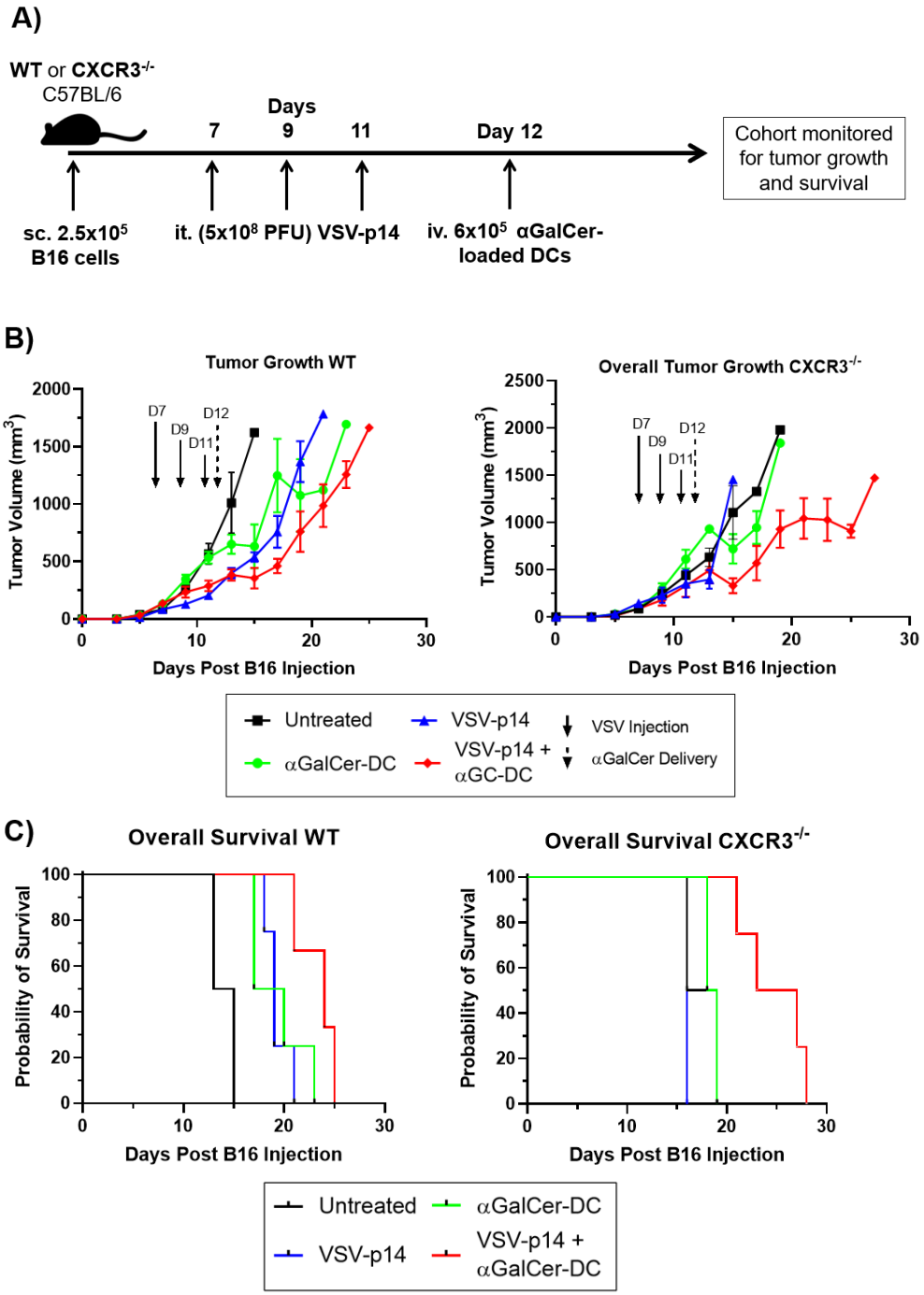

Figure 15. Earlier treatment does not alter efficacy of combined VSV-p14 and NKT cell therapies in WT and CXCR3$^{-/-}$ mice. A) Schematic of B16 tumor induction and treatment timeline. WT and CXCR3$^{-/-}$ C57BL/6 mice were subcutaneously inoculated with 2.5x10^5 B16 cells on day 0. Mice received intratumoral VSV-p14 (5x10^8 PFU) on days 7, 9, and 11. Mice receiving NKT cell activation treatment received 6x10^5 αGalCer-loaded DCs intravenously on day 12. B) B16 tumor volume and C) overall survival were assessed in WT and CXCR3$^{-/-}$ untreated mice, those receiving VSV-p14 alone, NKT cell activation treatment alone, or VSV-p14 + NKT cell activation (n=4-6 per group for WT cohort, 2-7 for CXCR3$^{-/-}$ cohort).

3.4 Enhanced viral persistence in the absence of CXCR3

To follow up on the unexpected efficacy of VSV-p14 in the CXCR3$^{-/-}$ cohort, I conducted tumor plaque assays to assess potential differences in viral persistence between WT and CXCR3$^{-/-}$ mice 24, 48, and 72-hours following VSV-p14 treatment. Mice were inoculated with B16 cells and treated with VSV-p14 9, 11, and 13 days after inoculation. Mice were then harvested on days 14, 15, and 16 and plaque assays were performed using tumor lysates, with intratumoral viral titres normalized to tumor weights (Figure 16A). I found that VSV-p14 was detectable in the tumor lysates of both cohorts up to 72-hours post-treatment, although decreasing over time (Figure 16B). At 24-hours post-treatment, VSV-p14 titres were significantly higher in CXCR3$^{-/-}$ versus WT tumors (Figure 16B), suggesting that loss of CXCR3 may in fact improve the ability of VSV to persist in the tumor in the short term. This could improve the magnitude of oncolytic effects and may account for the improved efficacy of VSV-p14 observed in the CXCR3$^{-/-}$ cohort.

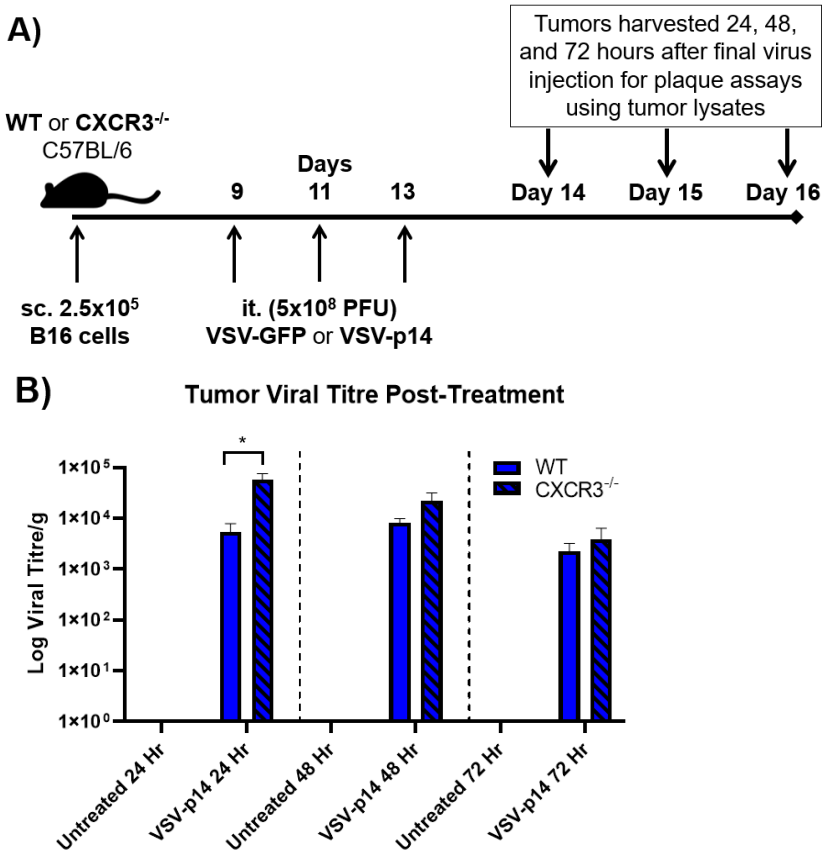

Figure 16. VSV-p14 persists in the tumors of mice for up to 72 hours following treatment. A) Schematic of B16 tumor induction and treatment timeline. WT and CXCR3$^{-/-}$ C57BL/6 mice were subcutaneously inoculated with 2.5x10^5 B16 cells on day 0. Mice received intratumoral VSV-p14 (5x10^8 PFU) on days 9, 11, and 13. Tumors were harvested on days 14, 15, and 16. B) Tumor lysates were used to perform plaque assays to assess viral titre (n=3-5 for untreated groups, n=4-9 for VSV-p14 groups). Titres are normalized to tumor weights. *p<0.05 CXCR3$^{-/-}$ VSV-p14 24 hours vs. WT VSV-p14 24 hours.

CHAPTER 4: DISCUSSION

4.1 Key findings

4.1.1 VSV infection induces production of CXCR3 ligands by B16 melanoma cells *in vitro*

One of the major challenges faced in treating cancers, particularly with immunotherapies, is the immunosuppressive tumor microenvironment [211]. Poor infiltration of key anti-tumor immune cell subsets, such as CD8+ T cells, is highly correlated with poor prognosis in many cancer types, including melanoma [47,212,213,214,215]. There is an ongoing search for therapies that can turn "cold" tumor microenvironments "hot" by increasing recruitment of anti-tumor immune cells. Oncolytic viruses are one promising tool to combat tumor immunosuppression, and have been shown to improve recruitment of anti-tumor immune cells such as CD8+ T cells into tumors, both alone and in combination with immunotherapies such as anti-PD-1 checkpoint blockade, in preclinical models as well as clinical trials [154,216,217]. Mechanisms by which oncolytic viruses might modulate the tumor microenvironment to promote immune infiltration include induction of ICD, release of novel tumor antigens, as well as cytokine and chemokine production. One promising group of chemokines that have been implicated in driving tumor immune infiltration and characterizing "hot" tumors are CXCL9, -10, and -11, which bind the CXCR3 receptor expressed on a range of immune cells including anti-tumor CD8+ T cells, CD4+ Th1 cells, NK cells, and NKT cells to orchestrate their infiltration into inflammatory sites [163,164].

I found that infection with oncolytic VSV-ΔM51 induced B16 melanoma cells to express high levels of CXCL9, -10, and -11 transcripts and produce high levels of CXCL9 and

CXCL10 protein *in vitro* (Figure 4). Both ancestral VSV-ΔM51 as well as VSV-ΔM51 constructs engineered to express a variety of reovirus FAST proteins could drive this CXCR3 ligand production. There was some variation between VSV-FAST constructs in the extent to which they upregulated CXCR3 ligands, but variation overall did not exceed a log difference and no clear patterns emerged, suggesting that observed differences may be due to factors such as minor differences in viral titre, or differences in the ability of VSV constructs to kill B16 cells. However, UV-VSV was unable to induce responses, indicating that CXCR3 ligand induction does require active viral infection and is not merely the result of virus binding to pattern recognition receptors.

These findings suggest that oncolytic VSV could increase immune activation in tumors, which may prime tumors for subsequent immunotherapies, such as NKT cell activation therapy. This is consistent with and extends previous work that found that VSV-ΔM51 increased expression of CXCL9, -10, and -11 transcripts in 4T1 murine breast cancer cells [128]. While this paper did not examine protein levels, it also investigated the ability of oncolytic reovirus to upregulate expression of these chemokines. Reovirus induced significantly lower expression of CXCR3 ligands, particularly CXCL9, suggesting that not all viruses have equivalent abilities to stimulate expression of inflammatory chemokines and other markers of potential immune activation [128].

Of note, CXCL10 has been recognized as a marker associated with ICD [133,218]. ICD is important for driving the indirect immune-activating effects of various oncolytic viruses [133,218,219]. The ability of VSV to upregulate CXCL10 in this model suggests that it may also be inducing ICD, which has been previously shown in both 4T1 and ID8 murine ovarian cancer models, where VSV-ΔM51 was able to upregulate surface calreticulin, as

well as release of ATP and HMGB1, classical markers of ICD [128]. This paper also found that reovirus was unable to stimulate these ICD markers, indicating virus-specific differences in the ability to induce ICD in specific tumor models, which has implications for their ability to potentiate immune activating effects and systemic anti-tumor immunity [128]. However, I did not examine the ability of our VSV constructs in this model to upregulate production of other markers of ICD. Given the inability of VSV, as discussed below, to significantly impact immune populations within tumors and spleens, it appears as if VSV may in fact not actually stimulate potent anti-tumor immunity in the B16 melanoma model *in vivo*, but it would be interesting to assess whether that is related to an inability of VSV to induce ICD in this model, or other reasons.

The ability of B16 melanoma cells to upregulate their own CXCR3 ligand production in culture in response to VSV infection is interesting given the IFN-induced nature of CXCR3 ligands. CXCL9 and CXCL10 are induced by IFNγ and CXCL11 is induced by both IFNγ and Type I IFNs, none of which should be readily produced by B16 cells. Like many cancer cells, they suffer defects in Type I IFN production as well as downstream signaling, as reflected by my finding that IFNα transcripts were not highly produced by B16 cells in response to VSV infection, with some exceptions (Figure 5). This is one feature which renders them more permissive to VSV-ΔM51 infection than healthy cells. Additionally, non-immune cells in general do not produce IFNγ. So, the question remains: how is production of these chemokines induced in the absence of strong IFN signaling? Several reports have outlined additional pathways which work both cooperatively with and potentially independently of IFNs to induce CXCR3 ligand production in various contexts [163]. In particular, CXCL10 has been reported to be induced

by NFκB, as well as IRF3, downstream of RIG-I and TLR signaling [163,220]. CXCL10 has also been shown to be weakly induced by TNF [221,222], which I found was upregulated in B16 cells upon VSV infection (Figure 5). The ability of other cancer cells, such as 4T1 mammary carcinoma cells, to also upregulate CXCR3 ligand production *in vitro* indicates that CXCR3 ligands must be induced to some degree in the absence of Type II IFN signaling and with only weak Type I IFN signaling. Overall, this remains to be further investigated, although it is likely not particularly physiologically relevant in cancer given that there are high levels of IFN production in tumor microenvironments *in vivo*, where CXCR3 ligands are produced to much higher levels by immune and stromal cells in addition to tumor cells themselves.

4.1.2 Combination VSV and NKT cell immunotherapy slows B16 melanoma tumor growth and prolongs survival

Melanoma patient outcomes are highly segregated based on the stage at which they are diagnosed. Melanoma caught early, before metastasis, has a robust cure rate for tumors that are surgically resectable [14,15]. Prior to checkpoint and targeted therapies, metastatic melanoma was considered incurable with a five-year survival rate under 10% [223]. Even with the development of targeted and checkpoint blockade therapies in the last ten years, the five-year survival rate for metastatic melanoma remains below 30% [1,14]. Despite the breakthrough provided by these therapies, they have significant limitations: only a subset of melanoma patients with BRAF-mutant tumors are eligible for targeted BRAF/MEK inhibitor therapies, and checkpoint blockade therapies such as anti-PD-1 and anti-CTLA-4 both have substantial toxicities, and only work for a period of time before the majority of patients relapse [18,25,30]. Another therapeutic strategy which has broken ground in

advanced melanoma treatment is oncolytic virus therapy, with the landmark clinical approval of oncolytic T-VEC in 2015 [34]. T-VEC (oncolytic HSV-1 encoding GM-CSF) highlights the promise of oncolytic virus therapy in treating advanced metastatic cancers, as it not only induces regression of primary tumors, but can target distant metastases due to systemic anti-tumor immune activation [33].

Given that VSV infection induced robust production of CXCR3 ligands in B16 melanoma cells, which indicated a potential for VSV to "prime" the B16 tumor environment to enhance subsequent immune infiltration, I investigated whether oncolytic VSV therapy combined with NKT cell activation immunotherapy would improve outcomes relative to individual therapies. Here, I report that the combination of oncolytic VSV therapy with NKT cell activation immunotherapy slowed B16 melanoma tumor growth and prolonged survival to a greater extent than monotherapies, but that ultimately there was limited synergy between the two therapies in this model (Figure 6, 7).

Both VSV and NKT cell activation therapies improved survival and slowed tumor growth individually. NKT cell activation monotherapy, which involved the activation of endogenous NKT cells by αGalCer-loaded DCs, was the least effective of our therapeutic interventions, by a small margin, although it still prolonged survival beyond the untreated baseline. Mice tended to experience a brief window of measurable tumor regression 3 to 5 days post-treatment followed by relapsed exponential tumor growth, potentially indicating an inability for NKT cell activation to overcome, in this model, a rapidly-proliferating tumor and/or immunosuppressive environment (Figure 6, 7). However, NKT cell activation by αGalCer-DCs did induce robust and significant increases in NKT cell levels in both tumors and spleens 5 days post-treatment, indicating that NKT cell therapy

was able to induce proliferation and/or recruitment of NKT cells (Figure 9). NKT cell levels were increased to the same extent by both NKT cell monotherapy and combination therapy, indicating that while combination therapy may have greater therapeutic efficacy, the addition of VSV was not measurably impacting tumor immune infiltration to increase NKT cell levels as we had initially expected (Figure 9). NKT cell activation, both alone and in combination therapy, also led to decreased expression of PD-1 on a variety of immune populations including CD8+ T, CD4+ T, and NK cells in spleens, but only CD4+ T cells in tumors (Figure 10). This suggests that NKT cells may be able to modulate the tumor microenvironment to some degree, as has been previously reported [92,106,107]. In order to tease out why NKT activation therapy was not particularly effective in this model, we assessed our treatment schedule. By the time mice were treated, 14 days post B16-tumor inoculation, tumors tended to be quite large, so we evaluated whether administering αGalCer-DCs at day 12 would improve the ability of NKT cell therapy to control tumor outgrowth. However, earlier treatment induced the same 3-to-5-day window of measurable tumor regression followed by a return to exponential tumor outgrowth, suggesting that tumor size at first treatment is not a major barrier to efficacy (Figure 15), at least within the timeframe examined. We also found limited differences in efficacy between delivery of αGalCer-loaded DCs delivered intravenously versus αGalCer delivered directly into the peritoneal cavity, with both delivery methods inducing similar levels of tumor regression and survival duration (Figure 13). This is interesting, as free αGalCer delivery is known to be less effective than delivery on DCs, which are able to provide additional signals such as CD40 and IL-12 which active NKT cells more strongly and avoid anergy induction [224,225]. Glycolipids loaded on non-

professional APCs are known to induce less favourable cytokine responses and NKT cell anergy [63,92,115]. Given this, we expected αGalCer-loaded DCs to mediate more robust anti-tumor effects. We did find, however, that αGalCer-DCs increased NKT cell levels in tumors and spleens to a significantly higher degree than free αGalCer, in line with previous work indicating loaded DCs lead to more robust activation (Figure 13). But, the fact that these increased NKT cell levels upon αGalCer-loaded DC treatment did not translate to increased therapeutic efficacy suggests that additional increases in NKT cell levels past a certain threshold may not contribute to further anti-tumor effects in this model. This concept of a "threshold" for NKT cell activity has been noted previously in a mouse model with humanized CD1d expression, where mice had tenfold fewer NKT cells but their activation cleared tumors just as effectively [93]. In this model, this threshold is likely due in part to the fact that B16 melanoma cells express limited to no CD1d, meaning that NKT cells have a limited capacity to directly target tumor cells in this model. Instead, anti-tumor effects of NKT cell therapy must rely primarily on activation of other immune cells such as NK cells and CD8+ T cells, or targeting of suppressive subsets like MDSCs [101,103,226]. This reliance on indirect anti-tumor effects may serve as a threshold for efficacy. Taken together, these results indicate that NKT cell activation therapy is not particularly effective in this model, and likely unable to mediate substantial anti-tumor effects as a monotherapy against B16 melanoma.

VSV monotherapy was marginally more effective than NKT cell monotherapy, though still less effective than combination therapy. I assessed both VSV-GFP as well as VSV-p14, a VSV construct encoding a FAST protein from reptilian reovirus [156]. VSV-GFP monotherapy led to more variable treatment responses than combination therapy, with a

greater proportion of mice reaching endpoint tumor volume at earlier time points, but it did lead to complete cures in 2 mice, one from the WT cohort and one from the CXCR3$^{-/-}$ cohort, whereas no complete cures were observed in the VSV-GFP combination therapy groups (Figure 6). The CXCR3$^{-/-}$ VSV-GFP monotherapy cohort experienced high levels of ulceration, which will be discussed in greater detail in the limitations section below, which resulted in incomplete collection of tumor growth and survival data for that cohort, although overall trends resembled the WT cohort (Figure 6). VSV-p14 monotherapy also induced more variable treatment responses than combination therapy, particularly in the WT cohort, but led to a complete cure in one VSV-p14 monotherapy treated CXCR3$^{-/-}$ mouse, as well as a complete cure in one VSV-p14 combination therapy treated CXCR3$^{-/-}$ mouse (Figure 7). The ability of VSV therapy to induce complete and sustained tumor regression in a small subset of mice indicates the potential for this therapy to be highly effective under specific conditions which remain to be fully elucidated.

In an attempt to untangle what some of the conditions driving the robust responses in a subset of our VSV-treated mice might be, I evaluated whether mice who had smaller tumors at first injection would respond more robustly to treatment, by initiating VSV-p14 treatment 7 days post- B16 tumor inoculation rather than 9 days post-inoculation. Seven days post-inoculation represents the first time point at which all tumors were consistently large enough to receive accurate intratumoral injections. I found no differences in treatment efficacy, suggesting that tumor volume at initial treatment does not substantially impact responses to VSV-p14 therapy (Figure 15). I also compared intravenous and intratumoral delivery of VSV-GFP and VSV-p14, and found that intratumoral delivery was modestly more effective than the intravenous route, perhaps

indicating some inability of intravenously-injected virus to reach the tumor site as effectively (Figure 12). This is a non-issue for targeting of primary tumors, such as melanoma, which are accessible by skin, but has implications for non-injectable primary tumor types as well as targeting of metastases. T-VEC is also delivered intratumorally in the clinic, but despite this intratumoral delivery it has shown the ability to target distant non-injected metastatic sites [34]. I did not assess the ability of intratumoral versus intravenous VSV to target metastases, which could be investigated in future in this model, as B16-F10 melanoma cells readily metastasize to the lungs.

I also found that VSV-p14 therapy did not substantially affect levels of most lymphoid and myeloid populations in spleens or tumors of mice (Figure 9, 10, 11). One exception includes a VSV-p14-driven trend towards increased splenic CD8+ T cells (Figure 10D), which was noted previously in a 4T1 breast cancer model [154]. However, this increase did not translate to increased levels of CD8+ T cells within melanoma tumors, which suggests it may not be relevant for anti-tumor effects, or that treatment-induced migration of CD8+ T cells was incomplete when immune populations were sampled, which was only 6 days following the third and final round of VSV-p14 injection (Figure 10). VSV-p14 treatment also increased levels of granulocytic cells within tumors, which may include granulocytic MDSCs, although no functional assays were performed to assess the suppressive capacity of these cells (Figure 11). Some viruses, such as influenza, have been shown to induce MDSC accumulation [106]. In contrast, oncolytic VSV constructs induced granulocytic myeloid cell infiltration in a pancreatic cancer model, but there was no increase in suppressive activity [129]. Overall, immune cell infiltration assays suggest that VSV-p14 may have minimal immune activating effects in the B16 model, and may

be mediating its anti-tumor effects primarily by direct tumor cell oncolysis. This conclusion was also reached in a Panc02 pancreatic cancer model, where both VSV-GFP and VSV-IL-15 monotherapies exhibited minimal immune activating effects on their own, but were able to enhance survival and decrease tumor weight, likely primarily through direct oncolysis [129]. Given time constraints, immune cell profiling following VSV-GFP monotherapy or combination therapy was not conducted in my work, but previous work has suggested that VSV-GFP induces less activation and infiltration of key immune subsets such as CD4+ T cells and CD8+ T cells than VSV-p14 in the 4T1 model and induced minimal immune activation in the Panc02 model as well [129,154].

Interestingly, I found that VSV-p14 therapy was overall slightly less effective than VSV-GFP, indicating that inclusion of a FAST protein did not significantly improve the efficacy of VSV therapy in this model, unlike in other tumor models [154]. VSV-p14 was previously compared with VSV-GFP in 4T1 breast cancer and CT26 colon cancer models in BALB/c mice, where it was found to improve survival and significantly decrease lung metastatic burden relative to VSV-GFP [154]. Our project did not directly examine the effects of either VSV-GFP or VSV-p14 on metastatic burden, although B16-F10 melanoma is known to aggressively metastasize to the lungs [227,228] –this is an oversight which could be addressed in the future. B16 melanoma differs from the 4T1 and CT26 models in several respects which may contribute to the observed lack of difference between VSV-GFP and VSV-p14. First, B16 melanoma is on the C57BL/6 genetic background, which is known to have a more Th1-skewed immune system compared to the Th2-skewed BALB/c background [229]. These differences result in well-documented differences in the susceptibility of C57BL/6 versus BALB/c mice to infections and

autoimmune diseases, and have implications for cancers which are conventionally best-targeted by Th1 immunity [229,230,231]. Given this, it is not unlikely that C57BL/6 and BALB/c mice may have different responses, or degrees of responsiveness, to VSV infection. It is possible that the increased immune activation observed as a result of VSV-p14 infection in the BALB/c model is a result of the viral infection shifting the balance toward a more Th1-dominant immune response, which would be more apparent on a more Th2-dominant immune background. Since the C57BL/6 background is more Th1-dominant at baseline, VSV-p14 infection may not be polarizing the immune response as noticeably or to the same extent. Additionally, as viral clearance is Th1-mediated, there may be better viral persistence in BALB/c mice, which could lead to enhanced viral efficacy. Secondly, B16 melanoma grows significantly faster than the primary 4T1 breast cancer model, and the compressed timeline of this model could potentially obscure subtler differences between treatments. Third, while B16 tumors are considered poorly immunogenic because of their limited expression of MHC Class I, they are still more immune-infiltrated and immunotherapy-responsive than 4T1 breast cancer tumors, which are poorly immunogenic and immunosuppressed [227,228].The baseline differences in these tumor microenvironments may mean that any immune activating effects potentiated by VSV-p14 have a greater, more noticeable impact on a very “cold” tumor model like 4T1 breast cancer.

Finally, as mentioned earlier, combination VSV and NKT cell activation therapy was more effective than either monotherapy. Combination therapy mediated the most consistent therapeutic responses, as seen in slower tumor outgrowth and increased overall survival duration in the largest proportion of treated mice (Figure 6, 7). While mice

treated with VSV or NKT cell monotherapies generally experienced tumor regression or slowed growth for a period of 3 to 5 days before relapse, combination-treated mice experienced benefits for up to 5 to 7 days before relapse, reflected by surviving on average for an additional 4 days (20% increase) relative to monotherapies for VSV-p14 combination therapy, and an additional 7 to 9 days (35-45% increase) relative to monotherapies for VSV-GFP combination therapy (Figure 6, 7). However, immune populations were surprisingly unchanged by combination therapy relative to monotherapies (Figure 9, 10). Although NKT cell therapy alone was less effective than combination therapy, it did induce comparable increases in NKT cells in tumors and spleens of untreated mice, suggesting that addition of VSV therapy does not significantly impact NKT cell recruitment or proliferation (Figure 9). Similar results were observed for other immune populations, including key anti-tumor immune subsets like NK cells, CD8+ T cells, and CD4+ T cells, which did not experience robust patterns of change in response to combination therapy (Figure 10). These results indicate that, although VSV may increase production of important immune-recruiting chemokines CXCL9 and CXCL10, this is not priming the tumor for subsequent increased immune infiltration as was initially hypothesized. One caveat to this observation is that immune profiling was conducted on a compressed timeframe because untreated mice reached endpoint tumor volume only 19 days post tumor-inoculation. Given this, immune profiling had to be conducted on day 19, which was only 5 days post-NKT cell therapy, and 6 days after the final dose of VSV was delivered, meaning that adaptive responses to combination therapy may not have been fully developed by this point. But, given this data, it appears that the enhanced efficacy of combination therapy compared to monotherapies is not due

to synergistic effects between the two therapies, as immune populations did not change in unique ways in response to combination therapy. Instead, the enhanced efficacy of combination therapy may be due to additive benefits from each therapy, with direct oncolysis mediating improved tumor control for a slightly longer period with the addition of NKT cell activation-mediated tumor regression.

However, despite the improved efficacy of combination therapy, only one VSV-p14 combination therapy treated mouse (in the CXCR3$^{-/-}$ cohort) experienced complete tumor regression (Figure 7). The remaining VSV-GFP and VSV-p14 combination therapy treated mice all relapsed and reached endpoint tumor volume by a maximum of 33 days post-tumor inoculation (Figure 6). So, what factors might be contributing to incomplete response and relapse? One factor might be the immunosuppressive tumor microenvironment. We observed very high levels of PD-1 expression on intratumoral CD8+ T cells (50-75%), indicating that this key anti-tumor immune population was highly exhausted, which results in reduced functionality (Figure 10). PD-1 was also highly expressed on other intratumoral immune populations, including CD4+ T cells (15-35%), NK cells (5-20%), and NKT cells (5-10%) (Figure 9, 10). PD-1 levels were generally highest in the untreated groups, which at day 19 were at endpoint, and slightly lower in treated groups (Figure 9, 10). Though tumors were not sampled for immune profiling at multiple time points, it is possible that PD-1 expression increases over time as a result of ongoing immune activation, which may be one mechanism mediating the loss of therapeutic efficacy over time. These results indicate that addition of anti-PD-1 checkpoint blockade as a triple therapy following NKT cell activation may prolong anti-tumor therapeutic responses, which will be discussed further below. Additionally, Tregs

comprised 5-15% of tumor-infiltrating CD4+ T cells and may also contribute to immunosuppression in this model (Figure 10). Other immunosuppressive mechanisms which were not assessed, such as recruitment of MDSCs, may also contribute to loss of immunotherapy efficacy, as has been reported in many other models [49]. Another mechanism contributing to loss of therapeutic efficacy in both VSV monotherapy and combination therapy is viral clearance. I found that VSV was able to persist in tumors for up to 72 hours post-treatment, but with decreasing viral titres over time ($5x10^8$ PFU/mL injected intratumorally versus $2\text{-}4x10^3$ PFU/mL recovered 72-hours post final injection), suggesting that VSV was in the process of being cleared from tumors (Figure 16). I did not follow intratumoral VSV levels beyond 72 hours, or assess the effects of combination therapy on intratumoral viral persistence, but decreasing viral titres indicate that oncolytic effects are lessening and likely being lost after the 3-5 day window of efficacy observed with VSV therapy.

Overall, while combination VSV and NKT cell immunotherapy was effective at delaying tumor growth and prolonging survival in a B16 melanoma model, incomplete responses and relapse of most mice indicate that this combination therapy will likely need to be further developed to exhibit clinical efficacy comparable to or greater than that currently being observed with the use of targeted therapies and checkpoint blockade immunotherapy.

4.1.3 CXCR3 axis is dispensable for NKT cell immunotherapy

The therapeutic responses outlined in the previous section were, with some key exceptions, comparable between WT and $CXCR3^{-/-}$ cohorts, indicating that loss of

CXCR3 does not significantly negatively affect overall therapeutic responses to NKT cell therapy, alone or in combination with VSV therapy.

CXCR3$^{-/-}$ mice also exhibited responses to VSV and NKT cell therapies, alone and in combination (Figure 6, 7). Other than NKT cells, loss of CXCR3 did not negatively impact intratumoral levels of other key anti-tumor immune populations, including CD8+ T cells and NK cells (Figure 10). This stands in contrast to previous work by Mikucki et al. [165] and Wendel et al. [73] which reported that CXCR3 was non-redundantly required for CD8+ T cell and NK cell trafficking into tumors, respectively. However, both of those papers utilized adoptive transfer models, and while it may be the case that CXCR3 is non-redundantly required for adoptive transfer of CD8+ T and NK cells into established tumors, other work has suggested that CXCR3 is not required for trafficking of endogenous T cells into B16 melanoma and other tumors, particularly in the early stages of tumor development, where other chemokine axes such as CCR5 may work cooperatively with CXCR3 to aid in trafficking of tumor-infiltrating immune cells [69,169,170]. Our results align more neatly with this second model of multi-stage, CXCR3-redundant infiltration of immune cells into tumors.

However, previous work in this area has focused primarily on CD8+ T cells and NK cells, and neglected to investigate the role of these chemokine axes on the tumor trafficking of NKT cells, which also express high levels of CXCR3 and lower levels of CCR5 [162,167,176]. We report that loss of CXCR3 significantly reduced levels of NKT cell levels within CXCR3$^{-/-}$ tumors upon αGalCer-loaded DC NKT cell activation therapy (Figure 9). This suggests that loss of CXCR3 negatively affects the recruitment and/or proliferation of NKT cells within tumors, particularly upon NKT cell activation therapy,

which causes NKT cell proliferation. Additionally, NKT cell levels trended lower in untreated CXCR3$^{-/-}$ tumors compared to WT, suggesting that loss of CXCR3 may reduce baseline infiltration of NKT cells into tumors (Figure 9). This pattern was reversed in spleens, where CXCR3$^{-/-}$ mice had significantly increased NKT cell levels, suggesting that loss of CXCR3 may impair migration of proliferating NKT cells out of the spleen into tumor sites, or result in NKT cell accumulation in the spleen if they cannot traffic elsewhere (Figure 9). These results are much more striking than the lack of difference observed for other key anti-tumor immune populations; however, as a point of consideration, our αGalCer-loaded DC therapy specifically induces activation and proliferation of NKT cells, which could be amplifying an effect that otherwise might not be particularly visible in the absence of treatment. While NKT cell accumulation in untreated and VSV-p14 treated tumors trend towards decrease in the CXCR3$^{-/-}$ cohort, these differences are not statistically significant without the administration of αGalCer-loaded DC therapy. Perhaps therapies specifically activating CD8+ T cells and NK cells would tease out the same CXCR3-dependent differences. Also, as mentioned briefly above, immune profiling was conducted less than a week after the delivery of NKT cell activation therapy and the final dose of VSV therapy, which may be a sufficient timeline for the activation and proliferation of more innate-like lymphoid populations like NK cells and NKT cells, but may be too short of a window to fully assess CD8+ and CD4+ T cell responses to therapy. Finally, it is worth noting that although NKT cell levels are lower in CXCR3$^{-/-}$ tumors, they are not absent, and they are still increased above the untreated baseline upon NKT cell activation therapy, indicating that while CXCR3 may be important for recruitment and/or proliferation of activated NKT cells within tumors, it

is not the only factor involved. Ultimately, these decreased NKT cell levels only modestly reduced efficacy of NKT cell therapy in CXCR3$^{-/-}$ mice (Figure 6,7). As mentioned previously, this suggests that there may be a threshold for NKT cell activation past which greater accumulation does not correlate with greater anti-tumor effects in this model, potentially due in part to limited CD1d expression on B16 cells resulting in the inability of NKT cells to mediate direct anti-tumor effects [93,101,226]. These results further highlight that NKT cell therapy overall may have limited efficacy in the B16 melanoma model, which ultimately suggests that this may not be the best tumor model in which to tease out CXCR3-dependent differences in therapeutic efficacy.

4.1.4 Loss of CXCR3 enhances response to VSV therapy

To add another layer to the story of CXCR3, I was surprised to find that loss of CXCR3, instead of negatively affecting therapeutic responsiveness, appeared to improve responses to VSV therapy. This trend towards improved efficacy was seen both in VSV monotherapy and in combination with NKT activation therapy using αGalCer-loaded DCs. This response was more pronounced with VSV-p14 than VSV-GFP, likely due to incomplete collection of VSV-GFP tumor growth and survival data due to ulceration. CXCR3$^{-/-}$ mice which received both VSV-p14 monotherapy and combination therapy experienced greater tumor regression and prolonged survival compared to their WT counterparts (Figure 7). WT VSV-p14 treated mice survived on average 19 days, compared to CXCR3$^{-/-}$ VSV-p14 monotherapy treated mice who survived on average 21 days, with one mouse experiencing complete tumor regression (Figure 7). WT VSV-p14 combination therapy treated mice survived on average 23 days, whereas CXCR3$^{-/-}$ combination therapy treated mice survived on average 25 days, with one mouse

experiencing complete tumor regression (Figure 7). No mice in the WT group experienced complete tumor regression in response to VSV-p14, although there was one WT complete responder with VSV-GFP treatment, along with a $CXCR3^{-/-}$ VSV-GFP complete responder (Figure 6).

This improved responsiveness did not correlate with any notable immune population changes in response to VSV-p14 therapy (Figure 10), suggesting once again that VSV may be mediating its effects primarily by direct oncolysis rather than indirect immune activation in this model. These differences in therapeutic response then, could be due to differences in viral persistence within tumors, which would affect the duration and strength of direct oncolytic effects. And in fact, I did find that $CXCR3^{-/-}$ tumors had greater than ten-fold higher VSV-p14 titres compared to WT mice at 24-hours post-treatment with VSV-p14, a highly significant increase (p=0.0009) (Figure 16). Viral titres decreased at 48 and 72-hours post-treatment, but still trended higher in $CXCR3^{-/-}$ mice (Figure 16). These results suggest that loss of CXCR3 may improve the ability of VSV to persist in the tumor, at least in the short term, which could improve the magnitude and duration of oncolysis and lead to the improved tumor regression and survival I observed in VSV-treated $CXCR3^{-/-}$ mice.

This finding is corroborated by previous work investigating the role of CXCR3 in viral infections which has suggested that loss of CXCR3 impairs the ability of immune cells at the site of infection to clear virus. A paper by Hickman et al. [168] demonstrated, in a model of skin vaccina virus infection, that global knockout of CXCR3 did not impair the ability of CD8+ T cells to migrate to skin, but did specifically impair the ability of $CXCR3^{-/-}$ CD8+ T cells to successfully locate virus-infected cells for killing, exacerbating infection

in CXCR3$^{-/-}$ mice. Another paper reported similar findings using epidermal infection with HSV-1, where they found that, although both virus-specific and bystander cytotoxic T lymphocytes migrated through the epidermis without any observable directional preference, there was a subtle CXCR3-dependent preference for migration towards local sites of infection, leading to increased efficiency of T cell accumulation in those sites that was only recognized upon quantitative analysis [232]. The importance of the CXCR3 axis was also reported in the colocalization of CD8+ T cells with lymphocytic choriomeningitis virus (LCMV) antigen in the spleen [233]. The CXCR3 axis was also found to play a key role in shaping CD8+ T cell immunity against HSV-2 infection locally within latently-infected tissues, and preventing recurrence of active viral infection [234]. Yet another paper reported that CXCR3 and CCR5 together were important for the ability of effector CD8+ T cells to re-encounter influenza antigen within specific microenvironments in the lung [235]. Together, this work in viral infection models mirrors findings by Chow et al. [69] which reported in a B16 melanoma model that CXCR3 was more important for immune cell positioning and interaction with other cells than it was for recruitment into the tumor itself. In the context of oncolytic viral infection of tumor cells, these findings may mean that the CXCR3 axis is important for mediating the ability of CD8+ T cells to target virus-infected cells within tumors, which has implications for how long the virus persists at the tumor site. Loss of CXCR3, by improving viral persistence, could improve the duration of oncolysis, which could lead to improved therapeutic responses in a model where the virus is acting primarily by direct oncolysis. On the other hand, if an oncolytic virus was mediating anti-tumor effects primarily by

inducing immune activation and recruitment, loss of CXCR3 might instead dampen its efficacy.

4.1.4 Combination therapy has the potential to stimulate long-lasting immune memory

Oncolytic VSV and NKT cell immunotherapy were able to generate complete tumor regression in a very small subset of treated mice, including two VSV-GFP monotherapy treated mice (one WT, one CXCR3$^{-/-}$), one VSV-p14 monotherapy treated CXCR3$^{-/-}$ mouse, and one VSV-p14 combination therapy treated CXCR3$^{-/-}$ mouse (Figure 6, 7). Although the two VSV-GFP complete responders were unable to be re-challenged and assessed for immune memory responses due to COVID-19-related shutdown of the animal care facility, the two VSV-p14 complete responders were re-challenged with B16 melanoma cells 60 days after initial inoculation. The complete responder from VSV-p14 monotherapy experienced tumor regrowth at a similar rate to naïve mice challenged with B16 cells for the first time, indicating that persistent anti-tumor immune memory had not formed in this mouse. The complete responder to VSV-p14 combination therapy, however, completely resisted B16 tumor re-challenge, indicating the potential formation of robust anti-tumor immune memory. This was further dissected by immune profiling 60 days following rechallenge. Compared to two completely naïve controls, the complete responder exhibited increased memory populations, including effector memory (CD44+) CD4+ and CD8+ T cell populations in the spleen and lymph nodes, alongside decreases in naïve (CD62L+CD44-) CD4+ and CD8+ T cells in the spleen as well as increased PD-1 expression on CD4+ and CD8+ T cells in the spleen, which may be a lingering consequence of immune activation upon initial B16 challenge and re-challenge (Figure

8). Central memory (CD44+ CD62L+) CD4+ and CD8+ T cell populations remained relatively unchanged (Figure 8). One caveat to our delineation of these memory populations was the failure of our anti-CCR7 fluorochrome, which was intended to more precisely delineate effector memory (CCR7-) from central memory and naïve T cell populations (CCR7+). In the absence of CCR7 staining, central and effector memory populations are less clearly distinguished, but we can still observe overall trends towards the formation of memory T cell and memory-like NKT cell populations upon combination therapy. All NKT cells have a "memory" phenotype upon exiting the thymus characterized by high CD44 expression [236], but more specific "memory-like" populations of NKT cells have been described which upregulate CD62L (which most NKT cells do not normally express) following glycolipid stimulation [162,167,237]. These CD62L+ NKT cells have "memory-like" features including increased persistence; resistance to acquisition of exhaustion markers and apoptosis; as well as continued proliferation and cytokine production [237]. Given this, I have used CD62L expression to delineate increases in "memory-like" NKT cells in our work. NKT cell activation therapy using αGalCer-loaded DCs has also been shown to amplify memory CD8+ T cells leading to persistent anti-tumor immunity in several tumor models [238,239]. This may be one reason why we observed robust anti-tumor immune memory in our combination therapy-treated complete responder, but not our VSV-p14 monotherapy-treated complete responder.

Notably, the mouse that developed this anti-tumor immune memory response upon combination therapy was from the CXCR3$^{-/-}$ cohort. Interestingly, the CXCR3 axis has also been implicated in the formation of immune memory populations, with loss of

CXCR3 (with a minor role for CCR5) on effector CD8+ T cells leading to formation of massive numbers of memory CD8+ T cells following influenza and *Mycobacterium tuberculosis* infection, as a result of effector CXCR3$^{-/-}$ CD8+ T cells being less likely to re-encounter antigen and thus undergo contraction [235]. A similar pattern was observed in LCMV infection, with absence of CD8+ T cell CXCR3 expression leading to fewer short-lived effector cells and a much larger central memory population, which had fewer effector memory cells and exhibited a greater recall response [233]. These findings do not fully align with our own observations, as our CXCR3$^{-/-}$ complete responder appeared to have greater effector memory populations, but again technical issues may have interfered with our ability to effectively delineate effector memory from central memory populations. This previous work corresponds interestingly with the fact that we observed three CXCR3$^{-/-}$ complete responders to therapy and only one WT complete responder to therapy, which could be investigated more rigorously in future studies. Overall, we found that combination VSV-p14 and NKT cell activation therapy were able to induce not only complete tumor regression but seemingly protective anti-tumor immunity in one CXCR3$^{-/-}$ mouse.

4.2 Limitations and challenges

4.2.1 Mouse models of melanoma

The work in this thesis used the transplantable syngeneic B16-F10 murine melanoma model on the C57BL/6 background. The B16 melanoma model has been in use since the late 1970s and remains one of the most common mouse melanoma models used experimentally [227,228]. It was a spontaneous melanoma first derived from a male C57BL/6 mouse, and several sublines have since been derived which vary in terms of their ability

to metastasize and their immunogenicity [227]. The most common variant, and the one used in this thesis, is B16-F10, which is highly aggressive and will rapidly form lung metastases after primary subcutaneous injection, as well as after intravenous delivery [227]. B16 melanoma is a fast-growing tumor, with untreated tumors reaching endpoint volumes 2 to 4 weeks after subcutaneous tumor inoculation depending on the volume inoculated. This compressed timeline has been noted previously to make it difficult to assess therapies because of the short therapeutic window [228].

B16 melanoma possesses several notable genetic differences from human melanomas which limit its ability to accurately model human melanoma. B16 melanoma tumors have been classified as poorly immunogenic, because B16 cells express low levels of MHC Class I, in contrast to human melanomas which vary more widely in their MHC I expression [227,228,240]. This low MHC I expression is also characteristic of untransformed C57BL/6 melanocytes, and so appears to be a characteristic retained after they became malignant [227]. B16 melanoma has long been regarded as difficult-to-treat for these reasons, and a tough test for the efficacy of therapies [227]. That being said, B16 melanoma is less immunologically "cold" than many other common murine cancer models, as it responds robustly to anti-PD-1 and anti-CTLA-4 checkpoint blockade [228,241]. B16 melanoma cells express PD-L1 and B7 molecules (CD80 and CD86) which are able to bind PD-1 and CTLA-4 on the surface of CD8+ T cells and other anti-tumor immune populations to induce immune exhaustion, effects reversible by checkpoint blockade [228]. B16 cells do also, despite their low MHC I expression, express high levels of T-cell targetable melanoma-associated self-antigens, including gp100 and tyrosinase related protein 2 (TRP2) [228,240]. Overall, though, B16 melanoma cells have much less genomic

heterogeneity and a lower mutational burden than most human melanomas, especially UV-driven melanomas, which are regarded as one of the most highly immunogenic cancers [228,242]. Importantly, B16 melanoma does not possess activating mutations in the BRAF oncogene, the most common driver mutation in human melanoma, expressed in over half of human melanoma cases [228,243]. This means that B16 melanoma cannot be used to test the efficacy of combination therapies with BRAF-targeted therapy, which is one of the most common therapies currently in clinical use [14]. B16 melanoma also possesses a functional phosphatase and tensin homologue deleted on chromosome 10 (PTEN) protein, which is lost in 30-60% of sporadic human melanomas [228,243]. However, B16 melanoma does possess deletions in the CDKN2A locus leading to inactivation of the $p16^{INK4a}$ and $p19^{Arf}$ ($p14^{ARF}$ in humans) tumor suppressor proteins which negatively regulate cell cycling [243]. These mutations have also been described in heritable as well as sporadic human melanoma [243]. Overall, these genetic differences represent a major limitation of B16 melanoma as a model of human melanoma. Additionally, as a subcutaneous transplantation model, B16 melanoma is unable to model the natural spontaneous development of melanoma as well as how melanoma spreads through the layers of the skin [240].

Given the limitations of the B16 melanoma model, other mouse melanoma models which more accurately mimic human melanoma have been developed. Human xenograft models have been developed which involve the transplantation of either human melanoma cell lines, primary melanoma cells, or patient-derived tumor xenografts into immunodeficient nude athymic mice or non-obese diabetic/severe combined immunodeficiency (NOD/SCID) mice [240]. These models on their own are excellent for better understanding

pathways driving malignancy, metastasis, and treatment resistance in more relevant human melanomas, but the lack of an immune system in these models is a significant drawback which prevents immunotherapies from being tested [240]. Because of this, more recently, humanized mouse models have been developed which re-introduce humanized or partially humanized immune systems into these mice to re-capitulate the role of the immune system –however, such approaches are still technically challenging and can be expensive [240].

In addition to these xenograft models, there are genetically engineered mouse (GEM) models which have been critical in identifying key genes and factors driving melanoma tumorigenesis and progression [240,244]. GEM models are generated by the introduction of targeted driver mutations to model specific aspects of melanoma, such as loss of PTEN or overactivation of BRAF. The Cre recombinase/LoxP system is the most common technique to induce such conditional mutant mouse models. It involves expression of the Cre recombinase gene under the control of a tissue-specific promoter. Cre recombinase recognizes the LoxP DNA sequence, and catalyzes recombination between two repeated LoxP sites, resulting in the deletion of any sequence between the two LoxP sites, which has been used to either knock out a tumor suppressor gene or constitutively activate an oncogene [244]. It has been refined to allow for precise spatiotemporal targeting of genes for conditional knockout or overexpression using a mutant Cre recombinase fused to the ligand binding portion of the estrogen receptor (ER) [244]. Cre-ER will remain inactive until the administration of tamoxifen, the ligand for ER, which activates the Cre-ER recombinase, allowing for the deletion or activation of a gene at a specific timepoint [244]. This Cre-ER/LoxP system has been used to generate conditional knockouts of PTEN,

loss of which is normally embryonic lethal, as well as activation of the most common human BRAF mutation $BRAF^{V600E}$ [240]. Importantly, a GEM model has been generated which possesses both mutations at the same time under the control of the melanocyte-specific Tyr promoter, leading to the formation of spontaneous metastatic melanoma in these mice [245,246]. This model, which is denoted as the Tyr::$CreER^{T2}$, $BRAF^{V600E}$, $Pten^{lox/lox}$ model, has been extensively used to assess how BRAF mutations drive melanoma tumorigenesis, how resistance to targeted $BRAF^{V600E}$ inhibitors develops, and to test other therapeutics [247,248,249,250].

In addition to GEM models which recapitulate common human drivers of melanoma in mice, there are models which aim to simulate the natural development of melanoma, such as UV-radiation induced melanoma. Although development of mouse and human melanocytes is highly similar, there are several anatomical and functional differences between mouse and human skin which render mouse melanocytes highly resistant to UV-radiation-induced melanoma [244]. In human skin, melanocytes can be found along the basal layer of the epidermis as well as in hair follicles. Mouse melanocytes, by contrast, are found primarily at the bottom of hair follicles and in the dermal layer [240]. Because of these differences between mouse and human skin, mice rarely develop spontaneous melanomas, and those which do develop are histologically different from human melanomas, as they are primarily located in the dermis, whereas human melanomas are found primarily in the epidermis or at the junction between those two layers [244]. Specific genetic modifications, such as constitutive expression of a hepatocyte growth factor/scatter factor (HGF/SF) transgene, can modify the distribution of melanocytes in mouse skin, enhancing their susceptibility to transformation by UV radiation and the

similarity of the melanomas which develop to human melanoma [240,244]. This HGF/SF GEM model has been instrumental in better understanding how UV radiation drives melanoma tumorigenesis, and the kinds of mutations that arise from this radiation-driven damage, and can be combined with additional genetic modifications such as inactivating CDKN2A or PTEN, or activating mutant BRAF [240,251,252].

All of these models represent steps beyond the B16 melanoma model which more accurately model human melanoma in a variety of ways, from the use of human melanoma cells in immunodeficient mice, to GEM models which recapitulate key driver mutations in human melanoma such as BRAF mutations, or simulate the natural progression of UV radiation-driven melanoma development. More complex and robust melanoma models should be considered in future to more rigorously test prospective immunotherapies, including and beyond VSV therapy and NKT cell activation therapy.

4.2.2 Tumor ulceration

The most significant technical challenge encountered during this project was related to tumor ulceration. High levels of tumor ulceration interfered with data collection across the course of this project. Ulceration is defined as the loss of the epidermal layer at the surface of the tumor, with some loss of deeper skin layers as well [253]. Ulcerations occur in subcutaneous tumor models, like B16 melanoma, typically as a result of tumor cell necrosis. Ulceration can be driven by rapid tumor growth leading to skin rupture, alterations in blood supply leading to hypoxic tumor areas, mechanical trauma, and cancer therapies, particularly those which involve intratumoral injection and stimulate tumor lysis (such as oncolytic virus therapy) [253]. Throughout this project, 25-50% of mice

in individual experiments developed ulcerations. Ulceration frequencies were similar between WT and CXCR3$^{-/-}$ cohorts and affected both treated and untreated mice in similar proportions, although VSV-treated groups had a slightly higher ulceration rate than NKT cell immunotherapy groups, likely due to the intratumoral delivery strategy as well as oncolytic effects. Ulcerations began early in the experimental course, as early as 7 days after B16 tumor inoculation and frequently resulted in the premature sacrifice of mice before endpoint tumor volume was reached, interfering with my ability to collect complete and coherent tumor growth and survival data that evaluated treatment efficacy.

To combat this issue, I increased the number of mice in each experimental group to account for loss due to ulceration. I was also permitted to conducted a pilot study using ulceration scoring guidelines developed based on the University of British Columbia and McGill University's ulceration scoring guidelines to guide more consistent assessment of our mice [253,254], with the hope that it would allow us use mice more effectively, even when the early stages of ulceration were beginning. Canadian Council on Animal Care (CCAC) guidelines developed in 1998 state that ulceration of tumors should be considered a humane endpoint, but more recent work has indicated that there is scientific rationale for keeping animals with ulcerated tumors; for example, to better model human cancer, as well as immunotherapies in which ulceration is frequently a sign of a successful anti-tumor response [253]. Ulcerations also have the capacity to stabilize, and in some cases heal, as we saw during our pilot study. We showed that monitoring mice using a defined set of ulceration scoring criteria prolonged the length of time that mice were allowed to remain in the study, and improved our completion of data collection by a significant margin. Unfortunately, I completed my thesis work before these ulceration

scoring guidelines were approved, and so I was not able to benefit from their implementation directly. CCAC has subsequently released updated guidelines for experimental endpoints related to tumor ulceration and monitoring of cancer therapy effects (March 2022 ISBN: 978-0-919087-95-8). Under these guidelines, I would not have been required to remove mice from my experiments.

4.2.3 VSV-N primers

Another challenge encountered at the end of this project was in developing VSV-N primers for RT-qPCR. We were hoping to verify our tumor plaque assay data by assessing intratumoral levels of VSV-N via RT-qPCR or digital droplet RT-PCR (ddPCR). I tested previously published VSV-N primer sequences and found poor and potentially non-specific amplification, as seen through the production of multiple-peaked melt curves. Unfortunately, we were unable to design VSV-N primers that did not have off-target amplification, and all new candidate VSV-N primer sequences we queried had significant sequence similarity with various mouse genes. We tested three new candidate VSV-N primer pairs and found that, although they induced high levels of amplification in our VSV-p14-treated pooled tumor samples, as well as pooled VSV-infected CMT167 cells, they also induced lower levels of background amplification in our untreated pooled tumor samples as well as pooled media-control CMT167 cells. Interestingly, a single melt curve peak, as well as specific band formation on endpoint PCR gels indicated that this background amplification was not due to non-specific formation of primer-dimers or other artifacts. We considered contamination as a potential source, but all non-template controls run, including those for housekeeping genes, were clean. We subsequently

found a paper which also reported a high level of false positive signal generated by use of internal VSV-N primers for RT-qPCR, due to RNA self-priming causing a lack of strand specificity [255]. To work around this, the authors used a tagged-primer approach, where they generated a VSV-N-specific forward primer tagged with an unrelated nucleotide sequence at the 5' end, and a reverse primer complementary to the tag sequence [255]. The authors found that this approach completely eliminated amplification of DNA made by RNA self-priming, as they found no background signal [255]. This approach is likely more stringent than necessary, as they were trying to specifically distinguish between positive-sense VSV-N mRNA and negative-sense VSV-N genomic RNA. A simpler version of their approach could be utilized to simply minimize background signal, by carrying out a specific reverse transcription step with VSV-N primers to produce specifically VSV-N cDNA rather than the random primer approach for reverse transcription we used initially. Moving forward, this VSV-N specific RT step should be considered to minimize non-specific background signal, and perhaps a tagged-primer approach could be considered to more accurately assess levels of replication-competent VSV with RT-qPCR.

4.3 Future directions

4.3.1 Effect of CXCR3 on recruitment, proliferation, and functionality of immune populations

This work evaluated the impact of CXCR3 loss on overall accumulation of key immune populations within tumors, but did not thoroughly dissect the contributions of recruitment versus intratumoral proliferation of immune cells to this accumulation. Teasing out these differences may be important to understand the role of the CXCR3 axis more fully in response to these therapies. For example, Chow et al. [69] established that loss of CXCR3

did not affect recruitment of CD8+ T cells into tumors regardless of anti-PD-1 therapy. But, in the absence of CXCR3, anti-PD-1 therapy was unable to induce intratumoral CD8+ T cell proliferation to the same extent, resulting in an increased level of CD8+ T cells in the WT relative to the CXCR3$^{-/-}$ cohort that was due not to impaired recruitment in the absence of CXCR3, but impaired proliferation. Understanding the relative contributions of recruitment versus intratumoral proliferation to the increased levels of NKT cells within WT versus CXCR3$^{-/-}$ tumors upon NKT cell activation therapy would help us better understand what role CXCR3 is mediating in that increase. Differences in recruitment could be assessed via adoptive transfer of CD45.2 NKT cells into CD45.1 congenic C57BL/6 mice, and proliferation could be measured using Ki67 expression as a proliferation marker.

Additionally, while I looked at surface expression of CD69, a marker of early activation, and PD-1, a co-inhibitory marker associated with functional immune exhaustion, I did not delve into the effects of CXCR3 on immune cell functionality or activation by, for example, profiling the ability of NKT cells to make IFNγ or other cytokines, or assessing the relative cytotoxic ability of these populations upon different treatments and in the absence of CXCR3. I attempted to perform cytotoxicity assays on CD8+ T cells, NK cells, and NKT cells purified from WT and CXCR3$^{-/-}$ spleens following VSV-p14 treatment and NKT cell therapy using Annexin V and 7-AAD staining, but ran into technical difficulties that I was unable to resolve.

4.3.2 Role of CXCR3 in other cancer models

Melanoma is generally considered to be a highly immunogenic and well immune-infiltrated cancer, and unlike other cancer types, such as pancreatic cancer, shows a high degree of responsiveness to immunotherapies like anti-PD-1 and anti-CTLA-4 checkpoint blockade [242,256,257]. Given this, it may be beneficial to examine the role of the CXCR3 axis in other cancer types, particularly those which are highly immune-excluded at baseline. Assessing the role of CXCR3, particularly with therapies like oncolytic VSV that stimulate production of CXCR3 ligands, in a cancer type that has significantly less immune infiltration prior to treatment may allow one to delineate the role of CXCR3 more clearly during the later stages of immune cell recruitment into an established tumor. This would also allow an assessment of the importance of the CXCR3 axis for turning a truly "cold" immune-excluded tumor "hot".

4.3.3 Alternate chemokine axes

As has been discussed at length already, the role of the CXCR3 axis in cancer is complicated by its relationships with other chemokine axes which may act in a redundant or cooperative fashion. Of particular note is the CCR5 axis, which has been implicated as a potential collaborator with CXCR3 in the recruitment of key anti-tumor immune populations such as CD8+ T cells and NK cells into tumors, particularly in the early stages of tumor development, where it has been suggested to drive later CXCR3-dependent recruitment [169,234]. This redundancy could help explain why we observed minimal changes in several key anti-tumor immune populations, such as CD8+ T cells, NK cells, and CD4+ T cells, in CXCR3-deficient mice. CCR5 has also been shown to be highly upregulated on NKT cells following αGalCer treatment, and $CCR5^{-/-}$ NKT cells have shown impaired recruitment into B16 tumors relative to WT NKT cells in co-

adoptive transfer experiments, further highlighting a potential role for the CCR5 axis to work in concert with CXCR3 in recruiting key anti-tumor immune populations in the context of our immunotherapies [258]. However, like the CXCR3 axis, the CCR5 axis is a double-edged sword in cancer, and has also been implicated in pro-tumorigenic functions including promoting tumor survival and metastasis in CCR5-expressing tumors, recruiting CCR5+ Tregs, and promoting the formation of MDSCs [160,259,260,261]. To better understand the combined roles of CXCR3 and CCR5, CXCR3/CCR5 double-knockouts could be generated to assess whether redundancy or early CCR5-driven seeding of immune populations in the tumor are able to compensate for loss of CXCR3 in our model.

Beyond CCR5, several other chemokine axes may play important roles in the complicated recruitment of immune cells into tumor sites. Most relevant for this work is CXCR6, which is constitutively expressed on NKT cells and has been shown to be important for their recruitment into the liver, tumor, and other sites [167,258,262]. Previous work has shown that CXCL16 (the ligand for CXCR6) produced by glycolipid-loaded DCs induced higher production of IFNγ by NKT cells, and that loss of CXCL16 expression by DCs resulted in impaired protection from metastasis and tumor control [263]. $CXCR6^{-/-}$ NKT cells have impaired recruitment into B16 tumors when co-adoptively transferred with WT NKT cells into $J\alpha18^{-/-}$ mice, further highlighting a role for CXCR6 in the recruitment of NKT cells into tumors [258]. This work indicates that the CXCR6/CXCL16 chemokine axis may also play an important role in mediating the efficacy of NKT cell therapy in cancer, and should be considered along with the CXCR3 axis. However, the CXCR6 axis is also highly associated with poor prognosis in

numerous cancers, and has been reported to drive tumorigenesis by enhancing angiogenesis, promoting metastasis, and inducing proliferation of CXCR6-expressing tumor cells [264,265,266,267]. Additionally, it has been shown that CXCR6$^{-/-}$ mice have defective NKT cell accumulation and activation, making it difficult to untangle the specific role of CXCR6 in NKT cell recruitment alone and the implications of that recruitment for cancer [262]. Blocking CXCL16 or adoptive transfer of CXCR6$^{-/-}$ NKT cells or CXCR3$^{-/-}$/CXCR6$^{-/-}$ NKT cells into tumor-bearing Jα18$^{-/-}$ mice may be ways to correct for the reduced NKT cell numbers in CXCR6$^{-/-}$ mice when examining the role of both chemokine axes in immune cell recruitment and tumorigenesis, but there are still challenges with these models.

Finally, to get a fuller but perhaps less flattering picture of the role of CXCR3 in B16 melanoma, lung metastatic burden could also be assessed in the presence and absence of CXCR3, as CXCR3 has been previously implicated in driving metastasis of melanoma tumor cells [197].

Ultimately, the CXCR3 axis likely does not have a single clear-cut role in cancer, but instead plays multiple important roles which are interconnected and cooperate with a variety of other chemokine axes. Given this, unraveling the roles of, and harnessing the CXCR3 axis in cancer immunotherapies will likely prove to be therapy and tumor-specific.

4.3.4 Improving treatment responsiveness with checkpoint blockade triple therapy

Despite the ability of oncolytic VSV and NKT activation therapy to slow tumor growth and prolong survival, particularly in combination therapy, most of our mice relapsed by

day 25 and therapeutic benefits were lost. If VSV and NKT activation combination therapy were to move forward in this model, it would likely require the addition of a third therapy to improve treatment responsiveness past day 25. One appealing candidate for triple therapy is checkpoint blockade, such as anti-PD-1, anti-PD-L1, or anti-CTLA-4. As previously mentioned, B16 melanoma cells express PD-L1 and B7, and show robust responses to checkpoint blockade therapies [228]. We showed in this work that tumor-infiltrating immune cells such as CD8+ T cells expressed high levels of PD-1, indicative of immune exhaustion, which may be contributing to the limited window of efficacy we observed with our therapies. Our laboratory has recently demonstrated that PD-1 therapy can combine effectively with oncolytic VSV and NKT cell activation therapy in a model of pancreatic cancer [129]. As melanoma is a "hotter" tumor microenvironment, adding anti-PD-1 therapy following NKT cell activation could help re-invigorate the immunosuppressed tumor microenvironment and prolong the duration of therapeutic efficacy in the B16 melanoma model.

4.3.5 Other oncolytic viruses

VSV is only one of many oncolytic virus platforms. Another means of improving therapeutic efficacy in future may be to replace oncolytic VSV with another oncolytic virus better suited for combination therapy with NKT cell activation –namely, an oncolytic virus able to stimulate significant immune-activating effects in addition to direct tumor oncolysis.

Beyond VSV, reovirus has also been tested in combination with NKT cell activation therapy, where it was able to augment NKT cell therapy in murine ID8 ovarian cancer but

not 4T1 breast cancer, demonstrating that specific oncolytic viruses may interact with NKT cell therapies to a different extent in different models [128]. Given this, it is possible that other oncolytic viruses may work more synergistically with NKT cell therapy than VSV has in B16 melanoma. The oncolytic reovirus construct Pelareorep has been previously tested in a clinical trial for metastatic melanoma, where it had no measurable objective responses, suggesting that additional modifications are likely needed to make it an effective candidate for melanoma therapy [268].

Another promising oncolytic platform is HSV-1, which forms the backbone of T-VEC and has shown great success in melanoma [132]. T-VEC has more recently been combined in clinical trials with other immunotherapies, such as anti-PD-1 checkpoint blockade, where it has improved response rates over anti-PD-1 alone without significantly increasing toxicity [216]. This indicates that T-VEC may be an appealing candidate for combination with NKT cell therapy as it has been shown to have potent immune-stimulating effects that could augment the efficacy of other immunotherapies [132]. T-VEC is also an excellent example of an oncolytic virus which has been genetically engineered to encode immunomodulatory genes. Specifically, T-VEC encodes the cytokine GM-CSF which leads to the recruitment and maturation of antigen-presenting cells to increase their potential to activate anti-tumor immune populations like cytotoxic CD8+ T cells [132,269]. Other HSV-1-based oncolytics have also been tested in clinical trials for melanoma, with limited efficacy, indicating that even with the same viral backbone, different oncolytic constructs can have very different efficacy [269,270].

Oncolytic coxsackie virus CVA21 has also been tested in a clinical trial for advanced metastatic melanoma, where it induced an overall response rate of 28% and durable

response rate of 19%, comparable to T-VEC in clinical trial, but with no associated toxicities, suggesting that it may be another appealing option for further development [271]. This trial also showed that CVA21 was able to drive influx of tumor-infiltrating CD8+ T cells, as well as increased expression of PD-L1 and other immune checkpoints within tumors, indicating that it has immune-activating effects [271]. CVA21 has since been used with great success in combination with checkpoint blockade in multiple clinical trials [132,272]. One ongoing clinical trial combining CVA21 with pembrolizumab (anti-PD-1) is reporting an interim objective response rate of 73% for all patients enrolled, and 100% objective response rate for patients with stage IV disease [272]. Given the strength of these responses, with tolerable toxicity, the study has been opened to enroll up to 50 patients [272]. The ability of CVA21 to mediate both direct oncolysis as well as improve immune infiltration into tumors makes it a very promising candidate for combination with additional, cell-based immunotherapies like NKT cell therapy.

Oncolytic adenoviruses and poxviruses are additional appealing options which, like HSV-1 based oncolytics, have the benefit of being larger double-stranded DNA viruses which can be engineered to express larger or multiple genes compared to smaller viruses like VSV-ΔM51, although DNA viruses do have the added risk of DNA insertion [273]. Oncolytic adenoviruses have been engineered to express several different immunomodulatory genes which increase their immunostimulatory effects [273]. Poxviruses have even been engineered to express multiple immunostimulatory genes at once. For example, PROSTVAC, which has been tested as a neoadjuvant vaccine in prostate cancer, is a combination of vaccinia virus and fowlpox which express prostate-specific antigen (PSA) as well as three costimulatory molecules (B7.1, ICAM-1, and LFA-3) to

enhance antigen presentation and activate tumor-specific cytotoxic T cells [273,274]. Though not used as an oncolytic specifically, this provides a blueprint for the delivery of multiple immunomodulatory genes at once in a single oncolytic vector to improve its ability to carry out not only direct tumor lysis but also potentiate broader anti-tumor immunity. For oncolytic viruses to be most effective, both alone and in combination therapies, they must be able to stimulate robust anti-tumor immunity, and engineering oncolytic viruses that contain immunomodulatory domains to help drive these immune stimulating effects is a promising way forward.

4.3.6 Beyond NKT cell activation therapy

NKT cell activation therapy alone did not exhibit substantial efficacy in our B16 melanoma model. To combat that, it can be combined with additional therapies to potentially boost its efficacy, including oncolytic virus therapy, or checkpoint blockade. Another option is to harness NKT cells themselves in a different way. Previous work has looked at transferring autologous, *ex vivo* expanded NKT cells back into patients, and more recent work has begun to build on NKT cells as a potential allogeneic "off-the-shelf" option for adoptive cell transfer [109]. Beyond either of those options, however, is the design of genetically modified "enhanced" NKT cells, as an expansion of the promising chimeric antigen receptor (CAR) T cell therapy. Briefly, CARs are modular synthetic receptors with four main components. First, they have an extracellular target antigen binding domain, generally targeted against a tumor antigen, derived from the variable heavy (V_H) and light (V_L) chains of a monoclonal antibody forming a single chain variable fragment (scFv) [275]. Because of this structure, CAR recognition of target antigens is MHC-independent. This antigen binding domain is connected to the plasma

membrane by a hinge region, followed by a membrane-spanning domain, and one or more intracellular signaling units [275]. These intracellular signaling units have diversified across the generations of CAR therapy to transmit stronger and more robust immune activating signals [275]. CAR constructs have most commonly been transduced into T cells, to generate CAR-T cells with redirected specificity for tumor antigens. CAR-T cells have had great success in treating blood cancers, with the FDA approval of anti-CD19 CAR-T cell therapy for B cell malignancies in 2017 [275]. However, CAR-T cells still possess significant limitations, including potentially life-threatening CAR-T cell associated toxicities mediated by graft vs. host disease, cytokine release syndrome, and other off-target effects. CAR-T cells also have limited efficacy against solid tumors, in part due to antigen escape, poor trafficking and infiltration, as well as immunosuppressive tumor microenvironments [275].

CAR-NKT cells, which are NKT cells engineered to express a CAR on their surface in addition to their semi-invariant TCR, overcome many of the limitations faced by CAR-T cells. First, they have an improved safety profile due to their expression of a distinct cytokine repertoire which limits cytokine storms [109]. They also recognize glycolipid antigens presented on non-polymorphic CD1d, which limits the potential toxicity of NKT cells in allogeneic settings [276]. CAR-NKT cells are also positioned to resist antigen escape, due to their ability to dually target tumor antigens using their CAR as well as their semi-invariant TCR in cancers that express CD1d [277]. Previous work has reported that anti-CD19 CAR-NKT cells are more effective than anti-CD19 CAR-T cells against CD1d-expressing lymphomas, including those in the brain [277]. They also showed that administration of αGalCer was able to further drive the activation of these CAR-NKT

cells, suggesting that αGalCer delivery may be another way to enhance CAR-NKT cell therapy [277]. CAR-NKT cells also express a variety of other receptors such as NK cell receptors which allow them to be activated by other mechanisms [109]. NKT cells have also been shown to be able to overcome immunosuppressive tumor environments by inhibiting MSDCs and TAMs via direct cytotoxic effects or release of immune polarizing cytokines [109]. CAR-NKT cells, then, are also uniquely positioned to help reverse tumor immunosuppression in solid tumors. These NKT cell characteristics make them highly effective candidates for use in CAR therapy.

CAR-NKT cells have been used in clinical trials to target neuroblastoma with great success and lower toxicity than CAR-T cells [278]. Anti-GD2 CAR-NKT cells localized to tumors, exhibited strong cytotoxic effects, and had a good safety profile [278]. Of the ten patients enrolled, one patient exhibited a complete response, another patient responded partially, and three patients had stable disease [278]. CAR-NKT cells have not been tested in clinical trials for melanoma, but they have been generated to recognize melanoma, through the production of anti-CSPG4 CAR-NKT cells which have shown strong cytotoxic effects and anti-tumor benefits in pre-clinical melanoma models [279].

Overall, NKT cells have many characteristics which make them ideal candidates for cancer immunotherapy. Finding new ways to harness NKT cells, for example, through the engineering of CAR-NKT cells, will allow them to break ground in the next generation of cancer immunotherapies.

4.4 Concluding remarks

To summarize, NKT cells are an often-overlooked immune population which play important roles in anti-tumor immunity. Activation of NKT cells with αGalCer-loaded DCs has been shown to induce tumor regression and prolong survival in various cancer models, but has variable efficacy in the clinic. Oncolytic viruses are another promising anti-cancer therapy which have been effective in a variety of cancers, including melanoma. Oncolytic viruses mediate their anti-tumor effects through both direct tumor lysis and indirect immune activation, which has been shown to potentiate subsequent immune infiltration and immunotherapies. The CXCR3 chemokine axis is one mechanism governing the migration of immune cells, including NKT cells, and has been shown to be important for immune infiltration into tumors. In this work, I not only attempted to improve the efficacy of NKT cell activation therapy and oncolytic VSV-ΔM51 therapies through combination therapy, but was interested in elucidating the importance of the CXCR3 axis for the functionality of these two therapies, alone and in combination.

I found that combining VSV-ΔM51 (expressing GFP or expressing the FAST protein p14) with NKT cell activation therapy delayed tumor outgrowth and significantly prolonged survival in a murine B16 melanoma model. However, the loss of CXCR3 did not negatively impact overall responses to treatment, suggesting that the CXCR3 axis may be ultimately dispensable for our combined therapy. NKT cell therapy increased accumulation of NKT cells in WT mice, but $CXCR3^{-/-}$ mice exhibited reduced NKT cell levels within tumors, indicating that loss of CXCR3 at least partially impaired their recruitment and/or proliferation within tumors. This ultimately did not translate to significantly reduced therapeutic efficacy, suggesting that NKT cell increases past a

certain threshold did not improve therapeutic efficacy, or that NKT cell therapy was not particularly effective in this model regardless of CXCR3 expression. Potentially, increased oncolytic VSV activity in CXCR3$^{-/-}$ mice may also have compensated for reduced NKT cell activity in combination therapy. Loss of CXCR3 did not reduce levels of other key anti-tumor subsets within tumors, including CD8+ T cells and NK cells, suggesting that redundancy in the chemokine system may be able to compensate for loss of this chemokine axis. However, CXCR3$^{-/-}$ mice exhibited surprisingly improved responses to VSV therapy, particularly with VSV-p14. Loss of CXCR3 improved the ability of VSV-p14 to persist in the tumor in the short-term, which could increase the magnitude of oncolysis, providing an explanation for the improved tumor regression and survival we observed in VSV-p14-treated CXCR3$^{-/-}$ mice. VSV-p14 therapy alone, or in combination with NKT cell therapy, did not induce significant changes in immune populations within tumors or spleens, suggesting that, although VSV was able to upregulate B16 melanoma cell production of CXCR3 ligands *in vitro*, this did not translate to significant immune activating effects or increased immune infiltration following VSV treatment *in vivo*. In total, four mice exhibited complete responses to treatment, two in response to VSV-GFP, one in response to VSV-p14, and one in response to VSV-p14 and NKT cell combination therapy. Of the VSV-p14 complete responders, only the combination therapy-treated responder exhibited persistent anti-tumor immune memory and an ability to resist tumor re-challenge. To conclude, combination VSV and NKT cell activation therapy exhibited modest anti-tumor effects in B16 melanoma, effects which did not appear reliant on the CXCR3 axis for either independent function or synergy.

Next steps include considering methods to improve the efficacy of VSV and NKT cell activation therapies in melanoma, including the addition of subsequent anti-PD-1 checkpoint blockade for triple therapy, as well as considering the contributions of additional chemokine axes such as CCR5 which may be working cooperatively or redundantly with CXCR3 in our tumor setting. Elucidating the roles of these chemokine axes in these therapies will allow for more precise targeting of the chemokine system to enhance immune infiltration and improve therapeutic efficacy. Moving forward, finding ways to enhance the immune-stimulating effects of oncolytic virus therapy will further enhance its efficacy in combination with immunotherapies such as NKT cell activation therapy, and considering ways to enhance the efficacy of NKT cells through genetic engineering or additional combination therapies, will pave the way for next-generation combination immunotherapies to more effectively treat cancers including and beyond melanoma.

REFERENCES

1. CCSA. 2021. Canadian Cancer Statistics 2021. cancer.ca/Canadian-Cancer-Statistics-2021-EN

2. Brenner DR, Poirier A, Woods RR, Ellison LF, Billette J-M, Demers AA, Zhang SX, Yao C, Finley C, Fitzgerald N, et al. 2022. Projected estimates of cancer in Canada in 2022. Can Med Assoc J. 194(17):E601–E607. doi:10.1503/cmaj.212097

3. Global Burden of Disease 2019 Cancer Collaboration, Kocarnik JM, Compton K, Dean FE, Fu W, Gaw BL, Harvey JD, Henrikson HJ, Lu D, Pennini A, et al. 2022. Cancer incidence, mortality, years of life lost, years lived with disability, and disability-adjusted life years for 29 cancer groups from 2010 to 2019: a systematic analysis for the global burden of disease study 2019. JAMA Oncol. 8(3):420. doi:10.1001/jamaoncol.2021.6987

4. Garaszczuk R, Yong JHE, Sun Z, de Oliveira C. 2022. The economic burden of cancer in Canada from a societal perspective. Curr Oncol. 29(4):2735–2748. doi:10.3390/curroncol29040223

5. Zugazagoitia J, Guedes C, Ponce S, Ferrer I, Molina-Pinelo S, Paz-Ares L. 2016. Current challenges in cancer Tteatment. Clin Ther. 38(7):1551–1566. doi:10.1016/j.clinthera.2016.03.026

6. Morad G, Helmink BA, Sharma P, Wargo JA. 2021. Hallmarks of response, resistance, and toxicity to immune checkpoint blockade. Cell. 184(21):5309–5337. doi:10.1016/j.cell.2021.09.020

7. Hanahan D, Weinberg RA. 2011. Hallmarks of cancer: the next generation. Cell. 144(5):646–674. doi:10.1016/j.cell.2011.02.013

8. Elder DE, Bastian BC, Cree IA, Massi D, Scolyer RA. 2020. The 2018 World Health Organization classification of cutaneous, mucosal, and uveal melanoma: detailed analysis of 9 distinct subtypes defined by their evolutionary pathway. Arch Pathol Lab Med. 144(4):500–522. doi:10.5858/arpa.2019-0561-RA

9. Kalaora S, Nagler A, Wargo JA, Samuels Y. 2022. Mechanisms of immune activation and regulation: lessons from melanoma. Nat Rev Cancer. 22(4):195–207. doi:10.1038/s41568-022-00442-9

10. Shaffer SM, Dunagin MC, Torborg SR, Torre EA, Emert B, Krepler C, Beqiri M, Sproesser K, Brafford PA, Xiao M, et al. 2017. Rare cell variability and drug-induced reprogramming as a mode of cancer drug resistance. Nature. 546(7658):431–435. doi:10.1038/nature22794

11. National Cancer Institute. 2020. International classification of diseases for oncology, second edition. NCI Thesaurus. Qeios; [accessed 2022 Nov 4]. doi:10.32388/5XG1QE

12. Amin MB, Greene FL, Edge SB, Compton CC, Gershenwald JE, Brookland RK, Meyer L, Gress DM, Byrd DR, Winchester DP. 2017. The eighth edition AJCC cancer staging manual: continuing to build a bridge from a population-based to a more “personalized” approach to cancer stagingw. CA Cancer J Clin. 67(2):93–99. doi:10.3322/caac.21388

13. Gershenwald JE, Scolyer RA, Hess KR, Sondak VK, Long GV, Ross MI, Lazar AJ, Faries MB, Kirkwood JM, McArthur GA, et al. 2017. Melanoma staging: evidence-based changes in the American Joint Committee on Cancer eighth edition cancer staging manual. CA Cancer J Clin. 67(6):472–492. doi:10.3322/caac.21409

14. Goepfert RP, Myers JN, Gershenwald JE. 2020. Updates in the evidence-based management of cutaneous melanoma. Head Neck. 42(11):3396–3404. doi:10.1002/hed.26398

15. Tracey EH, Vij A. 2019. Updates in melanoma. Dermatol Clin. 37(1):73–82. doi:10.1016/j.det.2018.08.003

16. Galon J, Bruni D. 2019. Approaches to treat immune hot, altered and cold tumours with combination immunotherapies. Nat Rev Drug Discov. 18(3):197–218. doi:10.1038/s41573-018-0007-y

17. Teixido C, Castillo P, Martinez-Vila C, Arance A, Alos L. 2021. Molecular markers and targets in melanoma. Cells. 10(9):2320. doi:10.3390/cells10092320

18. Rebecca VW, Somasundaram R, Herlyn M. 2020. Pre-clinical modeling of cutaneous melanoma. Nat Commun. 11(1):2858. doi:10.1038/s41467-020-15546-9

19. Hayward NK, Wilmott JS, Waddell N, Johansson PA, Field MA, Nones K, Patch A-M, Kakavand H, Alexandrov LB, Burke H, et al. 2017. Whole-genome landscapes of major melanoma subtypes. Nature. 545(7653):175–180. doi:10.1038/nature22071

20. Nasti TH, Timares L. 2015. MC1R, Eumelanin and pheomelanin: their role in determining the susceptibility to skin cancer. Photochem Photobiol. 91(1):188–200. doi:10.1111/php.12335

21. Ito T, Tanaka Y, Murata M, Kaku-Ito Y, Furue K, Furue M. 2021. BRAF heterogeneity in melanoma. Curr Treat Options Oncol. 22(3):20. doi:10.1007/s11864-021-00818-3

22. Garbe C, Amaral T, Peris K, Hauschild A, Arenberger P, Basset-Seguin N, Bastholt L, Bataille V, del Marmol V, Dréno B, et al. 2022. European consensus-based interdisciplinary guideline for melanoma. Part 2: treatment - update 2022. Eur J Cancer. 170:256–284. doi:10.1016/j.ejca.2022.04.018

23. Ethun CG, Delman KA. 2016. The importance of surgical margins in melanoma: melanoma margins. J Surg Oncol. 113(3):339–345. doi:10.1002/jso.24111

24. Howlader N, Noone AM, Krapcho M, Miller D, Brest A, Yu M, Ruhl J, Tatalovich Z, Mariotto A, Lewis DR, Chen HS, Feuer EJ, Cronin KA. SEER cancer statistics review, 1975-2016. Bethesda, MD: National Cancer Institute. https://seer.cancer.gov/csr/1975_2016/

25. Gellrich F, Schmitz M, Beissert S, Meier F. 2020. Anti-PD-1 and novel combinations in the treatment of melanoma—an update. J Clin Med. 9(1):223. doi:10.3390/jcm9010223

26. Adibzadeh R, Golhin MS, Sari S, Mohammadpour H, Kheirbakhsh R, Muhammadnejad A, Amanpour S, Moosavi MA, Rahmati M. 2021. Combination therapy with TiO2 nanoparticles and cisplatin enhances chemotherapy response in murine melanoma models. Clin Transl Oncol. 23(4):738–749. doi:10.1007/s12094-020-02463-y

27. Bender C, Hassel JC, Enk A. 2016. Immunotherapy of melanoma. Oncol Res Treat. 39(6):369–376. doi:10.1159/000446716

28. Carlino MS, Larkin J, Long GV. 2021. Immune checkpoint inhibitors in melanoma. The Lancet. 398(10304):1002–1014. doi:10.1016/S0140-6736(21)01206-X

29. Dummer R, Ascierto PA, Gogas HJ, Arance A, Mandala M, Liszkay G, Garbe C, Schadendorf D, Krajsova I, Gutzmer R, et al. 2018. Overall survival in patients with BRAF-mutant melanoma receiving encorafenib plus binimetinib versus vemurafenib or encorafenib (COLUMBUS): a multicentre, open-label, randomised, phase 3 trial. Lancet Oncol. 19(10):1315–1327. doi:10.1016/S1470-2045(18)30497-2

30. Schreuer M, Jansen Y, Planken S, Chevolet I, Seremet T, Kruse V, Neyns B. 2017. Combination of dabrafenib plus trametinib for BRAF and MEK inhibitor pretreated patients with advanced BRAFV600-mutant melanoma: an open-label, single arm, dual-centre, phase 2 clinical trial. Lancet Oncol. 18(4):464–472. doi:10.1016/S1470-2045(17)30171-7

31. Jerby-Arnon L, Shah P, Cuoco MS, Rodman C, Su M-J, Melms JC, Leeson R, Kanodia A, Mei S, Lin J-R, et al. 2018. A cancer cell program promotes T cell exclusion and resistance to checkpoint blockade. Cell. 175(4):984-997.e24. doi:10.1016/j.cell.2018.09.006

32. Andtbacka RHI, Kaufman HL, Collichio F, Amatruda T, Senzer N, Chesney J, Delman KA, Spitler LE, Puzanov I, Agarwala SS, et al. 2015. Talimogene Laherparepvec improves durable response rate in patients with advanced melanoma. J Clin Oncol. 33(25):2780–2788. doi:10.1200/JCO.2014.58.3377

33. Andtbacka RHI, Ross M, Puzanov I, Milhem M, Collichio F, Delman KA, Amatruda T, Zager JS, Cranmer L, Hsueh E, et al. 2016. Patterns of clinical response with Talimogene Laherparepvec (T-VEC) in patients with melanoma treated in the OPTiM phase III clinical trial. Ann Surg Oncol. 23(13):4169–4177. doi:10.1245/s10434-016-5286-0

34. Larocca CA, LeBoeuf NR, Silk AW, Kaufman HL. 2020. An update on the role of Talimogene Laherparepvec (T-VEC) in the treatment of melanoma: best practices and future directions. Am J Clin Dermatol. 21(6):821–832. doi:10.1007/s40257-020-00554-8

35. Dunn GP, Bruce AT, Ikeda H, Old LJ, Schreiber RD. 2002. Cancer immunoediting: from immunosurveillance to tumor escape. Nat Immunol. 3(11):991–998. doi:10.1038/ni1102-991

36. Cavallo F, De Giovanni C, Nanni P, Forni G, Lollini P-L. 2011. 2011: the immune hallmarks of cancer. Cancer Immunol Immunother. 60(3):319–326. doi:10.1007/s00262-010-0968-0

37. Veglia F, Perego M, Gabrilovich D. 2018. Myeloid-derived suppressor cells coming of age. Nat Immunol. 19(2):108–119. doi:10.1038/s41590-017-0022-x

38. Peng D, Kryczek I, Nagarsheth N, Zhao L, Wei S, Wang W, Sun Y, Zhao E, Vatan L, Szeliga W, et al. 2015. Epigenetic silencing of TH1-type chemokines shapes tumour immunity and immunotherapy. Nature. 527(7577):249–253. doi:10.1038/nature15520

39. Petro M, Kish D, Guryanova OA, Ilyinskaya G, Kondratova A, Fairchild RL, Gorbachev AV. 2013. Cutaneous tumors Cease CXCL9/Mig production as a result of IFN-γ–mediated immunoediting. J Immunol. 190(2):832–841. doi:10.4049/jimmunol.1201906

40. Vinay DS, Ryan EP, Pawelec G, Talib WH, Stagg J, Elkord E, Lichtor T, Decker WK, Whelan RL, Kumara HMCS, et al. 2015. Immune evasion in cancer: mechanistic basis and therapeutic strategies. Semin Cancer Biol. 35:S185–S198. doi:10.1016/j.semcancer.2015.03.004

41. Staveley-O'Carroll K, Sotomayor E, Montgomery J, Borrello I, Hwang L, Fein S, Pardoll D, Levitsky H. 1998. Induction of antigen-specific T cell anergy: an early event in the course of tumor progression. Proc Natl Acad Sci. 95(3):1178–1183. doi:10.1073/pnas.95.3.1178

42. Kudo-Saito C, Shirako H, Ohike M, Tsukamoto N, Kawakami Y. 2013. CCL2 is critical for immunosuppression to promote cancer metastasis. Clin Exp Metastasis. 30(4):393–405. doi:10.1007/s10585-012-9545-6

43. Ghiringhelli F, Puig PE, Roux S, Parcellier A, Schmitt E, Solary E, Kroemer G, Martin F, Chauffert B, Zitvogel L. 2005. Tumor cells convert immature myeloid dendritic cells into TGF-β–secreting cells inducing CD4+CD25+ regulatory T cell proliferation. J Exp Med. 202(7):919–929. doi:10.1084/jem.20050463

44. Ohue Y, Nishikawa H. 2019. Regulatory T (Treg) cells in cancer: can Treg cells be a new therapeutic target? Cancer Sci. 110(7):2080–2089. doi:10.1111/cas.14069

45. Pauken KE, Torchia JA, Chaudhri A, Sharpe AH, Freeman GJ. 2021. Emerging concepts in PD-1 checkpoint biology. Semin Immunol. 52:101480. doi:10.1016/j.smim.2021.101480

46. Iwai Y, Ishida M, Tanaka Y, Okazaki T, Honjo T, Minato N. 2002. Involvement of PD-L1 on tumor cells in the escape from host immune system and tumor immunotherapy by PD-L1 blockade. Proc Natl Acad Sci. 99(19):12293–12297. doi:10.1073/pnas.192461099

47. Galon J, Costes A, Sanchez-Cabo F, Kirilovsky A, Mlecnik B, Lagorce-Pagès C, Tosolini M, Camus M, Berger A, Wind P, et al. 2006. Type, density, and location of immune cells within human colorectal tumors predict clinical outcome. Science. 313(5795):1960–1964. doi:10.1126/science.1129139

48. Lei X, Lei Y, Li J-K, Du W-X, Li R-G, Yang J, Li J, Li F, Tan H-B. 2020. Immune cells within the tumor microenvironment: biological functions and roles in cancer immunotherapy. Cancer Lett. 470:126–133. doi:10.1016/j.canlet.2019.11.009

49. Umansky V, Blattner C, Gebhardt C, Utikal J. 2016. The role of myeloid-derived suppressor cells (MDSC) in cancer progression. Vaccines. 4(4):36. doi:10.3390/vaccines4040036

50. Huang B, Pan P-Y, Li Q, Sato AI, Levy DE, Bromberg J, Divino CM, Chen S-H. 2006. Gr-1+CD115+ immature myeloid suppressor cells mediate the development of tumor-induced T regulatory cells and T-cell anergy in tumor-bearing host. Cancer Res. 66(2):1123–1131. doi:10.1158/0008-5472.CAN-05-1299

51. Lu C, Redd PS, Lee JR, Savage N, Liu K. 2016. The expression profiles and regulation of PD-L1 in tumor-induced myeloid-derived suppressor cells. OncoImmunology. 5(12):e1247135. doi:10.1080/2162402X.2016.1247135

52. Gonzalez-Avila G, Sommer B, Mendoza-Posada DA, Ramos C, Garcia-Hernandez AA, Falfan-Valencia R. 2019. Matrix metalloproteinases participation in the metastatic process and their diagnostic and therapeutic applications in cancer. Crit Rev Oncol Hematol. 137:57–83. doi:10.1016/j.critrevonc.2019.02.010

53. Pan Y, Yu Y, Wang X, Zhang T. 2020. Tumor-associated macrophages in tumor immunity. Front Immunol. 11:583084. doi:10.3389/fimmu.2020.583084

54. Yin M, Li X, Tan S, Zhou HJ, Ji W, Bellone S, Xu X, Zhang H, Santin AD, Lou G, Min W. 2016. Tumor-associated macrophages drive spheroid formation during early transcoelomic metastasis of ovarian cancer. J Clin Invest. 126(11):4157–4173. doi:10.1172/JCI87252

55. Verma A, Mathur R, Farooque A, Kaul V, Gupta S, Dwarakanath BS. 2019. T-regulatory cells in tumor progression and therapy. Cancer Manag Res. 11:10731–10747. doi:10.2147/CMAR.S228887

56. Thornton AM, Shevach EM. 1998. CD4+CD25+ immunoregulatory T cells suppress polyclonal T cell activation *in vitro* by inhibiting interleukin 2 production. J Exp Med. 188(2):287–296. doi:10.1084/jem.188.2.287

57. Cai J, Wang D, Zhang G, Guo X. 2019. The role of PD-1/PD-L1 axis in Treg development and function: implications for cancer immunotherapy. OncoTargets Ther. 12:8437–8445. doi:10.2147/OTT.S221340

58. Schmidt A, Oberle N, Krammer PH. 2012. Molecular mechanisms of Treg-mediated T cell suppression. Front Immunol. 3. doi:10.3389/fimmu.2012.00051

59. Kurose K, Ohue Y, Wada H, Iida S, Ishida T, Kojima T, Doi T, Suzuki S, Isobe M, Funakoshi T, et al. 2015. Phase Ia study of FoxP3+ CD4 Treg depletion by infusion of a humanized anti-CCR4 antibody, KW-0761, in cancer patients. Clin Cancer Res. 21(19):4327–4336. doi:10.1158/1078-0432.CCR-15-0357

60. Zohar Y, Wildbaum G, Novak R, Salzman AL, Thelen M, Alon R, Barsheshet Y, Karp CL, Karin N. 2014. CXCL11-dependent induction of FOXP3-negative regulatory T cells suppresses autoimmune encephalomyelitis. J Clin Invest. 124(5):2009–2022. doi:10.1172/JCI71951

61. Lunardi S, Jamieson NB, Lim SY, Griffiths KL, Carvalho-Gaspar M, Al-Assar O, Yameen S, Carter RC, McKay CJ, Spoletini G, et al. 2014. IP-10/CXCL10 induction in human pancreatic cancer stroma influences lymphocytes recruitment and correlates with poor survival. Oncotarget. 5(22):11064–11080. doi:10.18632/oncotarget.2519

62. Redjimi N, Raffin C, Raimbaud I, Pignon P, Matsuzaki J, Odunsi K, Valmori D, Ayyoub M. 2012. CXCR3+ T regulatory cells selectively accumulate in human ovarian carcinomas to limit type I immunity. Cancer Res. 72(17):4351–4360. doi:10.1158/0008-5472.CAN-12-0579

63. Engelhard V, Conejo-Garcia JR, Ahmed R, Nelson BH, Willard-Gallo K, Bruno TC, Fridman WH. 2021. B cells and cancer. Cancer Cell. 39(10):1293–1296. doi:10.1016/j.ccell.2021.09.007

64. Laumont CM, Banville AC, Gilardi M, Hollern DP, Nelson BH. 2022. Tumour-infiltrating B cells: immunological mechanisms, clinical impact and therapeutic opportunities. Nat Rev Cancer. 22(7):414–430. doi:10.1038/s41568-022-00466-1

65. Cui C, Wang J, Fagerberg E, Chen P-M, Connolly KA, Damo M, Cheung JF, Mao T, Askari AS, Chen S, et al. 2021. Neoantigen-driven B cell and CD4 T follicular helper cell collaboration promotes anti-tumor CD8 T cell responses. Cell. 184(25):6101-6118.e13. doi:10.1016/j.cell.2021.11.007

66. Epeldegui M, Conti DV, Guo Y, Cozen W, Penichet ML, Martínez-Maza O. 2019. Elevated numbers of PD-L1 expressing B cells are associated with the development of AIDS-NHL. Sci Rep. 9(1):9371. doi:10.1038/s41598-019-45479-3

67. Sánchez-Paulete AR, Teijeira A, Cueto FJ, Garasa S, Pérez-Gracia JL, Sánchez-Arráez A, Sancho D, Melero I. 2017. Antigen cross-presentation and T-cell cross-priming in cancer immunology and immunotherapy. Ann Oncol. 28:xii44–xii55. doi:10.1093/annonc/mdx237

68. Spranger S, Dai D, Horton B, Gajewski TF. 2017. Tumor-residing Batf3 dendritic cells are required for effector T cell trafficking and adoptive T cell therapy. Cancer Cell. 31(5):711-723.e4. doi:10.1016/j.ccell.2017.04.003

69. Chow MT, Ozga AJ, Servis RL, Frederick DT, Lo JA, Fisher DE, Freeman GJ, Boland GM, Luster AD. 2019. Intratumoral activity of the CXCR3 chemokine system is required for the efficacy of anti-PD-1 therapy. Immunity. 50(6):1498-1512.e5. doi:10.1016/j.immuni.2019.04.010

70. Salmon H, Idoyaga J, Rahman A, Leboeuf M, Remark R, Jordan S, Casanova-Acebes M, Khudoynazarova M, Agudo J, Tung N, et al. 2016. Expansion and activation of CD103+ dendritic cell progenitors at the tumor site enhances tumor responses to therapeutic PD-L1 and BRAF inhibition. Immunity. 44(4):924–938. doi:10.1016/j.immuni.2016.03.012

71. Wu S-Y, Fu T, Jiang Y-Z, Shao Z-M. 2020. Natural killer cells in cancer biology and therapy. Mol Cancer. 19(1):120. doi:10.1186/s12943-020-01238-x

72. Fuertes MB, Domaica CI, Zwirner NW. 2021. Leveraging NKG2D ligands in immuno-oncology. Front Immunol. 12:713158. doi:10.3389/fimmu.2021.713158

73. Wendel M, Galani IE, Suri-Payer E, Cerwenka A. 2008. Natural killer cell accumulation in tumors is dependent on IFN-γ and CXCR3 ligands. Cancer Res. 68(20):8437–8445. doi:10.1158/0008-5472.CAN-08-1440

74. Kim S, Iizuka K, Aguila HL, Weissman IL, Yokoyama WM. 2000. *In vivo* natural killer cell activities revealed by natural killer cell-deficient mice. Proc Natl Acad Sci. 97(6):2731–2736. doi:10.1073/pnas.050588297

75. Ruterbusch M, Pruner KB, Shehata L, Pepper M. 2020. *In vivo* CD4 $^{+}$ T cell differentiation and function: revisiting the Th1/Th2 paradigm. Annu Rev Immunol. 38(1):705–725. doi:10.1146/annurev-immunol-103019-085803

76. Laidlaw BJ, Craft JE, Kaech SM. 2016. The multifaceted role of CD4+ T cells in CD8+ T cell memory. Nat Rev Immunol. 16(2):102–111. doi:10.1038/nri.2015.10

77. Bos R, Sherman LA. 2010. CD4+ T-cell help in the tumor milieu is required for recruitment and cytolytic function of CD8+ T lymphocytes. Cancer Res. 70(21):8368–8377. doi:10.1158/0008-5472.CAN-10-1322

78. Nishimura T, Iwakabe K, Sekimoto M, Ohmi Y, Yahata T, Nakui M, Sato T, Habu S, Tashiro H, Sato M, Ohta A. 1999. Distinct role of antigen-specific T helper type 1 (Th1) and Th2 cells in tumor eradication *in vivo*. J Exp Med. 190(5):617–628. doi:10.1084/jem.190.5.617

79. Kennedy R, Celis E. 2008. Multiple roles for CD4 $^{+}$ T cells in anti-tumor immune responses. Immunol Rev. 222(1):129–144. doi:10.1111/j.1600-065X.2008.00616.x

80. Chang SH. 2019. T helper 17 (Th17) cells and interleukin-17 (IL-17) in cancer. Arch Pharm Res. 42(7):549–559. doi:10.1007/s12272-019-01146-9

81. Rossin A, Miloro G, Hueber A-O. 2019. TRAIL and FasL functions in cancer and autoimmune diseases: towards an increasing complexity. Cancers. 11(5):639. doi:10.3390/cancers11050639

82. Park SL, Gebhardt T, Mackay LK. 2019. Tissue-resident memory T cells in cancer immunosurveillance. Trends Immunol. 40(8):735–747. doi:10.1016/j.it.2019.06.002

83. Zhang Y, Springfield R, Chen S, Li X, Feng X, Moshirian R, Yang R, Yuan W. 2019. α-GalCer and iNKT cell-based cancer immunotherapy: realizing the therapeutic potentials. Front Immunol. 10:1126. doi:10.3389/fimmu.2019.01126

84. Matsuda JL, Mallevaey T, Scott-Browne J, Gapin L. 2008. CD1d-restricted iNKT cells, the 'Swiss-Army knife' of the immune system. Curr Opin Immunol. 20(3):358–368. doi:10.1016/j.coi.2008.03.018

85. Fujii S-I, Shimizu K. 2019. Immune networks and therapeutic targeting of iNKT cells in cancer. Trends Immunol. 40(11):984–997. doi:10.1016/j.it.2019.09.008

86. Kato S, Berzofsky JA, Terabe M. 2018. Possible therapeutic application of targeting Type II natural killer T cell-mediated suppression of tumor immunity. Front Immunol. 9:314. doi:10.3389/fimmu.2018.00314

87. Ishihara S, Nieda M, Kitayama J, Osada T, Yabe T, Ishikawa Y, Nagawa H, Muto T, Juji T. 1999. CD8+NKR-P1A+ T cells preferentially accumulate in human liver. Eur J Immunol. 29(8):2406–2413. doi:10.1002/(SICI)1521-4141(199908)29:08<2406::AID-IMMU2406>3.0.CO;2-F

88. Fujii S, Shimizu K, Kronenberg M, Steinman RM. 2002. Prolonged IFN-γ–producing NKT response induced with α-galactosylceramide–loaded DCs. Nat Immunol. 3(9):867–874. doi:10.1038/ni827

89. Coquet JM, Chakravarti S, Kyparissoudis K, McNab FW, Pitt LA, McKenzie BS, Berzins SP, Smyth MJ, Godfrey DI. 2008. Diverse cytokine production by NKT cell subsets and identification of an IL-17–producing CD4 $^{-}$ NK1.1 $^{-}$ NKT cell population. Proc Natl Acad Sci. 105(32):11287–11292. doi:10.1073/pnas.0801631105

90. Wingender G, Sag D, Kronenberg M. 2015. NKT10 cells: a novel iNKT cell subset. Oncotarget. 6(29):26552–26553. doi:10.18632/oncotarget.5270

91. Rampuria P, Lang ML. 2015. CD1d-dependent expansion of NKT follicular helper cells *in vivo* and *in vitro* is a product of cellular proliferation and differentiation. Int Immunol. 27(5):253–263. doi:10.1093/intimm/dxv007

92. Bedard M, Salio M, Cerundolo V. 2017. Harnessing the power of invariant natural killer T cells in cancer immunotherapy. Front Immunol. 8:1829. doi:10.3389/fimmu.2017.01829

93. Wen X, Rao P, Carreño LJ, Kim S, Lawrenczyk A, Porcelli SA, Cresswell P, Yuan W. 2013. Human CD1d knock-in mouse model demonstrates potent antitumor potential of human CD1d-restricted invariant natural killer T cells. Proc Natl Acad Sci. 110(8):2963–2968. doi:10.1073/pnas.1300200110

94. Slauenwhite D, Johnston B. 2015. Regulation of NKT cell localization in homeostasis and infection. Front Immunol. 6. doi:10.3389/fimmu.2015.00255

95. Fujii S-I, Shimizu K, Hemmi H, Steinman RM. 2007. Innate Vα14 $^{+}$ natural killer T cells mature dendritic cells, leading to strong adaptive immunity. Immunol Rev. 220(1):183–198. doi:10.1111/j.1600-065X.2007.00561.x

96. Crowe NY, Smyth MJ, Godfrey DI. 2002. A critical role for natural killer T cells in immunosurveillance of methylcholanthrene-induced sarcomas. J Exp Med. 196(1):119–127. doi:10.1084/jem.20020092

97. Smyth MJ, Thia KYT, Street SEA, Cretney E, Trapani JA, Taniguchi M, Kawano T, Pelikan SB, Crowe NY, Godfrey DI. 2000. Differential tumor surveillance by natural killer (NK) and NKT Cells. J Exp Med. 191(4):661–668. doi:10.1084/jem.191.4.661

98. Tachibana T, Onodera H, Tsuruyama T, Mori A, Nagayama S, Hiai H, Imamura M. 2005. Increased intratumor Vα24-positive natural killer T cells: a prognostic factor for primary colorectal carcinomas. Clin Cancer Res. 11(20):7322–7327. doi:10.1158/1078-0432.CCR-05-0877

99. Exley MA, Friedlander P, Alatrakchi N, Vriend L, Yue S, Sasada T, Zeng W, Mizukami Y, Clark J, Nemer D, et al. 2017. Adoptive transfer of invariant NKT cells as immunotherapy for advanced melanoma: a phase I clinical trial. Clin Cancer Res. 23(14):3510–3519. doi:10.1158/1078-0432.CCR-16-0600

100. Pei B, Speak AO, Shepherd D, Butters T, Cerundolo V, Platt FM, Kronenberg M. 2011. Diverse endogenous antigens for mouse NKT cells: self-antigens that are not glycosphingolipids. J Immunol. 186(3):1348–1360. doi:10.4049/jimmunol.1001008

101. Fiedler T, Walter W, Reichert TE, Maeurer MJ. 2002. Regulation of CD1d expression by murine tumor cells: escape from immunosurveillance or alternate target molecules? Int J Cancer. 98(3):389–397. doi:10.1002/ijc.10141

102. Gerlini G, Tun-Kyi A, Dudli C, Burg G, Pimpinelli N, Nestle FO. 2004. Metastatic melanoma secreted IL-10 down-regulates CD1 molecules on dendritic cells in metastatic tumor lesions. Am J Pathol. 165(6):1853–1863. doi:10.1016/S0002-9440(10)63238-5

103. Shimizu K, Goto A, Fukui M, Taniguchi M, Fujii S. 2007. Tumor cells loaded with α-Galactosylceramide induce innate NKT and NK cell-dependent resistance to tumor implantation in mice. J Immunol. 178(5):2853–2861. doi:10.4049/jimmunol.178.5.2853

104. Weber F, Junger H, Werner JM, Velez Char N, Rejas C, Schlitt HJ, Hornung M. 2019. Increased cytoplasmatic expression of cancer immune surveillance receptor CD1d in anaplastic thyroid carcinomas. Cancer Med. 8(16):7065–7073. doi:10.1002/cam4.2573

105. Song L, Asgharzadeh S, Salo J, Engell K, Wu H, Sposto R, Ara T, Silverman AM, DeClerck YA, Seeger RC, Metelitsa LS. 2009. Vα24-invariant NKT cells mediate antitumor activity via killing of tumor-associated macrophages. J Clin Invest. 119(6):1524–1536. doi:10.1172/JCI37869

106. De Santo C, Salio M, Masri SH, Lee LY-H, Dong T, Speak AO, Porubsky S, Booth S, Veerapen N, Besra GS, et al. 2008. Invariant NKT cells reduce the immunosuppressive activity of influenza A virus–induced myeloid-derived suppressor cells in mice and humans. J Clin Invest. 118(12):4036–4048. doi:10.1172/JCI36264

107. De Santo C, Arscott R, Booth S, Karydis I, Jones M, Asher R, Salio M, Middleton M, Cerundolo V. 2010. Invariant NKT cells modulate the suppressive activity of IL-10-secreting neutrophils differentiated with serum amyloid A. Nat Immunol. 11(11):1039–1046. doi:10.1038/ni.1942

108. Liu D, Song L, Wei J, Courtney AN, Gao X, Marinova E, Guo L, Heczey A, Asgharzadeh S, Kim E, et al. 2012. IL-15 protects NKT cells from inhibition by tumor-associated macrophages and enhances antimetastatic activity. J Clin Invest. 122(6):2221–2233. doi:10.1172/JCI59535

109. Nelson A, Lukacs JD, Johnston B. 2021. The current landscape of NKT cell immunotherapy and the hills ahead. Cancers. 13(20):5174. doi:10.3390/cancers13205174

110. McEwen-Smith RM, Salio M, Cerundolo V. 2015. The regulatory role of invariant NKT cells in tumor immunity. Cancer Immunol Res. 3(5):425–435. doi:10.1158/2326-6066.CIR-15-0062

111. Clark K, Yau J, Bloom A, Wang J, Venzon DJ, Suzuki M, Pasquet L, Compton BJ, Cardell SL, Porcelli SA, et al. 2019. Structure-function implications of the ability of monoclonal antibodies against α-galactosylceramide-CD1d complex to recognize β-mannosylceramide presentation by CD1d. Front Immunol. 10:2355. doi:10.3389/fimmu.2019.02355

112. Lu X, Song L, Metelitsa LS, Bittman R. 2006. Synthesis and evaluation of an α-C-galactosylceramide analogue that induces Th1-biased responses in human natural killer T cells. ChemBioChem. 7(11):1750–1756. doi:10.1002/cbic.200600197

113. Tefit JN, Crabé S, Orlandini B, Nell H, Bendelac A, Deng S, Savage PB, Teyton L, Serra V. 2014. Efficacy of ABX196, a new NKT agonist, in prophylactic human vaccination. Vaccine. 32(46):6138–6145. doi:10.1016/j.vaccine.2014.08.070

114. Giaccone G, Punt CJA, Ando Y, Ruijter R, Nishi N, Peters M, Blomberg BME von, Scheper RJ, Vliet HJJ van der, Eertwegh AJM van den, et al. 2005. A phase I study of the natural killer T-cell ligand alpha-galactosylceramide (KRN7000) in patients with solid tumors. Clin Cancer Res . 8(12):3702–9.

115. Parekh VV. 2005. Glycolipid antigen induces long-term natural killer T cell anergy in mice. J Clin Invest. 115(9):2572–2583. doi:10.1172/JCI24762

116. Thapa P, Zhang G, Xia C, Gelbard A, Overwijk WW, Liu C, Hwu P, Chang DZ, Courtney A, Sastry JK. 2009. Nanoparticle formulated alpha-galactosylceramide activates NKT cells without inducing anergy. Vaccine. 27(25–26):3484–3488. doi:10.1016/j.vaccine.2009.01.047

117. Richter J, Neparidze N, Zhang L, Nair S, Monesmith T, Sundaram R, Miesowicz F, Dhodapkar KM, Dhodapkar MV. 2013. Clinical regressions and broad immune activation following combination therapy targeting human NKT cells in myeloma. Blood. 121(3):423–430. doi:10.1182/blood-2012-06-435503

118. Uchida T, Horiguchi S, Tanaka Y, Yamamoto H, Kunii N, Motohashi S, Taniguchi M, Nakayama T, Okamoto Y. 2008. Phase I study of α-galactosylceramide-pulsed antigen presenting cells administration to the nasal submucosa in unresectable or recurrent head and neck cancer. Cancer Immunol Immunother. 57(3):337–345. doi:10.1007/s00262-007-0373-5

119. Motohashi S, Nagato K, Kunii N, Yamamoto H, Yamasaki K, Okita K, Hanaoka H, Shimizu N, Suzuki M, Yoshino I, et al. 2009. A phase I-II study of α-galactosylceramide-pulsed IL-2/GM-CSF-cultured peripheral blood mononuclear cells in patients with advanced and recurrent non-small cell lung cancer. J Immunol. 182(4):2492–2501. doi:10.4049/jimmunol.0800126

120. Ishikawa A, Motohashi S, Ishikawa E, Fuchida H, Higashino K, Otsuji M, Iizasa T, Nakayama T, Taniguchi M, Fujisawa T. 2005. A phase I study of α-galactosylceramide (KRN7000)–pulsed dendritic cells in patients with advanced and recurrent non–small cell lung cancer. Clin Cancer Res. 11(5):1910–1917. doi:10.1158/1078-0432.CCR-04-1453

121. Yanagisawa K, Seino K, Ishikawa Y, Nozue M, Todoroki T, Fukao K. 2002. Impaired proliferative response of Vα24 NKT cells from cancer patients against α-galactosylceramide. J Immunol. 168(12):6494–6499. doi:10.4049/jimmunol.168.12.6494

122. Molling JW, Kölgen W, van der Vliet HJJ, Boomsma MF, Kruizenga H, Smorenburg CH, Molenkamp BG, Langendijk JA, Leemans CR, von Blomberg BME, et al. 2005. Peripheral blood IFN-γ-secreting Vα24+Vβ11+ NKT cell numbers are decreased in cancer patients independent of tumor type or tumor load. Int J Cancer. 116(1):87–93. doi:10.1002/ijc.20998

123. Yamasaki K, Horiguchi S, Kurosaki M, Kunii N, Nagato K, Hanaoka H, Shimizu N, Ueno N, Yamamoto S, Taniguchi M, et al. 2011. Induction of NKT cell-specific immune responses in cancer tissues after NKT cell-targeted adoptive immunotherapy. Clin Immunol. 138(3):255–265. doi:10.1016/j.clim.2010.11.014

124. Bagnara D, Ibatici A, Corselli M, Sessarego N, Tenca C, De Santanna A, Mazzarello A, Daga A, Corvo R, De Rossi G, et al. 2009. Adoptive immunotherapy mediated by *ex vivo* expanded natural killer T cells against CD1d-expressing lymphoid neoplasms. Haematologica. 94(7):967–974. doi:10.3324/haematol.2008.001339

125. Yu W, Ye F, Yuan X, Ma Y, Mao C, Li X, Li J, Dai C, Qian F, Li J, et al. 2021. A phase I/II clinical trial on the efficacy and safety of NKT cells combined with gefitinib for advanced EGFR-mutated non-small-cell lung cancer. BMC Cancer. 21(1):877. doi:10.1186/s12885-021-08590-1

126. Yu W, Yuan X, Ye F, Mao C, Li J, Zhang M, Chen D, Xia S. 2022. Role of allogeneic natural killer T cells in the treatment of a patient with gefitinib-sensitive lung adenocarcinoma. Immunotherapy. 14(16):1291–1296. doi:10.2217/imt-2022-0178

127. Chang DH, Liu N, Klimek V, Hassoun H, Mazumder A, Nimer SD, Jagannath S, Dhodapkar MV. 2006. Enhancement of ligand-dependent activation of human natural killer T cells by lenalidomide: therapeutic implications. Blood. 108(2):618–621. doi:10.1182/blood-2005-10-4184

128. Gebremeskel S, Nelson A, Walker B, Oliphant T, Lobert L, Mahoney D, Johnston B. 2021. Natural killer T cell immunotherapy combined with oncolytic vesicular stomatitis virus or reovirus treatments differentially increases survival in mouse models of ovarian and breast cancer metastasis. J Immunother Cancer. 9(3):e002096. doi:10.1136/jitc-2020-002096

129. Nelson A, Gebremeskel S, Lichty BD, Johnston B. 2022. Natural killer T cell immunotherapy combined with IL-15-expressing oncolytic virotherapy and PD-1 blockade mediates pancreatic tumor regression. J Immunother Cancer. 10(3):e003923. doi:10.1136/jitc-2021-003923

130. Bayan C-AY, Lopez AT, Gartrell RD, Komatsubara KM, Bogardus M, Rao N, Chen C, Hart TD, Enzler T, Rizk EM, et al. 2018. The role of oncolytic viruses in the treatment of melanoma. Curr Oncol Rep. 20(10):80. doi:10.1007/s11912-018-0729-3

131. Kaufman HL, Kohlhapp FJ, Zloza A. 2015. Oncolytic viruses: a new class of immunotherapy drugs. Nat Rev Drug Discov. 14(9):642–662. doi:10.1038/nrd4663

132. Rothermel LD, Zager JS. 2018. Engineered oncolytic viruses to treat melanoma: where are we now and what comes next? Expert Opin Biol Ther. 18(12):1199–1207. doi:10.1080/14712598.2018.1544614

133. Guo ZS, Liu Z, Bartlett DL. 2014. Oncolytic immunotherapy: dying the right way is a key to eliciting potent antitumor immunity. Front Oncol. 4. doi:10.3389/fonc.2014.00074

134. de Vries CR, Kaufman HL, Lattime EC. 2015. Oncolytic viruses: focusing on the tumor microenvironment. Cancer Gene Ther. 22(4):169–171. doi:10.1038/cgt.2015.11

135. Pan C, Liu H, Robins E, Song W, Liu D, Li Z, Zheng L. 2020. Next-generation immuno-oncology agents: current momentum shifts in cancer immunotherapy. J Hematol OncolJ Hematol Oncol. 13(1):29. doi:10.1186/s13045-020-00862-w

136. Breitbach CJ, De Silva NS, Falls TJ, Aladl U, Evgin L, Paterson J, Sun YY, Roy DG, Rintoul JL, Daneshmand M, et al. 2011. Targeting tumor vasculature with an oncolytic virus. Mol Ther. 19(5):886–894. doi:10.1038/mt.2011.26

137. Maroun J, Muñoz-Alía M, Ammayappan A, Schulze A, Peng K-W, Russell S. 2017. Designing and building oncolytic viruses. Future Virol. 12(4):193–213. doi:10.2217/fvl-2016-0129

138. Frampton JE. 2022. Teserpaturev/G47Δ: first approval. BioDrugs. 36(5):667–672. doi:10.1007/s40259-022-00553-7

139. Garber K. 2006. China approves world's first oncolytic virus therapy for cancer treatment. JNCI J Natl Cancer Inst. 98(5):298–300. doi:10.1093/jnci/djj111

140. Pol J, Buqué A, Aranda F, Bloy N, Cremer I, Eggermont A, Erbs P, Fucikova J, Galon J, Limacher J-M, et al. 2016. Trial watch—oncolytic viruses and cancer therapy. OncoImmunology. 5(2):e1117740. doi:10.1080/2162402X.2015.1117740

141. Hastie E, Cataldi M, Marriott I, Grdzelishvili VZ. 2013. Understanding and altering cell tropism of vesicular stomatitis virus. Virus Res. 176(1–2):16–32. doi:10.1016/j.virusres.2013.06.003

142. Fultz PN, Holland JJ. 1985. Differing responses of hamsters to infection by vesicular stomatitis virus Indiana and New Jersey serotypes. Virus Res. 3(2):129–140. doi:10.1016/0168-1702(85)90003-6

143. Stojdl DF, Lichty BD, tenOever BR, Paterson JM, Power AT, Knowles S, Marius R, Reynard J, Poliquin L, Atkins H, et al. 2003. VSV strains with defects in their ability to shutdown innate immunity are potent systemic anti-cancer agents. Cancer Cell. 4(4):263–275. doi:10.1016/S1535-6108(03)00241-1

144. Velazquez-Salinas L, Naik S, Pauszek SJ, Peng K-W, Russell SJ, Rodriguez LL. 2017. Oncolytic recombinant vesicular stomatitis virus (VSV) is nonpathogenic and nontransmissible in pigs, a natural host of VSV. Hum Gene Ther Clin Dev. 28(2):108–115. doi:10.1089/humc.2017.015

145. Obuchi M, Fernandez M, Barber GN. 2003. Development of recombinant vesicular stomatitis viruses that exploit defects in host defense to augment specific oncolytic activity. J Virol. 77(16):8843–8856. doi:10.1128/JVI.77.16.8843-8856.2003

146. Felt SA, Grdzelishvili VZ. 2017. Recent advances in vesicular stomatitis virus-based oncolytic virotherapy: a 5-year update. J Gen Virol. 98(12):2895–2911. doi:10.1099/jgv.0.000980

147. Roslan Z, Muhamad M, Selvaratnam L, Ab-Rahim S. 2019. The roles of low-density lipoprotein receptor-related proteins 5, 6, and 8 in cancer: a review. J Oncol. 2019:1–6. doi:10.1155/2019/4536302

148. Shen W, Patnaik MM, Ruiz A, Russell SJ, Peng K-W. 2016. Immunovirotherapy with vesicular stomatitis virus and PD-L1 blockade enhances therapeutic outcome in murine acute myeloid leukemia. Blood. 127(11):1449–1458. doi:10.1182/blood-2015-06-652503

149. Lichty BD, Breitbach CJ, Stojdl DF, Bell JC. 2014. Going viral with cancer immunotherapy. Nat Rev Cancer. 14(8):559–567. doi:10.1038/nrc3770

150. Cook J, Peng KWW, Witzig TE, Broski SM, Villasboas JC, Paludo J, Patnaik MM, Rajkumar V, Dispenzieri A, Leung N, et al. 2022. Clinical activity of single dose systemic oncolytic VSV virotherapy in patients with relapsed refractory T-cell lymphoma. Blood Adv. doi:10.1182/bloodadvances.2021006631

151. Peruzzi P, Chiocca EA. 2018. Viruses in cancer therapy — from benchwarmers to quarterbacks. Nat Rev Clin Oncol. 15(11):657–658. doi:10.1038/s41571-018-0077-0

152. Patel MR, Jacobson BA, Ji Y, Drees J, Tang S, Xiong K, Wang H, Prigge JE, Dash AS, Kratzke AK, et al. 2015. Vesicular stomatitis virus expressing interferon-β is oncolytic and promotes antitumor immune responses in a syngeneic murine model of non-small cell lung cancer. Oncotarget. 6(32):33165–33177. doi:10.18632/oncotarget.5320

153. Shin EJ, Wanna GB, Choi B, Aguila D, Ebert O, Genden EM, Woo SL. 2007. Interleukin-12 expression enhances vesicular stomatitis virus oncolytic therapy in murine squamous cell carcinoma. The Laryngoscope. 117(2):210–214. doi:10.1097/01.mlg.0000246194.66295.d8

154. Le Boeuf F, Gebremeskel S, McMullen N, He H, Greenshields AL, Hoskin DW, Bell JC, Johnston B, Pan C, Duncan R. 2017. Reovirus FAST protein enhances vesicular stomatitis virus oncolytic virotherapy in primary and metastatic tumor models. Mol Ther Oncolytics. 6:80–89. doi:10.1016/j.omto.2017.08.001

155. Duncan R. 2019. Fusogenic reoviruses and their fusion-associated small transmembrane (FAST) proteins. Annu Rev Virol. 6(1):341–363. doi:10.1146/annurev-virology-092818-015523

156. Salsman J, Top D, Boutilier J, Duncan R. 2005. Extensive syncytium formation mediated by the reovirus FAST proteins triggers apoptosis-induced membrane instability. J Virol. 79(13):8090–8100. doi:10.1128/JVI.79.13.8090-8100.2005

157. Nelson A. 2022. Natural killer T cell immunotherapy in combination with recombinant oncolytic vesicular stomatitis virus and immune checkpoint therapy reduces tumor burden in models of pancreatic and breast cancer [PhD]. Halifax, NS: Dalhousie University.

158. Griffith JW, Sokol CL, Luster AD. 2014. Chemokines and chemokine receptors: positioning cells for host defense and immunity. Annu Rev Immunol. 32(1):659–702. doi:10.1146/annurev-immunol-032713-120145

159. Nagarsheth N, Wicha MS, Zou W. 2017. Chemokines in the cancer microenvironment and their relevance in cancer immunotherapy. Nat Rev Immunol. 17(9):559–572. doi:10.1038/nri.2017.49

160. Schlecker E, Stojanovic A, Eisen C, Quack C, Falk CS, Umansky V, Cerwenka A. 2012. Tumor-infiltrating monocytic myeloid-derived suppressor cells mediate CCR5-dependent recruitment of regulatory T cells favoring tumor growth. J Immunol. 189(12):5602–5611. doi:10.4049/jimmunol.1201018

161. Metelitsa LS, Wu H-W, Wang H, Yang Y, Warsi Z, Asgharzadeh S, Groshen S, Wilson SB, Seeger RC. 2004. Natural killer T cells infiltrate neuroblastomas expressing the chemokine CCL2. J Exp Med. 199(9):1213–1221. doi:10.1084/jem.20031462

162. Kim CH, Johnston B, Butcher EC. 2002. Trafficking machinery of NKT cells: shared and differential chemokine receptor expression among Vα24+Vβ11+ NKT cell subsets with distinct cytokine-producing capacity. Blood. 100(1):11–16. doi:10.1182/blood-2001-12-0196

163. Tokunaga R, Zhang W, Naseem M, Puccini A, Berger MD, Soni S, McSkane M, Baba H, Lenz H-J. 2018. CXCL9, CXCL10, CXCL11/CXCR3 axis for immune activation – a target for novel cancer therapy. Cancer Treat Rev. 63:40–47. doi:10.1016/j.ctrv.2017.11.007

164. Kuo PT, Zeng Z, Salim N, Mattarollo S, Wells JW, Leggatt GR. 2018. The role of CXCR3 and its chemokine ligands in skin disease and cancer. Front Med. 5:271. doi:10.3389/fmed.2018.00271

165. Mikucki ME, Fisher DT, Matsuzaki J, Skitzki JJ, Gaulin NB, Muhitch JB, Ku AW, Frelinger JG, Odunsi K, Gajewski TF, et al. 2015. Non-redundant requirement for CXCR3 signalling during tumoricidal T-cell trafficking across tumour vascular checkpoints. Nat Commun. 6(1):7458. doi:10.1038/ncomms8458

166. Mullins IM, Slingluff CL, Lee JK, Garbee CF, Shu J, Anderson SG, Mayer ME, Knaus WA, Mullins DW. 2004. CXC chemokine receptor 3 expression by activated CD8+ T cells is associated with survival in melanoma patients with stage III disease. Cancer Res. 64(21):7697–7701. doi:10.1158/0008-5472.CAN-04-2059

167. Johnston B, Kim CH, Soler D, Emoto M, Butcher EC. 2003. Differential chemokine responses and homing patterns of murine TCRαβ NKT cell subsets. J Immunol. 171(6):2960–2969. doi:10.4049/jimmunol.171.6.2960

168. Hickman HD, Reynoso GV, Ngudiankama BF, Cush SS, Gibbs J, Bennink JR, Yewdell JW. 2015. CXCR3 chemokine receptor enables local CD8+ T cell migration for the destruction of virus-infected cells. Immunity. 42(3):524–537. doi:10.1016/j.immuni.2015.02.009

169. Dangaj D, Bruand M, Grimm AJ, Ronet C, Barras D, Duttagupta PA, Lanitis E, Duraiswamy J, Tanyi JL, Benencia F, et al. 2019. Cooperation between constitutive and inducible chemokines enables T cell engraftment and immune attack in solid tumors. Cancer Cell. 35(6):885-900.e10. doi:10.1016/j.ccell.2019.05.004

170. Srivastava S, Furlan SN, Jaeger-Ruckstuhl CA, Sarvothama M, Berger C, Smythe KS, Garrison SM, Specht JM, Lee SM, Amezquita RA, et al. 2021. Immunogenic chemotherapy enhances recruitment of CAR-T cells to lung tumors and improves antitumor efficacy when combined with checkpoint blockade. Cancer Cell. 39(2):193-208.e10. doi:10.1016/j.ccell.2020.11.005

171. Russo E, Laffranchi M, Tomaipitinca L, Del Prete A, Santoni A, Sozzani S, Bernardini G. 2021. NK cell anti-tumor surveillance in a myeloid cell-shaped environment. Front Immunol. 12:787116. doi:10.3389/fimmu.2021.787116

172. Bedognetti D, Spivey TL, Zhao Y, Uccellini L, Tomei S, Dudley ME, Ascierto ML, De Giorgi V, Liu Q, Delogu LG, et al. 2013. CXCR3/CCR5 pathways in metastatic melanoma patients treated with adoptive therapy and interleukin-2. Br J Cancer. 109(9):2412–2423. doi:10.1038/bjc.2013.557

173. Mlecnik B, Tosolini M, Charoentong P, Kirilovsky A, Bindea G, Berger A, Camus M, Gillard M, Bruneval P, Fridman W, et al. 2010. Biomolecular network reconstruction identifies T-cell homing factors associated with survival in colorectal cancer. Gastroenterology. 138(4):1429–1440. doi:10.1053/j.gastro.2009.10.057

174. Reschke R, Yu J, Flood BA, Higgs EF, Hatogai K, Gajewski TF. 2021. Immune cell and tumor cell-derived CXCL10 is indicative of immunotherapy response in metastatic melanoma. J Immunother Cancer. 9(9):e003521. doi:10.1136/jitc-2021-003521

175. Harlin H, Meng Y, Peterson AC, Zha Y, Tretiakova M, Slingluff C, McKee M, Gajewski TF. 2009. Chemokine expression in melanoma metastases associated with CD8+ T-cell recruitment. Cancer Res. 69(7):3077–3085. doi:10.1158/0008-5472.CAN-08-2281

176. Russo E, Santoni A, Bernardini G. 2020. Tumor inhibition or tumor promotion? The duplicity of CXCR3 in cancer. J Leukoc Biol. 108(2):673–685. doi:10.1002/JLB.5MR0320-205R

177. Brownell J, Bruckner J, Wagoner J, Thomas E, Loo Y-M, Gale M, Liang TJ, Polyak SJ. 2014. Direct, interferon-independent activation of the CXCL10 promoter by NF-κB and interferon regulatory factor 3 during Hepatitis C virus infection. J Virol. 88(3):1582–1590. doi:10.1128/JVI.02007-13

178. Merad M, Sathe P, Helft J, Miller J, Mortha A. 2013. The dendritic cell lineage: ontogeny and function of dendritic cells and their subsets in the steady state and the inflamed setting. Annu Rev Immunol. 31(1):563–604. doi:10.1146/annurev-immunol-020711-074950

179. Ohtani H, Jin Z, Takegawa S, Nakayama T, Yoshie O. 2009. Abundant expression of CXCL9 (MIG) by stromal cells that include dendritic cells and accumulation of CXCR3 $^{+}$ T cells in lymphocyte-rich gastric carcinoma: chemokines in lymphocyte-rich gastric cancers. J Pathol. 217(1):21–31. doi:10.1002/path.2448

180. Wightman SC, Uppal A, Pitroda SP, Ganai S, Burnette B, Stack M, Oshima G, Khan S, Huang X, Posner MC, et al. 2015. Oncogenic CXCL10 signalling drives metastasis development and poor clinical outcome. Br J Cancer. 113(2):327–335. doi:10.1038/bjc.2015.193

181. Dengel LT, Norrod AG, Gregory BL, Clancy-Thompson E, Burdick MD, Strieter RM, Slingluff CL, Mullins DW. 2010. Interferons induce CXCR3-cognate chemokine production by human metastatic melanoma. J Immunother. 33(9):965–974. doi:10.1097/CJI.0b013e3181fb045d

182. Pan J, Burdick MD, Belperio JA, Xue YY, Gerard C, Sharma S, Dubinett SM, Strieter RM. 2006. CXCR3/CXCR3 ligand biological axis impairs RENCA tumor growth by a mechanism of immunoangiostasis. J Immunol. 176(3):1456–1464. doi:10.4049/jimmunol.176.3.1456

183. Arenberg D, White E, Burdick M, Strom S, Strieter R. 2001. Improved survival in tumor-bearing SCID mice treated with interferon-γ-inducible protein 10 (IP-10/CXCL10). Cancer Immunol Immunother. 50(10):533–538. doi:10.1007/s00262-001-0231-9

184. Mohty A-M, Grob J-J, Mohty M, Richard M-A, Olive D, Gaugler B. 2010. Induction of IP-10/CXCL10 secretion as an immunomodulatory effect of low-dose adjuvant interferon-alpha during treatment of melanoma. Immunobiology. 215(2):113–123. doi:10.1016/j.imbio.2009.03.008

185. Barreira da Silva R, Laird ME, Yatim N, Fiette L, Ingersoll MA, Albert ML. 2015. Dipeptidylpeptidase 4 inhibition enhances lymphocyte trafficking, improving both naturally occurring tumor immunity and immunotherapy. Nat Immunol. 16(8):850–858. doi:10.1038/ni.3201

186. Specht K, Harbeck N, Smida J, Annecke K, Reich U, Naehrig J, Langer R, Mages J, Busch R, Kruse E, et al. 2009. Expression profiling identifies genes that predict recurrence of breast cancer after adjuvant CMF-based chemotherapy. Breast Cancer Res Treat. 118(1):45–56. doi:10.1007/s10549-008-0207-y

187. Hong M, Puaux A-L, Huang C, Loumagne L, Tow C, Mackay C, Kato M, Prévost-Blondel A, Avril M-F, Nardin A, Abastado J-P. 2011. Chemotherapy induces intratumoral expression of chemokines in cutaneous melanoma, favoring T-cell infiltration and tumor control. Cancer Res. 71(22):6997–7009. doi:10.1158/0008-5472.CAN-11-1466

188. Sistigu A, Yamazaki T, Vacchelli E, Chaba K, Enot DP, Adam J, Vitale I, Goubar A, Baracco EE, Remédios C, et al. 2014. Cancer cell–autonomous contribution of type I interferon signaling to the efficacy of chemotherapy. Nat Med. 20(11):1301–1309. doi:10.1038/nm.3708

189. Liu W, Liu Y, Fu Q, Zhou L, Chang Y, Xu L, Zhang W, Xu J. 2016. Elevated expression of IFN-inducible CXCR3 ligands predicts poor prognosis in patients with non-metastatic clear-cell renal cell carcinoma. Oncotarget. 7(12):13976–13983. doi:10.18632/oncotarget.7468

190. Shiels MS, Katki HA, Hildesheim A, Pfeiffer RM, Engels EA, Williams M, Kemp TJ, Caporaso NE, Pinto LA, Chaturvedi AK. 2015. Circulating inflammation markers, risk of lung cancer, and utility for risk stratification. JNCI J Natl Cancer Inst. 107(10). doi:10.1093/jnci/djv199

191. Shi T, Gao G. 2022. Identify potential prognostic indicators and tumor-infiltrating immune cells in pancreatic adenocarcinoma. Biosci Rep. 42(2):BSR20212523. doi:10.1042/BSR20212523

192. Zhang C, Li Z, Xu L, Che X, Wen T, Fan Y, Li C, Wang S, Cheng Y, Wang X, et al. 2018. CXCL9/10/11, a regulator of PD-L1 expression in gastric cancer. BMC Cancer. 18(1):462. doi:10.1186/s12885-018-4384-8

193. Yang C, Zheng W, Du W. 2016. CXCR3A contributes to the invasion and metastasis of gastric cancer cells. Oncol Rep. 36(3):1686–1692. doi:10.3892/or.2016.4953

194. Cambien B, Karimdjee BF, Richard-Fiardo P, Bziouech H, Barthel R, Millet MA, Martini V, Birnbaum D, Scoazec JY, Abello J, et al. 2009. Organ-specific inhibition of metastatic colon carcinoma by CXCR3 antagonism. Br J Cancer. 100(11):1755–1764. doi:10.1038/sj.bjc.6605078

195. Kawada K, Sonoshita M, Sakashita H, Takabayashi A, Yamaoka Y, Manabe T, Inaba K, Minato N, Oshima M, Taketo MM. 2004. Pivotal role of CXCR3 in melanoma cell metastasis to lymph nodes. Cancer Res. 64(11):4010–4017. doi:10.1158/0008-5472.CAN-03-1757

196. Amatschek S, Lucas R, Eger A, Pflueger M, Hundsberger H, Knoll C, Grosse-Kracht S, Schuett W, Koszik F, Maurer D, Wiesner C. 2011. CXCL9 induces chemotaxis, chemorepulsion and endothelial barrier disruption through CXCR3-mediated activation of melanoma cells. Br J Cancer. 104(3):469–479. doi:10.1038/sj.bjc.6606056

197. Wightman SC, Uppal A, Pitroda SP, Ganai S, Burnette B, Stack M, Oshima G, Khan S, Huang X, Posner MC, et al. 2015. Oncogenic CXCL10 signalling drives metastasis development and poor clinical outcome. Br J Cancer. 113(2):327–335. doi:10.1038/bjc.2015.193

198. Zhang Y, Zhao W, Li S, Lv M, Yang X, Li M, Zhang Z. 2019. CXCL11 promotes self-renewal and tumorigenicity of α2δ1+ liver tumor-initiating cells through CXCR3/ERK1/2 signaling. Cancer Lett. 449:163–171. doi:10.1016/j.canlet.2019.02.016

199. Medoff BD, Wain JC, Seung E, Jackobek R, Means TK, Ginns LC, Farber JM, Luster AD. 2006. CXCR3 and its ligands in a murine model of obliterative bronchiolitis: regulation and function. J Immunol. 176(11):7087–7095. doi:10.4049/jimmunol.176.11.7087

200. Rosenblum JM, Shimoda N, Schenk AD, Zhang H, Kish DD, Keslar K, Farber JM, Fairchild RL. 2010. CXC chemokine ligand (CXCL) 9 and CXCL10 are antagonistic costimulation molecules during the priming of alloreactive T cell effectors. J Immunol. 184(7):3450–3460. doi:10.4049/jimmunol.0903831

201. Metzemaekers M, Vanheule V, Janssens R, Struyf S, Proost P. 2018. Overview of the mechanisms that may contribute to the non-redundant activities of interferon-inducible CXC chemokine receptor 3 ligands. Front Immunol. 8:1970. doi:10.3389/fimmu.2017.01970

202. Dalit L, Alvarado C, Küijper L, Kueh AJ, Weir A, D'Amico A, Herold MJ, Vince JE, Nutt SL, Groom JR. 2022. CXCL11 expressing C57BL/6 mice have intact adaptive immune responses to viral infection. Immunol Cell Biol. 100(5):312–322. doi:10.1111/imcb.12541

203. Dharmadhikari N, Mehnert JM, Kaufman HL. 2015. Oncolytic virus immunotherapy for melanoma. Curr Treat Options Oncol. 16(3):10. doi:10.1007/s11864-014-0326-0

204. Pfaffl MW. 2001. A new mathematical model for relative quantification in real-time RT-PCR. Nucleic Acids Res. 29(9):45e–445. doi:10.1093/nar/29.9.e45

205. Girbl T, Lenn T, Perez L, Rolas L, Barkaway A, Thiriot A, del Fresno C, Lynam E, Hub E, Thelen M, et al. 2018. Distinct compartmentalization of the chemokines CXCL1 and CXCL2 and the atypical receptor ACKR1 determine discrete stages of neutrophil diapedesis. Immunity. 49(6):1062-1076.e6. doi:10.1016/j.immuni.2018.09.018

206. Lepsenyi M, Algethami N, Al-Haidari AA, Algaber A, Syk I, Rahman M, Thorlacius H. 2021. CXCL2-CXCR2 axis mediates αV integrin-dependent peritoneal metastasis of colon cancer cells. Clin Exp Metastasis. 38(4):401–410. doi:10.1007/s10585-021-10103-0

207. Korbecki J, Kojder K, Simińska D, Bohatyrewicz R, Gutowska I, Chlubek D, Baranowska-Bosiacka I. 2020. CC chemokines in a tumor: a review of pro-cancer and anti-cancer properties of the ligands of receptors CCR1, CCR2, CCR3, and CCR4. Int J Mol Sci. 21(21):8412. doi:10.3390/ijms21218412

208. Balkwill F. 2009. Tumour necrosis factor and cancer. Nat Rev Cancer. 9(5):361–371. doi:10.1038/nrc2628

209. Rizza P, Moretti F, Belardelli F. 2010. Recent advances on the immunomodulatory effects of IFN-α: implications for cancer immunotherapy and autoimmunity. Autoimmunity. 43(3):204–209. doi:10.3109/08916930903510880

210. Teicher BA. 2001. Malignant cells, directors of the malignant process: role of transforming growth factor-beta. Cancer Metastasis Rev. 20(1/2):133–143. doi:10.1023/A:1013177011767

211. Binnewies M, Roberts EW, Kersten K, Chan V, Fearon DF, Merad M, Coussens LM, Gabrilovich DI, Ostrand-Rosenberg S, Hedrick CC, et al. 2018. Understanding the tumor immune microenvironment (TIME) for effective therapy. Nat Med. 24(5):541–550. doi:10.1038/s41591-018-0014-x

212. Galon J, Pagès F, Marincola FM, Angell HK, Thurin M, Lugli A, Zlobec I, Berger A, Bifulco C, Botti G, et al. 2012. Cancer classification using the Immunoscore: a worldwide task force. J Transl Med. 10(1):205. doi:10.1186/1479-5876-10-205

213. Maibach F, Sadozai H, Seyed Jafari SM, Hunger RE, Schenk M. 2020. Tumor-infiltrating lymphocytes and their prognostic value in cutaneous melanoma. Front Immunol. 11:2105. doi:10.3389/fimmu.2020.02105

214. Edwards J, Wilmott JS, Madore J, Gide TN, Quek C, Tasker A, Ferguson A, Chen J, Hewavisenti R, Hersey P, et al. 2018. CD103+ tumor-resident CD8+ T cells are associated with improved survival in immunotherapy-naïve melanoma patients and expand significantly during anti–PD-1 treatment. Clin Cancer Res. 24(13):3036–3045. doi:10.1158/1078-0432.CCR-17-2257

215. Thomas NE, Busam KJ, From L, Kricker A, Armstrong BK, Anton-Culver H, Gruber SB, Gallagher RP, Zanetti R, Rosso S, et al. 2013. Tumor-infiltrating lymphocyte grade in primary melanomas is independently associated with melanoma-specific survival in the population-based genes, environment and melanoma Study. J Clin Oncol. 31(33):4252–4259. doi:10.1200/JCO.2013.51.3002

216. Ribas A, Dummer R, Puzanov I, VanderWalde A, Andtbacka RHI, Michielin O, Olszanski AJ, Malvehy J, Cebon J, Fernandez E, et al. 2017. Oncolytic virotherapy promotes intratumoral T cell infiltration and improves anti-PD-1 immunotherapy. Cell. 170(6):1109-1119.e10. doi:10.1016/j.cell.2017.08.027

217. Garofalo M, Pancer KW, Wieczorek M, Staniszewska M, Salmaso S, Caliceti P, Kuryk L. 2022. From Immunosuppression to immunomodulation - turning cold tumours into hot. J Cancer. 13(9):2884–2892. doi:10.7150/jca.71992

218. Galluzzi L, Buqué A, Kepp O, Zitvogel L, Kroemer G. 2017. Immunogenic cell death in cancer and infectious disease. Nat Rev Immunol. 17(2):97–111. doi:10.1038/nri.2016.107

219. Ma J, Ramachandran M, Jin C, Quijano-Rubio C, Martikainen M, Yu D, Essand M. 2020. Characterization of virus-mediated immunogenic cancer cell death and the consequences for oncolytic virus-based immunotherapy of cancer. Cell Death Dis. 11(1):48. doi:10.1038/s41419-020-2236-3

220. Xia J-B, Liu G-H, Chen Z-Y, Mao C-Z, Zhou D-C, Wu H-Y, Park K-S, Zhao H, Kim S-K, Cai D-Q, Qi X-F. 2016. Hypoxia/ischemia promotes CXCL10 expression in cardiac microvascular endothelial cells by NFkB activation. Cytokine. 81:63–70. doi:10.1016/j.cyto.2016.02.007

221. Ohmori Y, Wyner L, Narumi S, Armstrong D, Stoler M, Hamilton T. 1993. Tumor necrosis factor-alpha induces cell type and tissue-specific expression of chemoattractant cytokines in vivo. Am J Pathol. 142(3):861-870.

222. Narumi S, Yoneyama H, Inadera H, Nishioji K, Itoh Y, Okanoue T, Matsushima K. 2000. TNF-α is a potent inducer for IFN-inducible protein-10 in hepatocytes and unaffected by GM-CSF *in vivo*, in contrast to IL-1β and IFN-γ. Cytokine. 12(7):1007–1016. doi:10.1006/cyto.1999.0672

223. Fisher RA, Larkin J. 2010. Malignant melanoma (metastatic). BMJ Clin Evid.(12):1–27.

224. Chang DH, Osman K, Connolly J, Kukreja A, Krasovsky J, Pack M, Hutchinson A, Geller M, Liu N, Annable R, et al. 2005. Sustained expansion of NKT cells and antigen-specific T cells after injection of α-galactosyl-ceramide loaded mature dendritic cells in cancer patients. J Exp Med. 201(9):1503–1517. doi:10.1084/jem.20042592

225. Fujii S, Shimizu K, Smith C, Bonifaz L, Steinman RM. 2003. Activation of natural killer T cells by α-galactosylceramide rapidly induces the full maturation of dendritic cells *in vivo* and thereby acts as an adjuvant for combined CD4 and CD8 T cell immunity to a coadministered protein. J Exp Med. 198(2):267–279. doi:10.1084/jem.20030324

226. Metelitsa LS. 2011. Anti-tumor potential of type-I NKT cells against CD1d-positive and CD1d-negative tumors in humans. Clin Immunol. 140(2):119–129. doi:10.1016/j.clim.2010.10.005

227. Overwijk WW, Restifo NP. 2000. B16 as a mouse model for human melanoma. Curr Protoc Immunol. 39(1). doi:10.1002/0471142735.im2001s39

228. Gregg RK. 2021. Model systems for the study of malignant melanoma. In: Melanoma. Vol. 2265. New York, NY: Springer US; p. 1–21. doi:10.1007/978-1-0716-1205-7_1

229. Trunova GV, Makarova OV, Diatroptov ME, Bogdanova IM, Mikchailova LP, Abdulaeva SO. 2011. Morphofunctional characteristic of the immune system in BALB/c and C57Bl/6 mice. Bull Exp Biol Med. 151(1):99–102. doi:10.1007/s10517-011-1268-1

230. Fornefett J, Krause J, Klose K, Fingas F, Hassert R, Eisenberg T, Schrödl W, Grunwald T, Müller U, Baums CG. 2018. Comparative analysis of clinics, pathologies and immune responses in BALB/c and C57BL/6 mice infected with Streptobacillus moniliformis. Microbes Infect. 20(2):101–110. doi:10.1016/j.micinf.2017.10.001

231. Chen L, Watanabe T, Watanabe H, Sendo F. 2001. Neutrophil depletion exacerbates experimental Chagas' disease in BALB/c, but protects C57BL/6 mice through modulating the Th1 / Th2 dichotomy in different directions. Eur J Immunol. 31(1):265–275. doi:10.1002/1521-4141(200101)31:1<265::AID-IMMU265>3.0.CO;2-L

232. Ariotti S, Beltman JB, Borsje R, Hoekstra ME, Halford WP, Haanen JBAG, de Boer RJ, Schumacher TNM. 2015. Subtle CXCR3-dependent chemotaxis of CTLs within infected tissue allows efficient target localization. J Immunol. 195(11):5285–5295. doi:10.4049/jimmunol.1500853

233. Hu JK, Kagari T, Clingan JM, Matloubian M. 2011. Expression of chemokine receptor CXCR3 on T cells affects the balance between effector and memory CD8 T-cell generation. Proc Natl Acad Sci. 108(21). doi:10.1073/pnas.1101881108

234. Srivastava R, Khan AA, Chilukuri S, Syed SA, Tran TT, Furness J, Bahraoui E, BenMohamed L. 2017. CXCL10/CXCR3-dependent mobilization of Herpes Simplex Virus-specific $CD8^+$ T_{EM} and $CD8^+$ T_{RM} cells within infected tissues allows efficient protection against recurrent herpesvirus infection and disease. J Virol. 91(14):e00278-17. doi:10.1128/JVI.00278-17

235. Kohlmeier JE, Reiley WW, Perona-Wright G, Freeman ML, Yager EJ, Connor LM, Brincks EL, Cookenham T, Roberts AD, Burkum CE, et al. 2011. Inflammatory chemokine receptors regulate CD8+ T cell contraction and memory generation following infection. J Exp Med. 208(8):1621–1634. doi:10.1084/jem.20102110

236. Pellicci DG, Koay H-F, Berzins SP. 2020. Thymic development of unconventional T cells: how NKT cells, MAIT cells and γδ T cells emerge. Nat Rev Immunol. 20(12):756–770. doi:10.1038/s41577-020-0345-y

237. Tian G, Courtney AN, Jena B, Heczey A, Liu D, Marinova E, Guo L, Xu X, Torikai H, Mo Q, et al. 2016. CD62L+ NKT cells have prolonged persistence and antitumor activity *in vivo*. J Clin Invest. 126(6):2341–2355. doi:10.1172/JCI83476

238. Reilly EC, Thompson EA, Aspeslagh S, Wands JR, Elewaut D, Brossay L. 2012. Activated iNKT cells promote memory CD8+ T cell differentiation during viral infection. PLoS ONE. 7(5):e37991. doi:10.1371/journal.pone.0037991

239. Macho-Fernandez E, Cruz LJ, Ghinnagow R, Fontaine J, Bialecki E, Frisch B, Trottein F, Faveeuw C. 2014. Targeted delivery of α-galactosylceramide to $CD8\alpha^+$ dendritic cells optimizes Type I NKT cell–based antitumor responses. J Immunol. 193(2):961–969. doi:10.4049/jimmunol.1303029

240. Kuzu OF, Nguyen FD, Noory MA, Sharma A. 2015. Current state of animal (mouse) modeling in melanoma research. Cancer Growth Metastasis. 8s1:CGM.S21214. doi:10.4137/CGM.S21214

241. Zhang Y, Fang C, Wang RE, Wang Y, Guo H, Guo C, Zhao L, Li S, Li X, Schultz PG, et al. 2019. A tumor-targeted immune checkpoint blocker. Proc Natl Acad Sci. 116(32):15889–15894. doi:10.1073/pnas.1905646116

242. Marzagalli M, Ebelt ND, Manuel ER. 2019. Unraveling the crosstalk between melanoma and immune cells in the tumor microenvironment. Semin Cancer Biol. 59:236–250. doi:10.1016/j.semcancer.2019.08.002

243. Melnikova VO, Bolshakov SV, Walker C, Ananthaswamy HN. 2004. Genomic alterations in spontaneous and carcinogen-induced murine melanoma cell lines. Oncogene. 23(13):2347–2356. doi:10.1038/sj.onc.1207405

244. Pérez-Guijarro E, Day C-P, Merlino G, Zaidi MR. 2017. Genetically engineered mouse models of melanoma: mouse models of melanoma. Cancer. 123(S11):2089–2103. doi:10.1002/cncr.30684

245. Dankort D, Curley DP, Cartlidge RA, Nelson B, Karnezis AN, Damsky Jr WE, You MJ, DePinho RA, McMahon M, Bosenberg M. 2009. BrafV600E cooperates with Pten loss to induce metastatic melanoma. Nat Genet. 41(5):544–552. doi:10.1038/ng.356

246. Bosenberg M, Muthusamy V, Curley DP, Wang Z, Hobbs C, Nelson B, Nogueira C, Horner JW, DePinho R, Chin L. 2006. Characterization of melanocyte-specific inducible Cre recombinase transgenic mice. Genesis. 44(5):262–267. doi:10.1002/dvg.20205

247. Smith MP, Sanchez-Laorden B, O'Brien K, Brunton H, Ferguson J, Young H, Dhomen N, Flaherty KT, Frederick DT, Cooper ZA, et al. 2014. The immune microenvironment confers resistance to MAPK pathway inhibitors through macrophage-derived TNFα. Cancer Discov. 4(10):1214–1229. doi:10.1158/2159-8290.CD-13-1007

248. Hooijkaas A, Gadiot J, Morrow M, Stewart R, Schumacher T, Blank CU. 2012. Selective BRAF inhibition decreases tumor-resident lymphocyte frequencies in a mouse model of human melanoma. OncoImmunology. 1(5):609–617. doi:10.4161/onci.20226

249. Zhou L, Yang K, Dunaway S, Abdel-Malek Z, Andl T, Kadekaro AL, Zhang Y. 2018. Suppression of MAPK signaling in BRAF-activated PTEN-deficient melanoma by blocking β-catenin signaling in cancer-associated fibroblasts. Pigment Cell Melanoma Res. 31(2):297–307. doi:10.1111/pcmr.12657

250. Swaminathan K, Campbell A, Papalazarou V, Jaber-Hijazi F, Nixon C, McGhee E, Strathdee D, Sansom OJ, Machesky LM. 2021. The RAC1 target NCKAP1 plays a crucial role in the progression of Braf;Pten-driven melanoma in mice. J Invest Dermatol. 141(3):628-637.e15. doi:10.1016/j.jid.2020.06.029

251. Leonard MK, Pamidimukkala N, Puts GS, Snyder DE, Slominski AT, Kaetzel DM. 2017. The HGF/SF mouse model of UV-induced melanoma as an *in vivo s*ensor for metastasis-regulating gene. Int J Mol Sci. 18(8):1647. doi:10.3390/ijms18081647

252. Recio JA, Noonan FP, Takayama H, Anver MR, Duray P, Rush WL, Lindner G, De Fabo EC, DePinho RA, Merlino G. 2002. Ink4a/arf deficiency promotes ultraviolet radiation-induced melanomagenesis. Cancer Res. 62(22):6724–6730.

253. UBC Animal Care Committee. 2018. UBC ACC guideline on rodents with ulcerated subcutaneous tumours: protocol requirements, monitoring, managing and humane endpoints. Vancouver (BC): University of British Columbia. [about 11 p.].

254. Gourdon J, Jiminez A. 2018. SOP 415.03- Humane intervention points for rodent cancer models. Montreal (QC): McGill University. [about 9 p.].

255. Simon ID, van Rooijen N, Rose JK. 2010. Vesicular stomatitis virus genomic RNA persists *in vivo* in the absence of viral replication. J Virol. 84(7):3280–3286. doi:10.1128/JVI.02052-09

256. Pan Y, Lu F, Fei Q, Yu X, Xiong P, Yu X, Dang Y, Hou Z, Lin W, Lin X, et al. 2019. Single-cell RNA sequencing reveals compartmental remodeling of tumor-infiltrating immune cells induced by anti-CD47 targeting in pancreatic cancer. J Hematol OncolJ Hematol Oncol. 12(1):124. doi:10.1186/s13045-019-0822-6

257. Blando J, Sharma A, Higa MG, Zhao H, Vence L, Yadav SS, Kim J, Sepulveda AM, Sharp M, Maitra A, et al. 2019. Comparison of immune infiltrates in melanoma and pancreatic cancer highlights VISTA as a potential target in pancreatic cancer. Proc Natl Acad Sci. 116(5):1692–1697. doi:10.1073/pnas.1811067116

258. Zatezalo N. 2015. The role of chemokines, chemokine receptors and glycolipid activation in NKT cell tumor infiltration [MSc]. Halifax, NS: Dalhousie University.

259. Aldinucci D, Colombatti A. 2014. The inflammatory chemokine CCL5 and cancer progression. Mediators Inflamm. 2014:1–12. doi:10.1155/2014/292376

260. Wu Y, Li Y-Y, Matsushima K, Baba T, Mukaida N. 2008. CCL3-CCR5 axis regulates intratumoral accumulation of leukocytes and fibroblasts and promotes angiogenesis in murine lung metastasis process. J Immunol. 181(9):6384–6393. doi:10.4049/jimmunol.181.9.6384

261. Zhang Y, Lv D, Kim H-J, Kurt RA, Bu W, Li Y, Ma X. 2013. A novel role of hematopoietic CCL5 in promoting triple-negative mammary tumor progression by regulating generation of myeloid-derived suppressor cells. Cell Res. 23(3):394–408. doi:10.1038/cr.2012.178

262. Germanov E, Veinotte L, Cullen R, Chamberlain E, Butcher EC, Johnston B. 2008. Critical role for the chemokine receptor CXCR6 in homeostasis and activation of CD1d-restricted NKT cells. J Immunol. 181(1):81–91. doi:10.4049/jimmunol.181.1.81

263. Veinotte L, Gebremeskel S, Johnston B. 2016. CXCL16-positive dendritic cells enhance invariant natural killer T cell-dependent IFNγ production and tumor control. OncoImmunology. 5(6):e1160979. doi:10.1080/2162402X.2016.1160979

264. Hu W, Liu Y, Zhou W, Si L, Ren L. 2014. CXCL16 and CXCR6 are coexpressed in human lung cancer *in vivo* and mediate the invasion of lung cancer cell lines *in vitro*. PLoS ONE. 9(6):e99056. doi:10.1371/journal.pone.0099056

265. Deng L, Chen N, Li Y, Zheng H, Lei Q. 2010. CXCR6/CXCL16 functions as a regulator in metastasis and progression of cancer. Biochim Biophys Acta BBA - Rev Cancer. 1806(1):42–49. doi:10.1016/j.bbcan.2010.01.004

266. Isozaki T, Arbab AS, Haas CS, Amin MA, Arendt MD, Koch AE, Ruth JH. 2013. Evidence that CXCL16 is a potent mediator of angiogenesis and is involved in endothelial progenitor cell chemotaxis: studies in mice with K/BxN serum-induced arthritis: endothelial progenitor cell recruitment to RA synovium via CXCL16. Arthritis Rheum. 65(7):1736–1746. doi:10.1002/art.37981

267. Darash-Yahana M, Gillespie JW, Hewitt SM, Chen Y-YK, Maeda S, Stein I, Singh SP, Bedolla RB, Peled A, Troyer DA, et al. 2009. The chemokine CXCL16 and its receptor, CXCR6, as markers and promoters of inflammation-associated cancers. PLoS ONE. 4(8):e6695. doi:10.1371/journal.pone.0006695

268. Galanis E, Markovic SN, Suman VJ, Nuovo GJ, Vile RG, Kottke TJ, Nevala WK, Thompson MA, Lewis JE, Rumilla KM, et al. 2012. Phase II trial of intravenous administration of Reolysin® (Reovirus Serotype-3-dearing Strain) in patients with metastatic melanoma. Mol Ther. 20(10):1998–2003. doi:10.1038/mt.2012.146

269. Ma W, He H, Wang H. 2018. Oncolytic herpes simplex virus and immunotherapy. BMC Immunol. 19(1):40. doi:10.1186/s12865-018-0281-9

270. Ferris RL, Gross ND, Nemunaitis JJ, Andtbacka RHI, Argiris A, Ohr J, Vetto JT, Senzer NN, Bedell C, Ungerleider RS, et al. 2014. Phase I trial of intratumoral therapy using HF10, an oncolytic HSV-1, demonstrates safety in HSV+/HSV- patients with refractory and superficial cancers. J Clin Oncol. 32:6082–6082. doi:10.1200/jco.2014.32.15_suppl.6082

271. Andtbacka RHI, Curti BD, Kaufman H, Daniels GA, Nemunaitis JJ, Spitler LE, Hallmeyer S, Lutzky J, Schultz SM, Whitman ED, et al. 2015. Final data from CALM: A phase II study of Coxsackievirus A21 (CVA21) oncolytic virus immunotherapy in patients with advanced melanoma. J Clin Oncol. 33(15_suppl):9030–9030. doi:10.1200/jco.2015.33.15_suppl.9030

272. Silk AW, Kaufman H, Gabrail N, Mehnert J, Bryan J, Norrell J, Medina D, Bommareddy P, Shafren D, Grose M, Zloza A. 2017. Abstract CT026: Phase 1b study of intratumoral Coxsackievirus A21 (CVA21) and systemic pembrolizumab in advanced melanoma patients: interim results of the CAPRA clinical trial. Cancer Res. 77:CT026–CT026. doi:10.1158/1538-7445.AM2017-CT026

273. Malogolovkin A, Gasanov N, Egorov A, Weener M, Ivanov R, Karabelsky A. 2021. Combinatorial approaches for cancer treatment using oncolytic viruses: projecting the perspectives through clinical trials outcomes. Viruses. 13(7):1271. doi:10.3390/v13071271

274. Gulley JL, Borre M, Vogelzang NJ, Ng S, Agarwal N, Parker CC, Pook DW, Rathenborg P, Flaig TW, Carles J, et al. 2019. Phase III trial of PROSTVAC in asymptomatic or minimally symptomatic metastatic castration-resistant prostate cancer. J Clin Oncol. 37(13):1051–1061. doi:10.1200/JCO.18.02031

275. Sterner RC, Sterner RM. 2021. CAR-T cell therapy: current limitations and potential strategies. Blood Cancer J. 11(4):69. doi:10.1038/s41408-021-00459-7

276. Heczey A, Liu D, Tian G, Courtney AN, Wei J, Marinova E, Gao X, Guo L, Yvon E, Hicks J, et al. 2014. Invariant NKT cells with chimeric antigen receptor provide a novel platform for safe and effective cancer immunotherapy. Blood. 124(18):2824–2833. doi:10.1182/blood-2013-11-541235

277. Rotolo A, Caputo VS, Holubova M, Baxan N, Dubois O, Chaudhry MS, Xiao X, Goudevenou K, Pitcher DS, Petevi K, et al. 2018. Enhanced Anti-lymphoma activity of CAR19-iNKT cells underpinned by dual CD19 and CD1d targeting. Cancer Cell. 34(4):596-610.e11. doi:10.1016/j.ccell.2018.08.017

278. Heczey A, Courtney AN, Montalbano A, Robinson S, Liu K, Li M, Ghatwai N, Dakhova O, Liu B, Raveh-Sadka T, et al. 2020. Anti-GD2 CAR-NKT cells in patients with relapsed or refractory neuroblastoma: an interim analysis. Nat Med. 26(11):1686–1690. doi:10.1038/s41591-020-1074-2

279. Simon B, Wiesinger M, März J, Wistuba-Hamprecht K, Weide B, Schuler-Thurner B, Schuler G, Dörrie J, Uslu U. 2018. The generation of CAR-transfected natural killer T cells for the immunotherapy of melanoma. Int J Mol Sci. 19(8):2365. doi:10.3390/ijms19082365